2009, VOLUME 3

PROGRESS IN PHYSICS

"All scientists shall have the right to present their scientific research results, in whole or in part, at relevant scientific conferences, and to publish the same in printed scientific journals, electronic archives, and any other media." — Declaration of Academic Freedom, Article 8

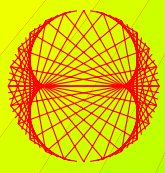

ISSN 1555-5534

The Journal on Advanced Studies in Theoretical and Experimental Physics, including Related Themes from Mathematics

PROGRESS IN PHYSICS

A quarterly issue scientific journal, registered with the Library of Congress (DC, USA). This journal is peer reviewed and included in the abstracting and indexing coverage of: Mathematical Reviews and MathSciNet (AMS, USA), DOAJ of Lund University (Sweden), Zentralblatt MATH (Germany), Scientific Commons of the University of St. Gallen (Switzerland), Open-J-Gate (India), Referativnyi Zhurnal VINITI (Russia), etc.

To order printed issues of this journal, contact the Editors. Electronic version of this journal can be downloaded free of charge:
http://www.ptep-online.com
http://www.geocities.com/ptep_online

Postal address

Chair of the Department
of Mathematics and Science,
University of New Mexico,
200 College Road,
Gallup, NM 87301, USA

This journal is powered by LaTeX

A variety of books can be downloaded free from the Digital Library of Science:
http://www.gallup.unm.edu/∼smarandache

ISSN: 1555-5534 (print)
ISSN: 1555-5615 (online)

Standard Address Number: 297-5092
Printed in the United States of America

JULY 2009 **VOLUME 3**

CONTENTS

Information for Authors and Subscribers

Progress in Physics has been created for publications on advanced studies in theoretical and experimental physics, including related themes from mathematics and astronomy. All submitted papers should be professional, in good English, containing a brief review of a problem and obtained results.

All submissions should be designed in LaTeX format using *Progress in Physics* template. This template can be downloaded from *Progress in Physics* home page http://www.ptep-online.com. Abstract and the necessary information about author(s) should be included into the papers. To submit a paper, mail the file(s) to the Editor-in-Chief.

All submitted papers should be as brief as possible. We usually accept brief papers, no larger than 8–10 typeset journal pages. Short articles are preferable. Large papers can be considered in exceptional cases to the section *Special Reports* intended for such publications in the journal. Letters related to the publications in the journal or to the events among the science community can be applied to the section *Letters to Progress in Physics*.

All that has been accepted for the online issue of *Progress in Physics* is printed in the paper version of the journal. To order printed issues, contact the Editors.

This journal is non-commercial, academic edition. It is printed from private donations. (Look for the current author fee in the online version of the journal.)

A New Cosmological Model: Black Hole Universe

Tianxi Zhang

Department of Physics, Alabama A & M University, Normal, Alabama
E-mail: tianxi.zhang@aamu.edu

A new cosmological model called black hole universe is proposed. According to this model, the universe originated from a hot star-like black hole with several solar masses, and gradually grew up through a supermassive black hole with billion solar masses to the present state with hundred billion-trillion solar masses by accreting ambient materials and merging with other black holes. The entire space is structured with infinite layers hierarchically. The innermost three layers are the universe that we are living, the outside called mother universe, and the inside star-like and supermassive black holes called child universes. The outermost layer is infinite in radius and limits to zero for both the mass density and absolute temperature. The relationships among all layers or universes can be connected by the universe family tree. Mathematically, the entire space can be represented as a set of all universes. A black hole universe is a subset of the entire space or a subspace. The child universes are null sets or empty spaces. All layers or universes are governed by the same physics - the Einstein general theory of relativity with the Robertson-walker metric of spacetime - and tend to expand outward physically. The evolution of the space structure is iterative. When one universe expands out, a new similar universe grows up from its inside. The entire life of a universe begins from the birth as a hot star-like or supermassive black hole, passes through the growth and cools down, and expands to the death with infinite large and zero mass density and absolute temperature. The black hole universe model is consistent with the Mach principle, the observations of the universe, and the Einstein general theory of relativity. Its various aspects can be understood with the well-developed physics without any difficulty. The dark energy is not required for the universe to accelerate its expansion. The inflation is not necessary because the black hole universe does not exist the horizon problem.

1 Introduction

In 1929, Edwin Hubble, when he analyzed the light spectra of galaxies, found that light rays from galaxies were all shifted toward the red [1, 2]. The more distant a galaxy is, the greater the light rays are shifted. According to the Doppler's effect, all the galaxies should be generally receding from us. The more distant a galaxy is, the faster it moves away from our Milky Way. This finding implies that our universe is expanding and thus had a beginning or an origin.

To explain the origin and evolution of the universe, Lemaitre [3–4] suggested that the universe began an explosion of a primeval atom. Around two decades later, George Gamow and his collaborators [5–9], when they synthesized elements in an expanding universe, devised the initial primordial fireball or big bang model based on the Lemaitre's superatom idea. To salvage the big bang model from some of its theoretical problems (e.g., flatness, relic particles, and event horizon), Guth [10] proposed the inflationary hypothesis based on the grand unification theory. The big bang model with an inflationary epoch has been widely accepted as the standard cosmological model because this model is the only one that can explain the three fundamental observations: the expansion of the universe, the 2.7°K cosmic microwave background radiation, and the abundances of helium and other light elements [11–15].

Although it has been declared to have successfully explained the three basic observations, the big bang theory is neither simple nor perfect because the explanations of the observations sensitively rely on many adjustable parameters and hypothesis that have not been or may never be tested [16–17]. In addition, the big bang theory has not yet told us a whole story for the origin and evolution of the universe with ninety-eight percent uncertainties of its composition. The past before 10^{-43} seconds, the outside, and the future of the universe are still unknown. As astronomers are able to observe the space deeper and deeper, the big bang theory may meet more and more severe difficulties with new evidences. In fact, that the newly observed distant quasars with a high fraction of heavy elements [18] has already brought the big bang model in a rather difficult situation. Cosmologists have being tried to mend this model for more than several decades. It is time for astronomers to open their minds to think the universe in different ways and develop a new model that is more convinced and competitive.

When the author was reading a paper [19] about the Mach principle and Brans-Dicke theory of gravity to develop his electric redshift mechanism in accord with the five-dimensional fully covariant Kaluza-Klein theory with a scalar field [20], an idea that the universe is a black hole came to his mind [21].

Upon this idea, a new cosmological model called black hole universe is then developed, which is consistent with the fundamental observations of the universe, the Mach principle, and the Einstein general theory of relativity. This new model provides us a simple and reasonable explanation for the origin, evolution, structure, and expansion of the universe. It also gives a better understanding of the 2.7°K cosmic microwave background radiation, the element abundances, and the high fraction of heavy elements in distant known quasars. Especially, the black hole universe model does not require new physics because the matter of the black hole universe would not be too dense and hot. Dark energy is not necessary for the universe to have an acceleration expansion. Inflation is not needed because there does not exist the horizon problem. Monopoles should not be created because it is not hot enough. Comparing to the standard big bang theory, the black hole universe model is more elegant, simple, and complete. The entire space is well structured hierarchically without outside, evolve iteratively forever without beginning and end, is governed by the simple well-developed physics, and does not exist other unable explained difficulties. The author has recently presented this new cosmological model on the 211th AAS meeting hold on January 7–11, 2008 at Austin, Texas [22] and the 213th AAS meeting hold on January 4–8, 2009 at Long Beach, California [23].

This paper gives a detail description of this new cosmological model. We will fully address why the universe behaves like a black hole, where the black hole universe originates from, how the entire space is structured, how the black hole universe evolves, why the black hole universe expands and accelerates, and what physics governs the black hole universe. Next studies will address how to explain the cosmic microwave background radiation, how quasars to form and release huge amount of energy, and how nuclear elements to synthesize, and so on.

2 Black hole universe

According to the Mach principle, the inertia of an object results as the interaction by the rest of the universe. A body experiences an inertial force when it accelerates relative to the center of mass of the entire universe. In short, mass there affects inertia here. In [24], Sciama developed a theoretical model to incorporate the Mach principle and obtained $GM_{\rm EF}/(c^2R_{\rm EF})\sim 1$, where $M_{\rm EF}$ and $R_{\rm EF}$ are the effective mass and radius of the universe (see also [19, 25]). Later on, it was shown by [26] that the Einstein general theory of relativity is fully consistent with the Sciama interpretation of the Mach principle and the relation between the effective mass and radius of the universe should be modified as $2GM_{\rm EF}/(c^2R_{\rm EF})\sim 1$.

According to the observations of the universe, the density of the present universe ρ_0 is about the critical density $\rho_0\sim\rho_c=3H_0^2/(8\pi G)\sim 9\times 10^{-30}\ \mathrm{g/cm^3}$ and the radius of the present universe is about $R_0\sim 13.7$ billion light years (or $\sim 1.3\times 10^{26}$ m). Here $G=6.67\times 10^{-11}\ \mathrm{N\,m^2\,kg^{-2}}$ is the gravitational constant and $H_0\sim 70\ \mathrm{km/s/Mpc}$ is the Hubble constant. Using the observed density (or the Hubble constant) and radius of the present universe, we have the total mass $M_0\sim 8\times 10^{52}$ kg and the mass-radius relation $2GM_0/(c^2R_0)=(H_0R_0/c)^2\sim 1$ for the present universe.

According to the Schwarzschild solution of the Einstein general theory of relativity [27], the radius of a black hole with mass $M_{\rm BH}$ is given by $R_{\rm BH}=2GM_{\rm BH}/c^2$ or by the relation $2GM_{\rm BH}/(c^2R_{\rm BH})=1$. For a black hole with mass equal to the mass of the present universe ($M_{\rm BH}=M_0$), the radius of the black hole should be about the radius of the present universe ($R_{\rm BH}\sim R_0$).

The results described above in terms of the Mach principle, the observations of the universe, and the Einstein general theory of relativity strongly imply that the universe is a Schwarzschild black hole, which is an extremely supermassive fully expanded black hole with a very big size and thus a very low density and temperature. The boundary of the universe is the Schwarzschild absolute event horizon described by

$$\frac{2GM}{c^2R}=1. \tag{1}$$

For convenience, this mass-radius relation (1) is named by Mach M-R relation. The black hole universe does not exist the horizon problem, so that it does not need an inflation epoch.

It is seen from equation (1) that the mass of a black hole including the universe is proportional to its radius ($M\propto R$). For a star-like black hole with 3 solar masses, its radius is about 9 km. For a supermassive black hole with 3 billion solar masses, its radius is about 9×10^9 km. For the present black hole universe with hundred billion-trillion solar masses, its radius is about 10^{23} km. Therefore, modeling the universe as a black hole is supported by the Mach principle, the observations of the universe, and the Einstein general theory of relativity.

The density of a black hole including the black hole universe can be determined as

$$\rho\equiv\frac{M}{V}=\frac{3c^6}{32\pi G^3M^2}=\frac{3c^2}{8\pi GR^2}, \tag{2}$$

i.e., $\rho R^2=\mathrm{constant}$ or $\rho M^2=\mathrm{constant}$. Here, we have used the Mach M-R relation (1) and $V=4\pi R^3/3$. It is seen that the density of a black hole including the black hole universe is inversely proportional to the square of the mass ($\rho\propto M^{-2}$) or to the square of the radius ($\rho\propto R^{-2}$). In other words, the mass of the black hole universe is proportional to its radius.

Figure 1 plots the density of a black hole as a function of its mass in the unit of the solar mass (the solid line) or a function of its radius in the unit of 3 kilometers (the same

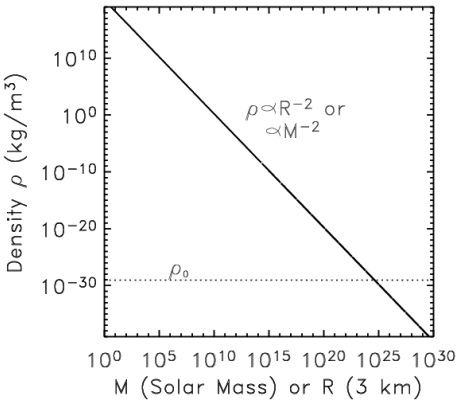

Fig. 1: The density of the black hole universe versus its mass or radius (solid line). The dotted line refers to $\rho = \rho_0$, so that the intersection of the two lines represents the density, radius, and mass of the present universe.

line). The dotted line marks the density of the present universe (ρ_0) and its intersection with the solid line shows the mass (M_0), density (ρ_0), and radius (R_0) of the present universe. Therefore, the black hole universe is not an isolated system because its mass increases as it expands. The density decreases by inversely proportional to the square of the radius (or the mass) of the black hole universe. Considering that matter can enter but cannot exit a black hole, we can suggest that the black hole universe is a semi-open system surrounded by outer space and matter.

In the black hole universe model, we have that the effective radius of the universe is about the actual radius of the universe (or $R_{\mathrm{EF}}/R \sim 1$) at all time. In the big bang theory, we have $R_{\mathrm{EF}}/R = [c^2 R/(2GM)]^{1/2}$ because $\rho R^3 = \mathtt{constant}$. This ratio R_{EF}/R increases as the universe expands and is equal to 1 only at the present time because the observation shows $2GM_0/(c^2 R_0) \sim 1$. In the past, the effective of radius is less than the radius of the universe ($R_{\mathrm{EF}} < R$). While, in future, the effective radius will be greater than the radius of the universe $R_{\mathrm{EF}} > R$, which is not physical, so that the Mach principle will lose its validity in future according to the big bang theory.

3 Origin, structure, and evolution of the black hole universe

In the black hole universe model, it is reasonable to suggest that the universe originated from a star-like black hole. According to the Einstein general theory of relativity, a star, if big enough, can form a star-like black hole when the inside thermonuclear fusion has completed. Once a star-like black hole is formed, an individual spacetime is created. The spacetime inside the event horizon is different from the outside, so that the densities and temperatures on both inside and outside are different. This origin of the universe is somewhat similar to the big bang model, in which the universe exploded from a singular point at the beginning, but the physics is quite different. Here, the star-like black hole with several solar masses (or several kilometers in radius) slowly grows up when it accretes materials from the outside and merges or packs with other black holes, rather than impulsively explodes from nothing to something in the big bang theory. It is also different from the Hoyle model, in which the universe expands due to continuous creation of matter inside the universe [28].

The star-like black hole gradually grows up to be a supermassive black hole as a milestone with billion solar masses and then further grows up to be one like the present universe, which has around hundred billion-trillion solar masses. It is generally believed that the center of an active galaxy exists a massive or supermassive black hole [29–32]. The present universe is still growing up or expanding due to continuously inhaling the matter from the outside called mother or parent universe. The star-like black hole may have a net angular momentum, an inhomogeneous and anisotropic matter distribution, and a net electric charge, etc., but all these effects become small and negligible when it sufficiently grows up.

The present universe is a fully-grown adult universe, which has many child universes such as the star-like and supermassive black holes as observed and one parent (or the mother universe). It may also have sister universes (some universes that are parallel to that we are living), aunt universes, grandmother universes, grand-grandmother universes, etc. based on how vast the entire space is. If the matter in the entire space is finite, then our universe will merge or swallow all the outside matter including its sisters, mother, aunts, grandmothers, and so on, and finally stop its growing. In the same way, our universe will also be finally swallowed by its children and thus die out. If the matter in the entire space is infinite, then the black hole universe will expand to infinitely large in size ($R \to \infty$), and infinitely low in both the mass density ($\rho \to 0$) and absolute temperature ($T \to 0$ K). In this case, the entire space has infinite size and does not have an edge. For completeness, we prefer the entire space to be infinite without boundary and hence without surroundings.

The entire space is structured with infinite layers hierarchically. The innermost three layers as plotted in Figure 2 include the universe that we are living, the outside called mother universe, and the inside star-like and supermassive black holes called child universes. In Figure 2, we have only plotted three child universes and did not plot the sister universes. There should have a number of child universes and may also have many sister universes.

The evolution of the space structure is iterative. In each iteration the matter reconfigures and the universe is renewed rather than a simple repeat or bouncing back. Figure 3 shows a series of sketches for the cartoon of the universe evolution in a single iteration from the present universe to the next similar one. This whole spacetime evolution process does not have the end and the beginning, which is similar to the Hawking's view of the spacetime [33]. As our universe expands,

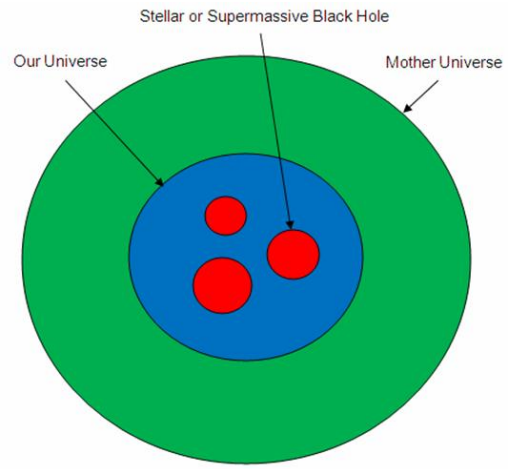

Fig. 2: The innermost three layers of the entire space that is structured hierarchically.

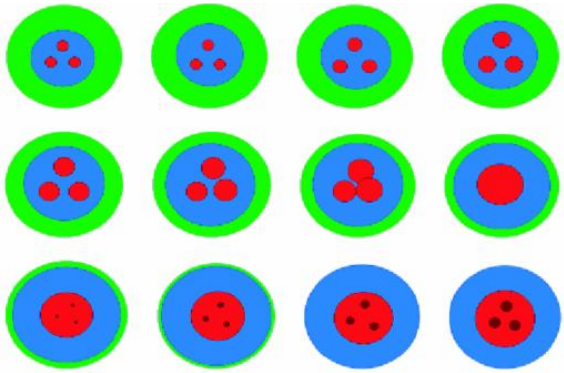

Fig. 3: A series of sketches (or a cartoon, from left to right and then top row to bottom row) for the black hole universe to evolve in a single iteration from the present universe to the next similar one. This is an irreversible process, in which matter and spacetime reconfigure rather than a simple repeat or bouncing back. One universe is expanded to die out and a new universe is born from inside.

the child universes (i.e., the inside star-like and supermassive black holes) grow and merge each other into a new universe. Therefore, when one universe expands out, a new similar universe is born from inside. As like the naturally living things, the universe passes through its own birth, growth, and death process and iterates this process endlessly. Its structure evolves iteratively forever without beginning and end.

To see the multi-layer structure of the space in a larger (or more complicate) view, we plot in Figure 4 the innermost four-layers of the black hole universe up to the grandmother universe. Parallel to the mother universe, there are aunt universes. Parallel to our universe, there are sister universes, which have their own child universes. Here again for simplicity, we have only plotted a few of universes for each layer. If the entire space is finite, then the number of layers is finite. Otherwise, it has infinite layers and the outermost layer corresponds to zero degree in the absolute temperature, zero in the density, and infinite in radius.

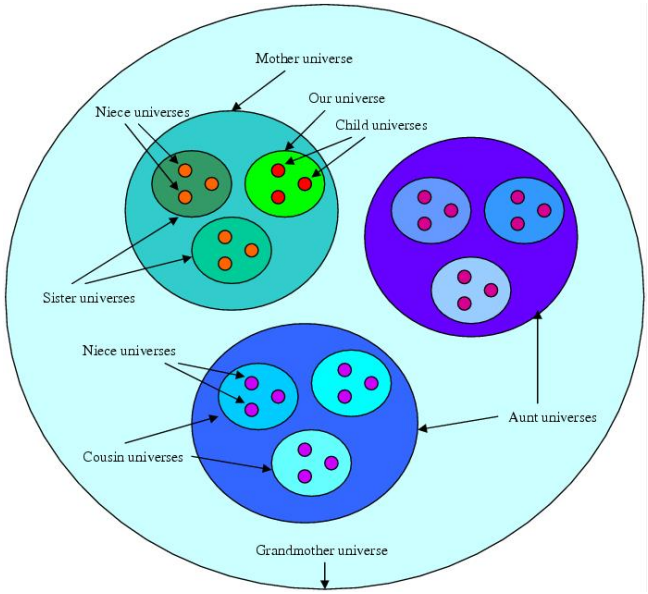

Fig. 4: A sketch of the innermost four layers of the black hole universe including grandmother universe, aunt universes, mother universe, sister universes, cousin universes, niece universes, and child universes.

This four generation universe family shown in Figure 4 can also be represented by a universe family tree (see Figure 5). The mother and aunt universes are children of the grandmother universe. The cousin universes are children of the aunt universes. Both our universe and the cousin universe have their own children, which are the star-like or supermassive black holes.

It is more natural to consider that the space is infinite large without an edge and has infinite number of layers. For the outermost layer, the radius tends to infinity, while the density and absolute temperature both tend to zero. We call this outermost layer as the entire space universe because it contains all universes. To represent this infinite layer structure of the entire space, we use the mathematical set concept (see Figure 6). We let the entire space universe be the set (denoted by U) of all universes; the child universes (also the niece universes) are null sets ($C = \{\}$ or $N = \{\}$); our universe is a set of the child universes ($O = \{C, C, C, \ldots, C\}$); the sister universes are sets of the niece universes $S = \{N, N, N, \ldots, N\}$); the mother universe is a set of our universe and the sister universes ($M = \{S, S, S, \ldots, O\}$); the aunt universes are sets of the cousin universes; the grandmother universe is a set of the aunt universes and the mother universe; and so on. The black hole universe model gives a fantastic picture of the entire space. All universes are self similar and governed by the same physics (the Einstein general theory of relativity with the Robertson-Walker metric) as shown later.

As a black hole grows up, it becomes nonviolent because its density and thus the gravitational field decrease. Matter being swallowed by a star-like black hole is extremely compressed and split into particles by the intense gravitational

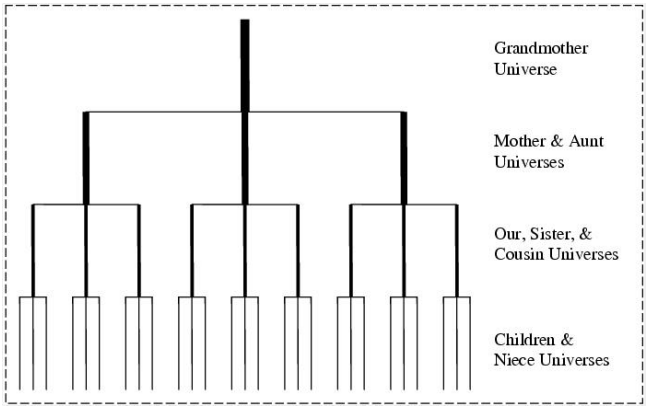

Fig. 5: A family tree for the youngest four generations of the universe family. The generation one includes the child and niece universes; the generation two includes our universe itself and the sister universes; the generation three includes the mother and aunt universes; and the generation four includes the grandmother universe.

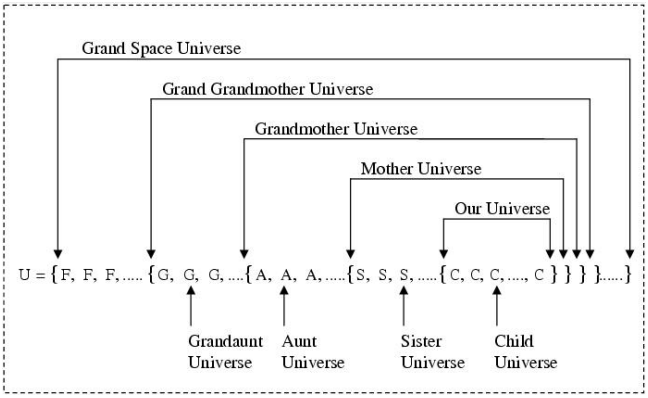

Fig. 6: Mathematical representation of sets of universes for an infinite large and layered space. An inner layer universe set is a subset of the outer layer universe set. The niece and child universes are null sets because they do not contain any sub-spacetime.

field; while that being swallowed by an extremely supermassive black hole (e.g., our universe) may not be compressed and even keeps the same state when it enters through the Schwarzschild absolute event horizon, because the gravitational field is very weak. To see more specifically on this aspect, we show, in Table 1, mass (M), radius (R), density (ρ), and gravitational field at surfaces (g_R) of some typical objects including the Earth, the Sun, a neutron star, a star-like black hole, a supermassive black hole, and the black hole universe. It is seen that the density of a star-like black hole is about that of a neutron star and 10^{14} times denser than the Sun and the Earth, while the density of supermassive black is less than or about that of water. The density of the black hole universe is only about 10^{-28} of supermassive black hole. The gravitational field of the supermassive black hole is only 10^{-8} of a star-like black hole. The gravitational field of the present universe at the surface is very weak ($g_R = c^2/(2R_0) \sim 3 \times 10^{-10}$N).

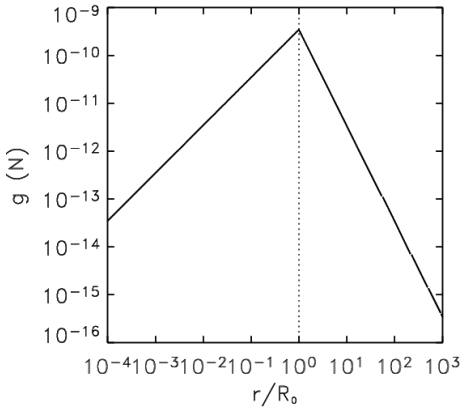

Fig. 7: The gravitational field of the present black hole universe. Inside the black hole universe, the gravity increases with the radial distance linearly from zero at the geometric center to the maximum value at the surface. While outside the black hole universe, the gravity decreases inversely with the square of the radial distance.

The total number of universes in the entire space is given by

$$n = \sum_{i=1}^{i=L} n_i \qquad (3)$$

where the subscript i is the layer number, n_i is the number of universes in the ith layer, and L refers to the number of layers in the entire space. For the four layer (or generation) black hole universe sketched in Figure 4 or 5, we have $L = 4$ and $n = 27 + 9 + 3 + 1 = 40$. If the entire space includes infinite number of layers (i.e., $L = \infty$), then the total number of universes is infinity.

The gravitational field of the black hole universe can be given by

$$g = \begin{cases} c^2 r/(2R_0^2) & \text{if} \quad r \leqslant R_0 \\ c^2 R_0/(2r^2) & \text{if} \quad r \geqslant R_0 \end{cases}, \qquad (4)$$

where r is the distance to the geometric center of the black hole universe. The gravity of the black hole universe increases linearly with r from zero at the center to the maximum (g_R) at the surface and then decreases inversely with r^2 (see Figure 7). In the present extremely expanded universe, the gravity is negligible (or about zero) everywhere, so that, physically, there is no special point (or center) in the black hole universe, which is equivalent to say that any point can be considered as the center. A frame that does not accelerate relative to the center of the universe is very like an inertial frame. The present universe appears homogeneous and isotropic.

4 The steady state and expansion of the black hole universe

In the black hole universe model, the physics of each universe is governed by the Einstein general theory of relativity. The matter density of each universe is inversely proportional to the square of the radius or, in other words, the mass

Object	M (kg)	R (m)	ρ (kg/m^3)	g_R (m/s^2)
Earth	6×10^{24}	6.4×10^6	5.5×10^3	9.8
Sun	2×10^{30}	7×10^8	1.4×10^3	270
Neutron Star	3×10^{30}	10^4	7.2×10^{17}	2×10^{12}
Starlike BH	10^{31}	3×10^3	8.8×10^{19}	7.4×10^{13}
Supermassive BH	10^{39}	3×10^{12}	22	7.4×10^3
Universe	10^{53}	1.4×10^{26}	8.7×10^{-27}	3.4×10^{-10}

Table 1: Mass, radius, density, and gravitational field at the surface of some typical objects.

is linearly proportional to the radius. The three dimensional space curvature of the black hole universe is positive, i.e., $k = 1$. The spacetime of each universe is described by the Robertson-Walker metric

$$ds^2 = c^2 dt^2 - a^2(t) \times \\ \times \left[\frac{1}{1 - r^2} dr^2 + r^2 d\theta^2 + r^2 \sin^2\theta \, d\phi^2 \right], \qquad (5)$$

where ds is the line element and $a(t)$ is the scale (or expansion) factor, which is proportional to the universe radius $R(t)$, and t is the time.

Substituting this metric into the field equation of the Einstein general relativity, we have the Friedmann equation [34]

$$H^2(t) \equiv \left[\frac{1}{R(t)} \frac{dR(t)}{dt} \right]^2 = \frac{8\pi G \rho(t)}{3} - \frac{c^2}{R^2(t)}, \qquad (6)$$

where $H(t)$ is the Hubble parameter (or the universe expansion rate) and $\rho(t)$ is the density of the universe. It should be noted that equation (6) can also be derived from the energy conservation in the classical Newton theory [35]. All layers or universes are governed by the same physics, i.e., the Einstein general theory of relativity with the Robertson-Walker metric, the Mach M-R relation, and the positive space curvature.

Substituting the density given by equation (2) into (6), we obtain

$$\frac{dR(t)}{dt} = 0, \qquad (7)$$

or $H(t) = 0$. Therefore, the black hole universe is usually in a steady state, although it has a positive curvature in the three dimensional space. The black hole universe is balanced when the mass and radius satisfy equation (1), or when the universe density is given by equation (2). The Einstein static universe model corresponds to a special case of the black hole universe model. The steady state remains until the black hole universe is disturbed externally, e.g., entering matter. In other words, when the universe is in a steady state, the Friedmann equation (6) reduces to the Mach M-R relation (1) or the density formula (2).

When the black hole universe inhales matter with an amount dM from the outside, we have

$$\frac{2G(M + dM)}{c^2 R} > 1. \qquad (8)$$

In this case, the black hole universe is not balanced. It will expand its size from R to $R + dR$, where the radius increment dR can be determined by

$$\frac{2G(M + dM)}{c^2(R + dR)} = 1, \qquad (9)$$

or

$$\frac{2G}{c^2} \frac{dM}{dR} = 1. \qquad (10)$$

Therefore, the black hole universe expands when it inhales matter from the outside. From equation (10), the expansion rate (or the rate of change in the radius of the universe) is obtained as

$$\frac{dR(t)}{dt} = \frac{2G}{c^2} \frac{dM(t)}{dt}, \qquad (11)$$

and the Hubble parameter is given by

$$H(t) = \frac{1}{R(t)} \frac{dR(t)}{dt} = \frac{1}{M(t)} \frac{dM(t)}{dt}. \qquad (12)$$

Equation (11) or (12) indicates that the rate at which a black hole including the black hole universe expands is proportional to the rate at which it inhales matter from its outside. Considering a black hole with three solar masses accreting 10^{-5} solar masses per year from its outside [36], we have $dR(t)/dt \sim 10^{-1}$ m/years and $H(t) \sim 10^7$ km/s/Mpc. Considering a supermassive black hole with one billion solar masses, which swallows one thousand solar masses in one year to run a quasar, we have $dR(t)/dt \sim 3 \times 10^3$ km/years and $H(t) \sim 10^6$ km/s/Mpc. When the black hole merges with other black holes, the growth rate should be larger. For our universe at the present state, the value of the Hubble parameter is measured as $H(t_0) \sim 70$ km/s/Mpc. If the radius of the universe is chosen as 13.7 billion light years, we have $dR(t_0)/dt \sim c$, which implies that our universe is expanding in about the light speed at present. To have such fast expansion, the universe must inhale about 10^5 solar masses in one second or swallows a supermassive black hole in about a few hours.

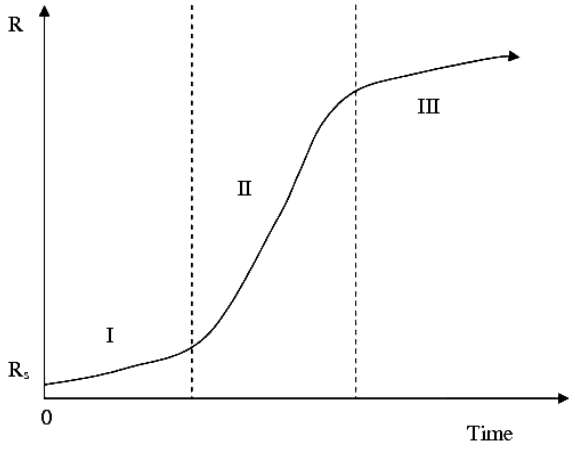

Fig. 8: A schematic sketch for the possible evolution of radius or mass of our black hole universe (solid line): R or M versus time. The two dashed vertical lines divide the plot into three regions, I: child universe, II: adult universe, and III: elder universe.

The whole life of our universe can be roughly divided into three time periods: I, II, and III (Figure 8). During the period I, the universe was a child (e.g., star-like or suppermassive black hole), which did not eat much and thus grew up slowly. During the period II, the universe is an adult (e.g., the present universe), which expands in the fastest speed. During the period III, the universe will become elder (e.g., the mother universe) and slow down the expansion till the end with an infinite radius, zero mass density, and zero absolute temperature. Figure 8 shows a possible variation of radius or mass of a black hole universe in its entire life. Since $dR(t)/dt < c$ in average, the age of the present universe must be greater than $R(t_0)/c$. The Hubble parameter represents the relative expansion rate, which decreases as the universe grows up.

The acceleration parameter is given by

$$q(t) \equiv \frac{1}{R^2(t)}\frac{d^2R(t)}{dt^2} = \frac{1}{M^2(t)}\frac{d^2M(t)}{dt^2}\,; \qquad (13)$$

therefore, if the universe inhales matter in an increasing rate ($d^2M(t)/dt^2 > 0$), the universe accelerates its expansion. Otherwise, it expands in a constant rate ($d^2M(t)/dt^2 = 0$) or expands in a decreasing rate ($d^2M(t)/dt^2 < 0$) or is at rest ($dM(t)/dt = 0$). In the black hole universe model, the dark energy is not required for the universe to accelerate. The black hole universe does not have the dark energy problem that exists in the big bang cosmological theory.

5 Discussions and conclusions

The black hole universe grows its space up by taking its mother's space as it inhales matter and radiation rather than by stretching the space of itself geometrically. As the black hole universe increases its size, the matter of the universe expands because its density must decrease according to equation (2). Since the planets are bound together with the Sun by the gravity, the solar system (also for galaxies and clusters) does not expand as the universe grows up. This is similar to that gases expand when its volume increases, but the atoms and molecules of the gases do not enlarge. Therefore, the expansion of the black hole universe is physical, not geometrical.

Conventionally, it has been suggested that, once a black hole is formed, the matter will further collapse into the center of the black hole, where the matter is crushed to infinitely dense and the pull of gravity is infinitely strong. The interior structure of the black hole consists of the singularity core (point-like) and the vacuum mantle (from the singularity core to the absolute even horizon). In the black hole universe model, our universe originated from a star-like black hole and grew up through a supermassive black hole. A star-like or supermassive black hole is just a child universe (or a mini spacetime). Physical laws and theories are generally applicable to all spacetimes or universes such as our universe, the mother universe, and the child universes (i.e., the star-like or supermassive black holes). The matter inside a black hole can also be governed by the Friedmann equation which is derived from the Einstein general relativity with the Robertson-Walker metric. Therefore, if a black hole does not inhale matter from its outside, it is in a steady state as described by equation (7). The matter inside a black hole distributes uniformly with a density given by equation (2). The highly curved spacetime of a black hole sustains its enormous gravity produced by the highly dense matter. If the black hole inhales the matter from its outside, it grows up and hence expands with a rate that depends on how fast it eats as described by equation (11) or (12).

A black hole, no matter how big it is, is an individual spacetime. From the view of us, a star-like black hole within our universe is a singularity sphere, from which the matter and radiation except for the Hawking radiation (a black body spectrum) cannot go out. Although it is not measurable by us, the temperature inside a star-like black hole should be higher than about that of a neutron star because the density of a star-like black hole is greater than about that of a neutron star, which may have a temperature as high as thousand billion degrees at the moment of its birth by following the explosion of a supernova and then be quickly cooled to hundred million degrees because of radiation [37]. A black hole can hold such high temperature because it does not radiate significantly. When a star-like black hole inhales the matter and radiation from its outside (i.e., the mother universe), it expands and cools down. From a star-like black hole to grow up to one as big as our universe, it is possible for the temperature to be decreased from thousand billion degrees (10^{12} K) to about 3 K. Therefore, in the black hole universe model, the cosmic microwave background radiation is the black body radiation of the black hole universe. In future study, we will explain the cosmic microwave background radiation in detail. We will analyze the nucleosynthesis of elements taken place

in the early (or child) black hole universe, which is dense and hot, grows slowly, and dominates by matter. The early black hole universe is hot enough for elements to synthesize, but not enough to create monopoles.

According to the Einstein general relativity, a main sequence star will, in terms of its mass, form a dwarf, a neutron star, or a black hole. After many stars in a normal galaxy have run out their fuels and formed dwarfs, neutron stars, and black holes, the galaxy will eventually shrink its size and collapse towards the center by gravity to form a supermassive black hole with billions of solar masses. This collapse leads to that extremely hot stellar black holes merge each other and further into the massive black hole at the center and meantime release intense radiation energies that can be as great as a quasar emits. Therefore, when the stellar black holes of a galaxy collapse and merge into a supermassive black hole, the galaxy is activated and a quasar is born. In the black hole universe model, the observed distant quasars can be understood as donuts from the mother universe. The observed distant quasars were formed in the mother universe as little sisters of our universe. When quasars entered our universe, they became children of our universe. The nearby galaxies are quiet at present because they are still very young. They will be activated with an active galactic nuclei and further evolve to quasars after billions of years. In future study, we will give a possible explanation for quasars to ignite and release huge amount of energy.

The black hole universe does not exist other significant difficulties. The dark energy is not necessary for the universe to accelerate its expansion. The expansion rate depends on the rate that the universe inhales matter from outside. When the black hole universe inhales the outside matter in an increasing rate, it accelerates its expansion. The boundary of the black hole universe is the Schwarzschild absolute event horizon, so that the black hole universe does not have the horizon problem. The inflation epoch is not required. The star-like or supermassive black holes are not hot enough to create monopoles. The present universe has been fully expanded and thus behaved as flat, homogeneous, and isotropic. The evolution and physical properties of the early universe are not critical to the present universe because matter and radiation of the present universe are mainly from the mother universe.

As a conclusion, we have proposed a new cosmological model, which is consistent with the Mach principle, the Einstein general theory of relativity, and the observations of the universe. The new model suggests that our universe is an extremely supermassive expanding black hole with a boundary to be the Schwarzschild absolute event horizon as described by the Mach M-R relation, $2GM/c^2R = 1$. The black hole universe originated from a hot star-like black hole with several solar masses, and gradually grew up (thus cooled down) through a supermassive black hole with billion solar masses as a milestone up to the present state with hundred billion-trillion solar masses due to continuously inhaling matter from its outside — the mother universe. The structure and evolution of the black hole universe are spatially hierarchical (or family like) and temporarily iterative. In each of iteration a universe passes through birth, growth, and death. The entire evolution of universe can be roughly divided into three periods with different expanding rates. The whole space is structured similarly and all layers of space (or universes) are governed by the same physics — the Einstein general relativity with the Robertson-Walker metric, the Mach M-R relation, and the positive space curvature. This new model brings us a natural, easily understandable, and reasonably expanding universe; thereby may greatly impact on the big bang cosmology. The universe expands physically due to inhaling matter like a balloon expands when gases are blown into instead of geometrically stretching. New physics is not required because the matter of the black hole universe does not go to infinitely dense and hot. The dark energy is not necessary for the universe to accelerate. There is not the horizon problem and thus not need an inflation epoch. The black hole universe is not hot enough to create monopoles. The black hole universe model is elegant, simple, and complete because the entire space is well structured, governed by the same physics, and evolved iteratively without beginning, end, and outside.

Acknowledgement

This work was supported by AAMU Title III. The author thanks Dr. Martin Rees for time in reading a draft of this paper.

Submitted on March 06, 2009 / Accepted on March 17, 2009

References

1. Hubble E. P. A clue to the structure of the Universe. *Leaflets of the Astronomical Society of the Pacific*, 1929, v. 1, 93–96.
2. Hubble E. P. A relation between distance and radial velocity among extra-galactic nebulae. *Proc. Nat. Acad. Sci.*, 1929, v. 15, 168–173.
3. Lemaitre G. *Annals of the Scientific Society of Brussels*, 1927, v. 47A, 41.
4. Lemaitre G. A homogeneous Universe of constant mass and growing radius accounting for the radial velocity of extragalactic nebulae. *MNRAS*, 1931, v. 91, 483–490.
5. Gamow G. The evolution of the Universe. *Nature*, 1948, v. 162, 680–682.
6. Gamow G. The origin of elements and the separation of galaxies. *Phys. Rev.*, 1948, v. 74, 505–506.
7. Alpher R. A., Bethe H. A., and Gamow G. The origin of chemical elements. *Phys. Rev.*, 1948, v. 73, 803–804.
8. Alpher R. A., Herman P., and Gamow G. Evolution of the Universe. *Nature*, 1948, v. 162, 774–775.
9. Alpher R. A., Herman P., and Gamow G. Thermonuclear reactions in the expanding Universe. *Phs. Rev.*, 1948, v. 74, 1198–1199.

10. Guth A. H. Iflationary universe: A possible solution to the horizon and flatness problems. *Phys. Rev. D* , 1981, v. 23, 347–356.
11. Dicke R. H., Peebles P. J. E., Roll P. G., and Wilkinson D. T. Cosmic black-body radiation. *Astrophys. J.*, 1965, v. 142, 414–419.
12. Penzias A., and Wilson R. W. A measurement of excess antenna temperature at 4080 Mc/s. *Astrophys. J.*, 1965, v. 142, 419–421.
13. Peebles P. J. E., and Yu J. T. Primeval adiabatic perturbation in an expanding universe. *Astrophys. J.*, 1970, v. 162, 815–836.
14. Boesgaard A. M. and Steigman G. Big bang nucleosynthesis — theories and observations. *ARA&A*, 1985, v. 23, 319–378.
15. Gilmore G., Edvardsson B., and Nissen P. E. First detection of beryllium in a very metal poor star — a test of the standard big bang model. *Astrophys. J.*, 1991, v. 378, 17–21.
16. Lerner E. J. et al. An open letter to the scientific community. *New Scientist*, 2004, v. 182, no. 2448, 20.
17. Alfvén H. Cosmology: myth or science. J. Astrophys. Astr., 1984, v. 5, 79–98.
18. Hasinger G., Schartel N., and Komossa S. Discovery of an ionized FeK edge in the Z=3.91 broad absorption line quasar APM 08279+5255 with XMM-Newton. *Astrophys. J.*, v. 573, L77–L80
19. Brans C. and Dicke R. H. Mach's principle and a relativistic theory of gravitation. Phys. Rev., 1961, v. 124, 925–935.
20. Zhang T. X. Electric redshift and quasars. *Astrophys. J.*, 2006, v. 636, L61–L64.
21. Zhang T. X. Black hole universe model. *Private Communication with Dr. Martin Rees*, 2005.
22. Zhang T. X. A new cosmological model: Black hole universe. *AAS 211th Meeting*, Jan. 7–11, 2008, Austin, Texas, 2007, Abstract no.: 152.04.
23. Zhang T. X. Anisotropic expansion of the black hole universe. *AAS 213th Meeting*, Jan. 4–8, 2009, Long Beach, California, 2008, Abstract no.: 357.03.
24. Sciama D. W. On the origin of inertia. *MNRAS*, 1953, v. 113, 34–42.
25. Dicke R. H. New research on old gravitation. *Science*, 1959, v. 129, 621–624.
26. Davidson W. General relativity and mach's principle. *MNRAS*, 1957, v. 117, 212–224.
27. Schwarzschild K. On the gravitational field of a mass point according to Einstein's theory. *Sitz. der Koniglich Preuss. Akad. der Wiss.*, 1916, v. 1, 189–196.
28. Hoyle F. A new model for the expanding universe. *MNRAS*, 1948, v. 108, 372–382.
29. Pringle J. E., Rees M. J., and Pacholczyk A. G. Accretion onto massive black holes. *Astron. Astrophys.*, 1973, v. 29, 179–184.
30. Gurzadian V. G. and Ozernoi L. M. Accretion on massive black holes in galactic nuclei. *Nature*, 1979, v. 280, 214–215.
31. Kormendy J. and Richstone D. Inward bound — The search for supermassive black holes in galactic nuclei. *ARA&A*, 1995, v. 33, 581–624.
32. Richstone D. et al. Supermassive black holes and the evolution of galaxies *Nature*, 1998, v. 395, 14–15.
33. Hawking S. W. Black hole explosions. *Nature*, 1974, v. 248, 30–31.
34. Friedmann A. On the curvature of space. *Z. Phys.*, 1922, v. 10, 377–386.
35. Duric N. Advanced Astrophysics. Cambridge Univ. Press, United Kingtom, 2004.
36. Shakura N. I., and Syunyaev R. A. Black holes in binary systems. Observational appearance. *Astron. Astrophys.*, 1973, v. 24, 337–355.
37. Yakovlev D. G., Gnedin O. Y., Kaminker A. D., Levenfish K. P., and Potekhin A. Y. Neutron star cooling: theoretical aspects and observational constraints. *Adv. Space Res.*, 2004, v. 33, 523–530.

Maxwell-Cattaneo Heat Convection and Thermal Stresses Responses of a Semi-infinite Medium due to High Speed Laser Heating

Ibrahim A. Abdallah

Department of Mathematics, Helwan University, Ain Helwan, 11795, Egypt
E-mail: iaawavelets@yahoo.com

Based on Maxwell-Cattaneo convection equation, the thermoelasticity problem is investigated in this paper. The analytic solution of a boundary value problem for a semi-infinite medium with traction free surface heated by a high-speed laser-pulses have Dirac temporal profile is solved. The temperature, the displacement and the stresses distributions are obtained analytically using the Laplace transformation, and discussed at small time duration of the laser pulses. A numerical study for Cu as a target is performed. The results are presented graphically. The obtained results indicate that the small time duration of the laser pulses has no effect on the finite velocity of the heat conductivity, but the behavior of the stress and the displacement distribution are affected due to the pulsed heating process and due to the structure of the governing equations.

1 Introduction

The induced thermoelastic waves in the material as a response to the pulsed laser heating becomes of great interest due to its wide applications inwelding, cutting, drilling surface hardening and machining of brittle materials. The classical linear theory of thermoelasticity [1] based on Fourier relation

$$q = -k\,\frac{\partial T}{\partial x} \tag{1}$$

together with the energy conservation produces the parabolic heat conduction equation;

$$\frac{\partial T}{\partial t} = \frac{k}{c}\,\frac{\partial T}{\partial x^2}\,. \tag{2}$$

Although this model solved some problems on the macroscale where the length and time scales are relatively large, but it have been proved to be unsuccessful in the microscales ($< 10^{-12}$ s) applications involving high heating rates by a short-pulse laser because Fourier's model implies an infinite speed for heat propagation and infinite thermal flux on the boundaries. To circumvent the deficiencies of Fourier's law in describing such problems involving high rate of temperature change; the concept of wave nature of heat transformation had been introduced [2, 3]. Beside the coupled thermoelasticity theory formulated by Biot [4], thermoelasticity theory with one relaxation time introduced by Lord and Shulman [5] and the two-temperature theory of thermoelasticity [6] which introduced to improve the classical thermoelasticity, there is the Maxwell-Cattaneo model of heat convection [9].

In the Maxwell-Cattaneo model the linkage between the heat conduction equation

$$q + \tau\,\frac{\partial q}{\partial t} = -k\,\frac{\partial T}{\partial x} \tag{3}$$

and the energy conservation introduces the hyperbolic equation

$$\tau\,\frac{\partial^2 T}{\partial t^2} + \frac{\partial T}{\partial t} = \frac{k}{c}\frac{\partial^2 T}{\partial x^2} \tag{4}$$

which describes a heat propagation with finite speed. The finiteness of heat propagation speed provided by the generalized thermoelasticity theories based on Maxwell- Cattaneo model of convection are supposed to be more realistic than the conventional theory to deal with practical problems with very large heat fluxes and/or short time duration.

Biot [4] formulated the theory of coupled thermoelasticity to eliminate the shortcoming of the classical uncoupled theory. In this theory, the equation of motion is a hyperbolic partial differential equation while the equation of energy is parabolic. Thermal disturbances of a hyperbolic nature have been derived using various approaches. Most of these approaches are based on the general notion of relaxing the heat flux in the classical Fourier heat conduction equation, thereby, introducing a non Fourier effect.

The first theory, known as theory of generalized thermoelasticity with one relaxation time, was introduced by Lord and Shulman [5] for the special case of an isotropic body. The extension of this theory to include the case of anisotropic body was developed by Dhaliwal and Sherief [7]. Recently, the author and co-workers investigated the problem of thermoelasticity, based on the theory of Lord and Shulman with one relaxation time, is used to solve a boundary value problem of one dimensional semiinfinite medium heated by a laser beam having a temporal Dirac distribution [8].

The purpose of the present work is to study the thermoelastic interaction caused by heating a homogeneous and isotropic thermoelastic semi-infinite body induced by a Dirac pulse having a homogeneous infinite cross-section by employing the theory of thermoelasticity with one relaxation time. The problem is solved by using the Laplace transform technique. Approximate small time analytical solutions to

stress, displacement and temperature are obtained. The convolution theorem is applied to get the spatial and temporal temperature distribution induced by laser radiation having a temporal Gaussian distribution. At the end of this work a numerical study for Cu as a target is performed and presented graphically and concluding remarks are given.

2 Formulation of the problem

We consider one-dimensional heating situation thermoelastic, homogeneous, isotropic semi-infinite target occupying the region $z \geqslant 0$, and initially at uniform temperature T_0. The surface of the target $z = 0$ is heated homogeneously by a leaser beam and assumed to be traction free. The Cartesian coordinates (x, y, z) are considered in the solution and z-axis pointing vertically into the medium. The governing equations are: The equation of motion in the absence of body forces

$$\sigma_{ji,j} = \rho\, \ddot{u}_i\,, \qquad i, j = x, y, z \tag{5}$$

where σ_{ij} is the components of stress tensor, u_i's are the displacement vector components and ρ is the mass density.

The Maxwell-Cattaneo convection equation

$$\frac{\partial \theta}{\partial t} + \tau\, \frac{\partial^2 \theta}{\partial t^2} = \frac{k}{\rho c_E} \frac{\partial^2 \theta}{\partial z^2} \tag{6}$$

where c_E is the specific heat at constant strain, τ is the relaxation time and k is the thermal conductivity.

The constitutive equation

$$\sigma_{ij} = (\lambda\, \mathrm{div}\, u - \gamma\, \theta)\, \delta_{ij} + 2\, \mu \epsilon_{ij} \tag{7}$$

where δ_{ij} is the delta Kronecker, $\gamma = \alpha_t(3\lambda + 2\mu)$, λ, μ are Lame's constants and α is the thermal expansion coefficient.

The strain-displacement relation

$$\epsilon_{ij} = \frac{1}{2}\,(u_{i,j} + u_{j,i})\,, \qquad i, j = x, y, z \tag{8}$$

The boundary conditions:

$$\sigma_{zz} = 0\,, \quad \text{at} \quad z = 0\,, \tag{9}$$

$$-k\, \frac{d\theta}{dz} = A_0\, q_0\, \delta(t)\,, \quad \text{at} \quad z = 0\,, \tag{10}$$

$$\sigma_{zz} = 0\,, \quad w = 0\,, \quad \theta = 0\,, \quad \text{as} \quad z \to \infty\,, \tag{11}$$

where A_0 is an absorption coefficient of the material, q_0 is the intensity of the laser beam and $\delta(t)$ is the Dirac delta function [10]. The initial conditions:

$$\left.\begin{aligned} &\theta(z,0) = \theta_0\,, \quad w(z,0) = 0\,, \quad \sigma_{ij}(z,0) = 0 \\ &\frac{\partial \theta}{\partial t} = \frac{\partial^2 \theta}{\partial t^2} = \frac{\partial w}{\partial t} = \frac{\partial^2 w}{\partial t^2} = \frac{\partial \sigma_{ij}}{\partial t} = \frac{\partial^2 \sigma_{ij}}{\partial t^2} = 0 \\ &\qquad\qquad\qquad\qquad \text{at} \quad t = 0\,, \ \forall z \end{aligned}\right\}. \tag{12}$$

Due to the symmetry of the problem and the external applied thermal field, the displacement vector u has the components:

$$u_x = 0\,, \quad u_y = 0\,, \quad u_z = w(z,t)\,. \tag{13}$$

From equation (12) the strain components ϵ_{ij}, read;

$$\left.\begin{aligned} &\epsilon_{xx} = \epsilon_{yy} = \epsilon_{xy} = \epsilon_{xz} = \epsilon_{yz} = 0 \\ &\epsilon_{zz} = \frac{\partial w}{\partial z} \\ &\epsilon_{ij} = \frac{1}{2}\,(u_{i,j} + u_{j,i})\,, \qquad i, j = x, y, z \end{aligned}\right\}. \tag{14}$$

The volume dilation e takes the form

$$e = \epsilon_{xx} + \epsilon_{yy} + \epsilon_{zz} = \frac{\partial w}{\partial z}\,. \tag{15}$$

The stress components in (8) can be written as:

$$\left.\begin{aligned} \sigma_{xx} = \sigma_{yy} &= \lambda\, \frac{\partial w}{\partial z} - \gamma\, \theta \\ \sigma_{zz} &= (2\,\mu + \lambda)\, \frac{\partial w}{\partial z} - \gamma\, \theta \end{aligned}\right\}, \tag{16}$$

where

$$\left.\begin{aligned} \sigma_{xy} &= 0 \\ \sigma_{xz} &= 0 \\ \sigma_{yz} &= 0 \end{aligned}\right\}. \tag{17}$$

The equation of motion (5) will be reduce to

$$\sigma_{xz,x} + \sigma_{yz,y} + \sigma_{zz,z} = \rho \ddot{u}_z\,. \tag{18}$$

Substituting from the constitutive equation (8) into the above equation and using $\theta = T - T_0$ we get,

$$(2\,\mu + \lambda)\, \frac{\partial^2 w}{\partial z^2} - \gamma\, \frac{\partial \theta}{\partial z} = \rho\, \frac{\partial^2 w}{\partial t^2} \tag{19}$$

where θ is the temperature change above a reference temperature T_0. Differentiating (19) with respect to z and using (15), we obtain

$$(2\,\mu + \lambda)\, \frac{\partial^2 e}{\partial z^2} - \gamma\, \frac{\partial^2 \theta}{\partial z^2} = \rho\, \frac{\partial^2 e}{\partial t^2} \tag{20}$$

after using (6) the energy equation can be written in the form:

$$(2\,\mu + \lambda)\, \frac{\partial^2 e}{\partial z^2} - \rho\, \frac{\partial^2 e}{\partial t^2} = \frac{\gamma \rho\, c_E}{k} \left(\frac{\partial}{\partial t} + \tau\, \frac{\partial^2}{\partial t^2}\right) \theta \tag{21}$$

by this equation one can determine the dilatation function e after determining θ which can be obtained by solving (6) using Laplace transformation; $\bar{f}(z,s) = \int_0^\infty e^{-st} f(z,t) dt$.

3 Analytic solution

In this section we introduce the analytical solutions of the system of equations (6), (16) and (19) based on the Laplace

transformation. Equation (6) after applying the Laplace transformation it will be;

$$\frac{d^2\bar{\theta}}{dz^2} - \alpha s\,(1+\tau s)\,\bar{\theta} = 0 \tag{22}$$

where $\alpha = \frac{\rho c_E}{k}$. By solving the above equation and using the boundary and the initial conditions (9)-(12); one can write the solution of equation (22) as

$$\bar{\theta} = \frac{A_0 q_0}{k f(s)} e^{-f(s)z}, \qquad \mathrm{Re}\,(f(s)) > 0\,. \tag{23}$$

Similarly the solution of equation (19) after Laplace transformation read;

$$\bar{w}(z,s) = B(s)\,e^{-asz} - \frac{\beta}{(f^2(s) - a^2 s^2)}\,e^{-f(s)z} \tag{24}$$

where

$$a^2 = \frac{\rho}{(2\mu+\lambda)}\,,\quad f(s) = \sqrt{\alpha s\,(1+\tau s)}\,,\quad \beta = \frac{\gamma A_0 q_0}{k(2\mu+\lambda)}\,,$$

$$B(s) = \frac{\beta f(s)}{sa\,(2\mu+\lambda)\,(f^2(s) - a^2 s^2)} - \frac{\beta}{asf(s)}\,.$$

Since we can use the Maclaurin series to write

$$\sqrt{s(1+\tau s)} = \sqrt{s^2\left(\tau + \frac{1}{s}\right)} \approx s\sqrt{\tau} + \frac{1}{2\sqrt{\tau}}\,. \tag{25}$$

Then the solution of the temperature distribution $\bar{\theta}$, and the displacement $\bar{w}$ can be written as

$$\bar{\theta}(z,s) = \left[\frac{C_1}{s} - \frac{C_2}{s^2} + \frac{C_3}{s^3}\right] e^{-z\left(s\sqrt{\alpha\tau} + \frac{1}{2}\sqrt{\frac{\alpha}{\tau}}\right)}, \tag{26}$$

$$\begin{aligned}\bar{w}(z,s) = &\left[\frac{w_1}{s} + \frac{w_2}{\frac{\alpha}{b}+s} + \frac{w_3}{s+\frac{1}{\tau}}\right] e^{-asz} - \\ &- \left[\frac{w_4}{s} + \frac{w_5}{\frac{\alpha}{b}+s}\right] e^{-z\left(s\sqrt{\alpha\tau} + \frac{1}{2}\sqrt{\frac{\alpha}{\tau}}\right)},\end{aligned} \tag{27}$$

therefore the stresses $\bar{\sigma}_{zz}$ and $\bar{\sigma}_{xx} = \bar{\sigma}_{yy}$ are obtained by applying the Laplace transformation to equation (16) and substituting by (26) and (27). Then using the inverse Laplace transformation, we obtain: the temperature θ

$$\begin{aligned}\theta(z,t) = &\Big[C_1 - C_2(t - \sqrt{\alpha\tau}z) + \\ &+ \frac{C_3}{2}(t - \sqrt{\alpha\tau}z)^2\Big] H(t - \sqrt{\alpha\tau}z) e^{-\frac{z}{2}\sqrt{\frac{\alpha}{\tau}}},\end{aligned} \tag{28}$$

the displacement w

$$\begin{aligned}w(z,t) = &\left[w_1 + \frac{w_2}{b}\,e^{-\frac{\alpha}{b}(t-az)} + w_3\,e^{-\frac{t-az}{\tau}}\right] H(t-az) - \\ &- \left[w_4 + \frac{w_5}{b}\,e^{-\frac{\alpha}{b}\left(t - \sqrt{\alpha\tau}z\right)}\right] H(t - \sqrt{\alpha\tau}\,z)\,e^{-\sqrt{\frac{\alpha}{\tau}}z},\end{aligned} \tag{29}$$

the stresses $\sigma_{xx} = \sigma_{yy}$

$$\begin{aligned}\sigma_{xx}(z,t) = &-a\lambda\Big[L_1\delta(t-az) - L_2 H(t-az)\,e^{-\frac{\alpha}{b}(t-az)} - \\ &- L_3 H(t-az) e^{-\frac{1}{\tau}(t-az)}\Big] + \\ &+ e^{-\frac{z}{2}\sqrt{\frac{\alpha}{\tau}}}\Big[L_4\delta(t - \sqrt{\alpha\tau}) + H(t - \sqrt{\alpha\tau}z) \times \\ &\times (L_5 + L_6 e^{-\frac{\alpha}{b}(t - \sqrt{\alpha\tau}z)})\Big] - \gamma\Big[C_1 - C_2(t - \sqrt{\alpha\tau}z) + \\ &+ \frac{C_3}{2}(t - \sqrt{\alpha\tau}z)^2\Big] H(t - \sqrt{\alpha\tau}z)\,e^{-\frac{z}{2}\sqrt{\frac{\alpha}{\tau}}},\end{aligned} \tag{30}$$

the stress σ_{zz}

$$\begin{aligned}\sigma_{zz}(z,t) = &-a(2\mu+\lambda)\Big[L_1\delta(t-az) - \\ &- L_2 H(t-az)\,e^{-\frac{\alpha}{b}(t-az)} - L_3 H(t-az)\,e^{-\frac{1}{\tau}(t-az)}\Big] + \\ &+ e^{-\frac{z}{2}\sqrt{\frac{\alpha}{\tau}}}\Big[L_4\delta(t - \sqrt{\alpha\tau}) + H(t - \sqrt{\alpha\tau}z) \times \\ &\times (L_5 + L_6\,e^{-\frac{\alpha}{b}(t - \sqrt{\alpha\tau}z)})\Big] - \gamma\Big[C_1 - C_2(t - \sqrt{\alpha\tau}z) + \\ &+ \frac{C_3}{2}(t - \sqrt{\alpha\tau}z)^2\Big] H(t - \sqrt{\alpha\tau}z)\,e^{-\frac{z}{2}\sqrt{\frac{\alpha}{\tau}}},\end{aligned} \tag{31}$$

$\delta(x)$ is Dirac delta function, and $H(x)$ is Heaviside unit step functions.

4 Results and discussions

We have calculated the spatial temperature, displacement and stress θ, w, σ_{xx}, σ_{yy} and σ_{zz} with the time as a parameter for a heated target with a spatial homogeneous laser radiation having a temporally Dirac distributed intensity with a width of (10^{-3} s). We have performed the computation for the physical parameters $T_0 = 293$ K, $\rho = 8954$ Kg/m^3, $A_0 = 0.01$, $c_E = 383.1$ J/kgK, $\alpha_t = 1.78\times10^{-5}$ K^{-1}, $k = 386$ W/mK, $\lambda = 7.76\times10^{10}$ kg/m sec^2, $\mu = 3.86\times10^{10}$ kg/m sec^2 and $\tau = 0.02$ sec for Cu as a target. Therefore the coefficients in the expressions (28)–(31)are

$$\left.\begin{array}{ll} C_1 = 1676.0\,, & C_2 = -83800.2 \\ C_3 = 1.57125\times10^6 & \\ w_1 = -5760.28\,, & w_2 = 44906.0 \\ \frac{w_2}{b} = 63506.0\,, & w_3 = 1.5589\times10^6 \\ w_4 = 0.1039\,, & w_5 = -0.7348 \\ \frac{\alpha}{b} = 1256.77\,, & L_1 = -3.0172\times10^{13} \\ L_2 = 1.4896\times10^5, & L_3 = 1.4547\times10^5 \\ L_4 = 2.7708\,, & L_5 = 34.6344 \\ L_6 = 1.7065\times10^3, & \frac{w_5}{b} = 0.103916 \end{array}\right\}. \tag{32}$$

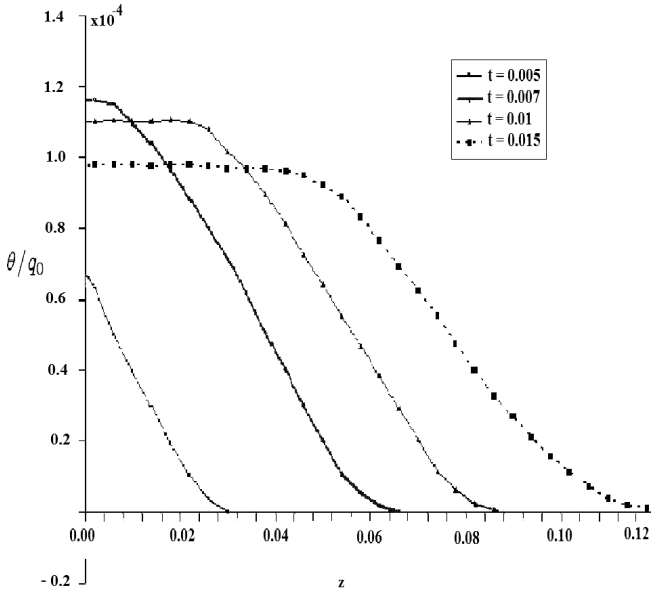

Fig. 1: The temperature distribution θ per unit intensity versus z with the time as a parameter.

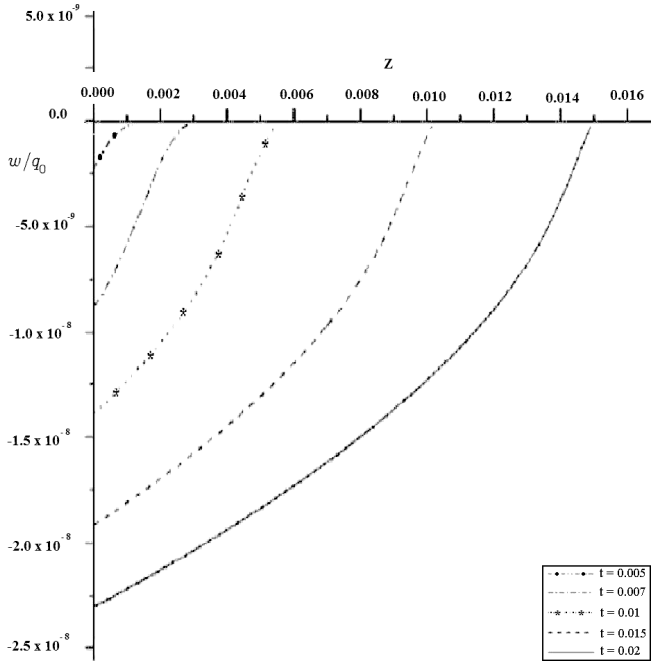

Fig. 2: The displacement distribution w per unit intensity versus z at different values of time as a parameter.

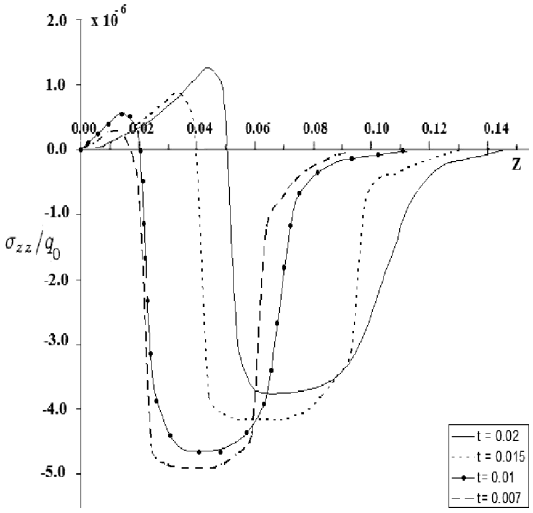

Fig. 3: The stress σ_{zz} distribution per unit intensity versus z with the time as a parameter.

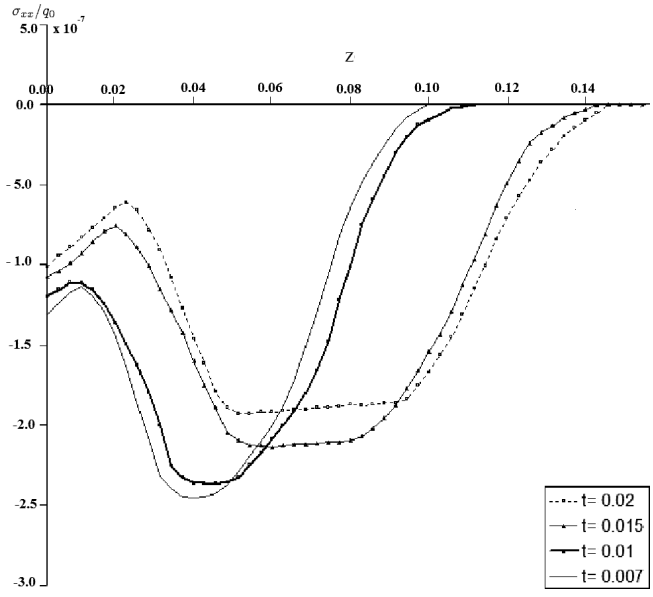

Fig. 4: The stress distribution $\sigma_{xx} = \sigma_{yy}$ per unit intensity versus z with the time as a parameter.

The obtained results are shown in the following figures.

Figure 1 illustrates the calculated spatial temperature distribution per unit intensity at different values of the time as a parameter $t = 0.005, 0.007, 0.01$ and 0.015. From the curves it is evident that the temperature has a finite velocity expressed through the strong gradient of the temperature at different locations which moves deeper in the target as the time increases.

Figure 2 represents the calculated spatial displacement per unit intensity for different values of time as a parameter. The displacement increases monotonically with increasing z. It Shows a smaller gradient with increasing z this behavior occurs at smaller z values than that of the temperature calculated at the corresponding time when it tends to zero. Both effects can be attributed to the temperature behavior and the finite velocity of the expansion which is smaller than that of the heat conduction. The negative displacement indicate the direction of the material expandion where the co-ordinate system is located at the front surface with positive direction of the $z-$axis pointing in the semi-infinite medium.

Figure 3 shows the calculated spatial stress σ_{zz} per unit intensity calculated at different times. It is given by $\sigma_{zz} = = \alpha e - \lambda_1 \theta$. For small z values and at the time $t = 0.005$ the temperature attains greater values than the gradient of the displacement, thus the stress in z direction becomes negative. After attaining z greater values both the temperature and the gradient of the displacement become smaller such that σ_{zz} takes greater values tending to zero. For $t = 0.007$ the effect of the temperature is dominant more than that of the gradient of the displacement this is leading to a more negative stress values shifted toward greater values of z. As the value $t = 0.01$ the effect of the gradient of the displacement over compensates that of the temperature leading to positive stress values lasting up to locations at which the gradient of the displacement and the temperature are practically equal. At this point the stress becomes maximum. As z takes greater values the gradient of the displacement decreases and the temperature becomes the upper hand leading to negative stress values. These behavior remains up to z values at which the temperature is practically zero where the stress tends also be zero. As t takes greater values the effect of the gradient will by more pronounced and thus the maximum of the stress becomes greater and shifts towards the greater z values.

Figure 4 depicts the calculated spatial stress distributions $\sigma_{xx} = \sigma_{yy}$ per unit intensity at different values of the time parameter. the same behavior as σ_{zz}. This is due to the same dependent relation of σ_{ij} on the strain and temperature except that the coefficient of the strain is different.

5 Conclusions

The thermoelastic waves in a semi infinite solid material indused by a Dirac pulsed laser heating are derived for non-Fourier effect based on the Maxwell-Cattaneo hyperbolic convection equation. Analytical solution for the temperature, the displacement and the stresses fields inside the material are derived using the Laplace transformation. The carried calculations enable us to model the thrmoelastic waves induced by a high speed Dirac laser pulse. From the figures it is evident that the temperature firstly increases with increasing the time this can be attributed to the increased absorbed energy which over compensates the heat losses given by the heat conductivity inside the material. As the absorbed power equals the conducted one inside the material the temperature attains its maximum value. the maximum of the temperature occurs at later time than the maximum of the radiation this is the result of the heat conductivity of Cu and the relatively small gradient of the temperature in the vicinity of $z = 0$. After the radiation becomes week enough such that it can not compensate the diffused power inside the material the temperature decreases monotonically with increasing time. Considering surface absorption the obtained results in Figure 1 shows the temperature θ, Figure 2 shows the displacement w, Figure 3 shows the the stress σ_{zz}, and Figure 4 shows the stresses $\sigma_{xx} = \sigma_{yy}$ respectively versus z. The solution of any of the considered function for this model vanishes identically to zero outside a bounded region. The response to the thermal effects by pulsed Laser heating does not reach infinity instantaneously but remains in a bounded region of z given by $0 < z < z^*(t)$ where t is the duration of the laser pulse used for heating. The stress exhibits like step-wise changes at the wave front. The stresses vanish quickly due to the dissipation of the thermal waves.

Submitted on February 25, 2009 / Accepted on March 18, 2009.

References

1. Chadwick L. P. Thermoelasticity: the dynamic theory. In: R. Hill and I. N. Sneddon (eds.), *Progress in Solid Mechanics*, v. I, North-Holland, Amsterdam, 1960, 263–328.
2. Müller L. and Rug-geri T. Extended thermodynamics. Springer, New York, 1993.
3. Özisik M. N. and Tzou D. Y. On the wave theory in heat conduction. *ASME J. of Heat Transfer*, 1994, v. 116, 526–535.
4. Biot M. Thermoelasticity and irreversible thermo-dynamics. *J. Appl. Phys.*, 1956, v. 27 240–253.
5. Lord H. and Shulman Y. A generalized dynamical theory of thermoelasticity. *J.Mech. Phys. Solid.*, 1967, v. 15 299–309.
6. Youssef H. M. and AlLehaibi E. A. State space approach of two temperature generalized thermoelasticity of one dimensional problem. *Intternational Journal of Solids and Structures*, 2007, v. 44, 1550–1562.
7. Dhaliwal R. and Sherief H. Generalized thermoelasticity for anisotropic media. *Quart. Appl. Math.*, 1980, v. 33, 1–8.
8. Abdallah I. A., Hassan A. F., and Tayel I. M. Thermoelastic property of a semi-infinite medium induced by a homogeneously illuminating laser radiation. *Progress In Physics*, 2008, v. 4, 44–50.

9. Andrea P. R., Patrizia B., Luigi M., and Agostino G. B. On the nonlinear Maxwell-Cattaneo equation with non-constant diffusivity: shock and discontinuity waves. *Int. J. Heat and Mass Trans.*, 2008, v. 51, 5327–5332.

10. Hassan A. F., et. al. Heating effects induced by a pulsed laser in a semi-infinite target in view of the theory of linear systems. *Optics and Laser Technology*, 1996, v. 28 (5), 337–343.

11. Hetnarski R. Coupled one-dimensional thermal shock problem for small times. *Arch. Mech. Stosow.*, 1961, v. 13, 295–306.

Relativistic Mechanics in Gravitational Fields Exterior to Rotating Homogeneous Mass Distributions within Regions of Spherical Geometry

Chifu Ebenezer Ndikilar*, Samuel Xede Kofi Howusu†, and Lucas Williams Lumbi‡

*Physics Department, Gombe State University, P.M.B. 127, Gombe, Gombe State, Nigeria
E-mail: ebenechifu@yahoo.com

†Physics Department, Kogi State University, Anyighba, Kogi State, Nigeria
E-mail: sxkhowusu@yahoo.co.uk

‡Physics Department, Nasarawa State University, Keffi, Nasarawa State, Nigeria
E-mail: williamslucas66@yahoo.com

General Relativistic metric tensors for gravitational fields exterior to homogeneous spherical mass distributions rotating with constant angular velocity about a fixed diameter are constructed. The coefficients of affine connection for the gravitational field are used to derive equations of motion for test particles. The laws of conservation of energy and angular momentum are deduced using the generalized Lagrangian. The law of conservation of angular momentum is found to be equal to that in Schwarzschild's gravitational field. The planetary equation of motion and the equation of motion for a photon in the vicinity of the rotating spherical mass distribution have rotational terms not found in Schwarzschild's field.

1 Introduction

General Relativity is the geometrical theory of gravitation published by Albert Einstein in 1915/1916 [1–3]. It unifies Special Relativity and Sir Isaac Newton's law of universal gravitation with the insight that gravitation is not due to a force but rather a manifestation of curved space and time, with the curvature being produced by the mass-energy and momentum content of the space time. After the publication of Einstein's geometrical field equations in 1915, the search for their exact and analytical solutions for all the gravitational fields in nature began [3].

The first method of approach to the construction of exact analytical solutions of Einstein's geometrical gravitational field equations was to find a mapping under which the metric tensor assumed a simple form, such as the vanishing of the off-diagonal elements. This method led to the first analytical solution — the famous Schwarzschild's solution [3]. The second method was to assume that the metric tensor contains symmetries — assumed forms of the associated Killing vectors. The assumption of axially asymmetric metric tensor led to the solution found by Weyl and Levi-Civita [4–11]. The fourth method was to seek Taylor series expansion of some initial value hyper surface, subject to consistent initial value data. This method has not proved successful in generating solutions [4–11].

We now introduce our method and approach to the construction of exact analytical solutions of Einstein's geometrical gravitational field equations [12, 13] as an extension of Schwarzschild analytical solution of Einstein's gravitational field equations. Schwarzschild's metric is well known to be the metric due to a static spherically symmetric body situated in empty space such as the Sun or a star [3, 12, 13]. Schwarzschild's metric is well known to be given as

$$g_{00} = 1 - \frac{2GM}{c^2 r}\,, \tag{1.1}$$

$$g_{11} = -\left[1 - \frac{2GM}{c^2 r}\right]^{-1}, \tag{1.2}$$

$$g_{22} = -r^2, \tag{1.3}$$

$$g_{33} = -r^2 \sin^2\theta\,, \tag{1.4}$$

$$g_{\mu\nu} = 0 \ \text{ otherwise}, \tag{1.5}$$

where $r > R$, the radius of the static spherical mass, G is the universal gravitational constant, M is the total mass of the distribution and c is the speed of light in vacuum. It can be easily recognized [12, 13] that the above metric can be written as

$$g_{00} = 1 + \frac{2f(r)}{c^2}\,, \tag{1.6}$$

$$g_{11} = -\left[1 + \frac{2f(r)}{c^2}\right]^{-1}, \tag{1.7}$$

$$g_{22} = -r^2, \tag{1.8}$$

$$g_{33} = -r^2 \sin^2\theta\,, \tag{1.9}$$

$$g_{\mu\nu} = 0 \ \text{ otherwise}, \tag{1.10}$$

where

$$f(r) = -\frac{GM}{r}\,. \tag{1.11}$$

We thus deduce that generally, $f(r)$ is an arbitrary function determined by the distribution. In this case, it is a function of the radial coordinate r only; since the distribution and hence its exterior gravitational field possess spherical symmetry. From the condition that these metric components should reduce to the field of a point mass located at the origin and contain Newton's equations of motion in the field of the spherical body, it follows that generally, $f(r)$ is approximately equal to the Newtonian gravitational scalar potential in the exterior region of the body, $\Phi(r)$ [12, 13].

Hence, we postulate that the arbitrary function f is solely determined by the mass or pressure distribution and hence possesses all the symmetries of the latter, a priori. Thus, by substituting the generalized arbitrary function possessing all the symmetries of the distribution in to Einstein's gravitational field equations in spherical polar coordinates, explicit equations satisfied by the single arbitrary function, $f(t, r, \theta, \phi)$, can be obtained. These equations can then be integrated exactly to obtain the exact expressions for the arbitrary function. Also, a sound and satisfactory approximate expression can be obtained from the well known fact of General Relativity [12, 13] that in the gravitational field of any distribution of mass;

$$g_{00} \approx 1 + \frac{2}{c^2}\,\Phi(t, r, \theta, \phi)\,. \tag{1.12}$$

It therefore follows that:

$$f(t, r, \theta, \phi) \approx \Phi(t, r, \theta, \phi)\,. \tag{1.13}$$

In a recent article [13], we studied spherical mass distributions in which the material inside the sphere experiences a spherically symmetric radial displacement. In this article, we now study general relativistic mechanics in gravitational fields produced by homogeneous mass distributions rotating with constant angular velocity about a fixed diameter within a static sphere placed in empty space.

2 Coefficients of affine connection

Consider a static sphere of total mass M and density ρ. Also, suppose the mass or pressure distribution within the sphere is homogeneous and rotating with uniform angular velocity about a fixed diameter. More concisely, suppose we have a static spherical object filled with a gas say and the gas is made to rotate with a constant velocity about a fixed diameter. In otherwords, the material inside the sphere is rotating uniformly but the sphere is static. Such a mass distribution might be hypothetical or exist physically or exist astrophysically. For this mass distribution, it is eminent that our arbitrary function will be independent of the coordinate time and azimuthal angle. Thus, the covariant metric for this gravitational field is given as

$$g_{00} = 1 + \frac{2f(r,\theta)}{c^2}\,, \tag{2.1}$$

$$g_{11} = -\left[1 + \frac{2f(r,\theta)}{c^2}\right]^{-1}, \tag{2.2}$$

$$g_{22} = -r^2, \tag{2.3}$$

$$g_{33} = -r^2\sin^2\theta\,, \tag{2.4}$$

$$g_{\mu\nu} = 0 \ \text{ otherwise}, \tag{2.5}$$

where $f(r,\theta)$ is an arbitrary function determined by the mass distribution within the sphere. It is instructive to note that our generalized metric tensor satisfy Einstein's field equations and the invariance of the line element; by virtue of their construction [1, 12]. An outstanding theoretical and astrophysical consequence of this metric tensor is that the resultant Einstein's field equations have only one unknown function, $f(r,\theta)$. Solutions to these field equations give explicit expressions for the function $f(r,\theta)$. In approximate gravitational fields, $f(r,\theta)$ can be conveniently equated to the gravitational scalar potential exterior to the homogeneous spherical mass distribution [1, 12–14]. It is most interesting and instructive to note that the rotation of the homogeneous mass distribution within the static sphere about a fixed diameter is taken care of by polar angle, θ in the function $f(r,\theta)$. Also, if the sphere is made to rotate about a fixed diameter, there will be additional off diagonal components to the metric tensor. Thus, in this analysis, the static nature of the sphere results in the vanishing of the off diagonal components of the metric.

The contravariant metric tensor for the gravitational field, obtained using the Quotient Theorem of tensor analysis [15] is given as

$$g^{00} = \left[1 + \frac{2f(r,\theta)}{c^2}\right]^{-1}, \tag{2.6}$$

$$g^{11} = -\left[1 + \frac{2f(r,\theta)}{c^2}\right], \tag{2.7}$$

$$g^{22} = -r^{-2}, \tag{2.8}$$

$$g^{33} = -\left(r^2\sin^2\theta\right)^{-1}, \tag{2.9}$$

$$g^{\mu\nu} = 0 \ \text{ otherwise}, \tag{2.10}$$

It is well known that the coefficients of affine connection for any gravitational field are defined in terms of the metric tensor [14, 15] as;

$$\Gamma^{\sigma}_{\mu\lambda} = \frac{1}{2}\,g^{\sigma\nu}\left(g_{\mu\nu,\lambda} + g_{\nu\lambda,\mu} - g_{\mu\lambda,\nu}\right), \tag{2.11}$$

$$\ddot{r} + \left[1 + \frac{2}{c^2} f(r,\theta)\right] \frac{\partial f(r,\theta)}{\partial r} \dot{t}^2 - \frac{1}{c^2} \left[1 + \frac{2}{c^2} f(r,\theta)\right]^{-1} \frac{\partial f(r,\theta)}{\partial r} \dot{r}^2 - \frac{2}{c^2} \left[1 + \frac{2}{c^2} f(r,\theta)\right]^{-1} \frac{\partial f(r,\theta)}{\partial \theta} \dot{r}\dot{\theta} - \\ - r \left[1 + \frac{2}{c^2} f(r,\theta)\right] \dot{\theta}^2 - r \sin^2\theta \left[1 + \frac{2}{c^2} f(r,\theta)\right]^{-2} \frac{\partial f(r,\theta)}{\partial \theta} \dot{\phi}^2 = 0 \tag{3.5}$$

where the comma as in usual notation designates partial differentiation with respect to x^λ, x^μ and x^ν. Thus, we construct the explicit expressions for the coefficients of affine connection in this gravitational field as;

$$\Gamma^0_{01} \equiv \Gamma^0_{10} = \frac{1}{c^2} \left[1 + \frac{2}{c^2} f(r,\theta)\right]^{-1} \frac{\partial f(r,\theta)}{\partial r}, \tag{2.12}$$

$$\Gamma^0_{02} \equiv \Gamma^0_{20} = \frac{1}{c^2} \left[1 + \frac{2}{c^2} f(r,\theta)\right]^{-1} \frac{\partial f(r,\theta)}{\partial \theta}, \tag{2.13}$$

$$\Gamma^1_{00} = \frac{1}{c^2} \left[1 + \frac{2}{c^2} f(r,\theta)\right] \frac{\partial f(r,\theta)}{\partial r}, \tag{2.14}$$

$$\Gamma^1_{11} = -\frac{1}{c^2} \left[1 + \frac{2}{c^2} f(r,\theta)\right]^{-1} \frac{\partial f(r,\theta)}{\partial r}, \tag{2.15}$$

$$\Gamma^1_{12} \equiv \Gamma^1_{21} = -\frac{1}{c^2} \left[1 + \frac{2}{c^2} f(r,\theta)\right]^{-1} \frac{\partial f(r,\theta)}{\partial \theta}, \tag{2.16}$$

$$\Gamma^1_{22} = -r \left[1 + \frac{2}{c^2} f(r,\theta)\right], \tag{2.17}$$

$$\Gamma^1_{33} = -r \sin^2\theta \left[1 + \frac{2}{c^2} f(r,\theta)\right]^{-2} \frac{\partial f(r,\theta)}{\partial \theta}, \tag{2.18}$$

$$\Gamma^2_{00} = \frac{1}{r^2 c^2} \frac{\partial f(r,\theta)}{\partial \theta}, \tag{2.19}$$

$$\Gamma^2_{11} = \frac{1}{r^2 c^2} \left[1 + \frac{2}{c^2} f(r,\theta)\right]^{-2} \frac{\partial f(r,\theta)}{\partial \theta}, \tag{2.20}$$

$$\Gamma^2_{12} \equiv \Gamma^2_{21} \equiv \Gamma^3_{13} \equiv \Gamma^3_{31} = -\frac{1}{r}, \tag{2.21}$$

$$\Gamma^2_{33} = -\frac{1}{2} \sin 2\theta, \tag{2.22}$$

$$\Gamma^3_{23} \equiv \Gamma^3_{32} = \cot\theta, \tag{2.23}$$

$$\Gamma^\sigma_{\mu\lambda} = 0 \text{ otherwise}, \tag{2.24}$$

Thus, the gravitational field exterior to a homogeneous rotating mass distribution within regions of spherical geometry has twelve distinct non zero affine connection coefficients. These coefficients are very instrumental in the construction of general relativistic equations of motion for particles of non-zero rest mass.

3 Motion of test particles

A test mass is one which is so small that the gravitational field produced by it is so negligible that it doesn't have any effect on the space metric. A test mass is a continuous body, which is approximated by its geometrical centre; it has nothing in common with a point mass whose density should obviously be infinite [16].

The general relativistic equation of motion for particles of non-zero rest masses is given [1, 12–14, 17] as

$$\frac{d^2 x^\mu}{d\tau^2} + \Gamma^\mu_{\nu\lambda} \left(\frac{dx^\nu}{d\tau}\right) \left(\frac{dx^\lambda}{d\tau}\right) = 0, \tag{3.1}$$

where τ is the proper time. To construct the equations of motion for test particles, we proceed as follows

Setting $\mu = 0$ in equation (3.1) and substituting equations (2.12) and (2.13) gives the time equation of motion as

$$\ddot{t} + \frac{2}{c^2} \left[1 + \frac{2}{c^2} f(r,\theta)\right]^{-1} \frac{\partial f(r,\theta)}{\partial r} \dot{t}\dot{r} + \\ + \frac{2}{c^2} \left[1 + \frac{2}{c^2} f(r,\theta)\right]^{-1} \frac{\partial f(r,\theta)}{\partial \theta} \dot{t}\dot{\theta} = 0, \tag{3.2}$$

where the dot denotes differentiation with respect to proper time. Equation (3.2) is the time equation of motion for particles of non-zero rest masses in this gravitational field. It reduces to Schwarzschild's time equation when $f(r,\theta)$ reduces to $f(r)$. The third term in equation (3.2) is the contribution of the rotation of the mass within the sphere; it does not appear in Schwarzschild's time equation of motion for test particles [1, 12–14, 17]. It is interesting and instructive to realize that equation (3.2) can be written equally as

$$\frac{d}{d\tau} \left(\ln \dot{t}\right) + \frac{d}{d\tau} \left[\ln \left(1 + \frac{2}{c^2} f(r,\theta)\right)\right] = 0. \tag{3.3}$$

Integrating equation (3.3) yields

$$\dot{t} = A \left(1 + \frac{2}{c^2} f(r,\theta)\right)^{-1}, \tag{3.4}$$

where A is the constant of integration (as $t \to \tau$, $f(r,\theta) \to 0$ and thus the constant A is equivalent to unity). Equation (3.4) is the expression for the variation of the time on a clock moving in this gravitational field. It is of same form as that in Schwarzschild's gravitational field [1, 12–14, 17].

Similarly, setting $\mu = 1$ in equation (3.1) gives the radial equation of motion as formula (3.5) on the top of this page.

For pure radial motion $\dot{\theta} \equiv \dot{\phi} = 0$ and hence equation (3.5) reduces to

$$\ddot{r} + \left[1 + \frac{2}{c^2} f(r,\theta)\right]^{-1} \frac{\partial f(r,\theta)}{\partial r} \left(1 - \frac{1}{c^2}\dot{r}^2\right) = 0 . \quad (3.6)$$

The instantaneous speed of a particle of non-zero rest mass in this gravitational field can be obtained from equations (3.5) and (3.6).

Also, setting $\mu = 2$ and $\mu = 3$ in equation (3.1) gives the respective polar and azimuthal equations of motion as

$$\ddot{\theta} + \frac{1}{r^2}\frac{\partial f(r,\theta)}{\partial \theta}\dot{t}^2 + \frac{1}{r^2 c^2}\left[1 + \frac{2}{c^2} f(r,\theta)\right]^{-2} \times \times \frac{\partial f(r,\theta)}{\partial \theta}\dot{r}^2 + \frac{2}{r}\dot{r}\dot{\theta} - \frac{1}{2}(\dot{\phi})^2 \sin 2\theta = 0 \quad (3.7)$$

and

$$\ddot{\phi} + \frac{2}{r}\dot{r}\dot{\phi} + 2\dot{\theta}\dot{\phi}\cot\theta = 0 . \quad (3.8)$$

It is instructive to note that equation (3.7) reduces satisfactorily to the polar equation of motion in Schwarzschild's gravitational field when $f(r,\theta)$ reduces to $f(r)$. Equation (3.8) is equal to the azimuthal equation of motion for particles of non-zero rest masses in Schwarzschild's field. Thus, the instantaneous azimuthal angular velocity from our field is exactly the same as that obtained from Newton's theory of gravitation [14] and Schwarzschild's metric [1, 12, 13, 17].

4 Orbits

The Lagrangian in the space time exterior to any mass or pressure distribution is defined as [17]

$$L = \frac{1}{c}\left(-g_{\alpha\beta}\frac{dx^\alpha}{d\tau}\frac{dx^\beta}{d\tau}\right)^{\frac{1}{2}} = 0 . \quad (4.1)$$

Thus, in our gravitational field, the Lagrangian can be written as

$$L = \frac{1}{c}\left[-g_{00}\left(\frac{dt}{d\tau}\right)^2 - g_{11}\left(\frac{dr}{d\tau}\right)^2\right]^{\frac{1}{2}} - - \frac{1}{c}\left[g_{22}\left(\frac{d\theta}{d\tau}\right)^2 - g_{33}\left(\frac{d\phi}{d\tau}\right)^2\right]^{\frac{1}{2}} = 0 . \quad (4.2)$$

Considering motion confined to the equatorial plane of the homogeneous spherical body, $\theta = \frac{\pi}{2}$ and hence $d\theta = 0$. Thus, in the equatorial plane, equation (4.2) reduces to

$$L = \frac{1}{c}\left[-g_{00}\left(\frac{dt}{d\tau}\right)^2 - - g_{11}\left(\frac{dr}{d\tau}\right)^2 - g_{33}\left(\frac{d\phi}{d\tau}\right)^2\right]^{\frac{1}{2}} = 0 . \quad (4.3)$$

Substituting the explicit expressions for the components of the metric tensor in the equatorial plane of the spherical body yields

$$L = \frac{1}{c}\left[-\left(1 + \frac{2}{c^2} f(r,\theta)\right)\dot{t}^2\right]^{\frac{1}{2}} + + \frac{1}{c}\left[\left(1 + \frac{2}{c^2} f(r,\theta)\right)^{-1}\dot{r}^2 + r^2\dot{\phi}^2\right]^{\frac{1}{2}} , \quad (4.4)$$

where the dot as in usual notation denotes differentiation with respect to proper time.

It is well known that the gravitational field is a conservative field. The Euler-lagrange equations of motion for a conservative system in which the potential energy is independent of the generalized velocities is written as [17]

$$\frac{\partial L}{\partial x^\alpha} = \frac{d}{d\tau}\left(\frac{\partial L}{\partial \dot{x}^\alpha}\right) , \quad (4.5)$$

but

$$\frac{\partial L}{\partial x^0} \equiv \frac{\partial L}{\partial t} = 0 , \quad (4.6)$$

by the time homogeneity of the field and thus from equation (4.5), we deduce that

$$\frac{\partial L}{\partial \dot{t}} = \text{constant} . \quad (4.7)$$

From equation (4.4), it can be shown using equation (4.7) that

$$\left(1 + \frac{2}{c^2} f(r,\theta)\right)\dot{t} = k , \qquad \dot{k} = 0 \quad (4.8)$$

where k is a constant. This the law of conservation of energy in the equatorial plane of the gravitational field [17]. It is of same form as that in Schwarzschild's field. Also, the Lagrangian for this gravitational field is invariant to azimuthal angular rotation (space is isotropic) and hence angular momentum is conserved, thus

$$\frac{\partial L}{\partial \phi} = 0 , \quad (4.9)$$

and from Lagrange's equation of motion and equation (4.4) it can be shown that

$$r^2\dot{\phi} = l , \qquad \dot{l} = 0 , \quad (4.10)$$

where l is a constant. This is the law of conservation of angular momentum in the equatorial plane of our gravitational field. It is equivalent to that obtained in Schwarzschild's gravitational field. Thus, we deduce that the laws of conservation of total energy and angular momentum are invariant in form in the two gravitational fields.

To describe orbits in Schwarzschild's space time, the Lagrangian for permanent orbits in the equatorial plane [17] is

given as;

$$L = \left\{ \left(1 - \frac{2GM}{c^2 r}\right)\left(\frac{dt}{d\tau}\right)^2 - \right. \\ \left. - \frac{1}{c^2}\left[\left(1 - \frac{2GM}{c^2 r}\right)^{-1}\left(\frac{dr}{d\tau}\right)^2 + r^2\left(\frac{d\phi}{d\tau}\right)^2\right]\right\}^{\frac{1}{2}}. \quad (4.11)$$

For time-like orbits, the Lagrangian gives the planetary equation of motion in Schwarzschild's space time as

$$\frac{d^2u}{d\phi^2} + u = \frac{GM}{h^2} + 3\frac{GM}{c^2}u^2, \quad (4.12)$$

where $u = \frac{1}{r}$ and h is a constant of motion. The solution to equation (4.12) depicts the famous perihelion precession of planetary orbits [1, 14, 17]. For null orbits, the equation of motion of a photon in the vicinity of a massive sphere in Schwarzschild's field is obtained as

$$\frac{d^2u}{d\phi^2} + u = 3\frac{GM}{c^2}u^2. \quad (4.13)$$

A satisfactory theoretical explanation for the deflection of light in the vicinity of a massive sphere in Schwarzschild's space time is obtained from the solution of equation (4.13).

It is well known [17] that the Lagrangian $L = \epsilon$, with $\epsilon = 1$ for time like orbits and $\epsilon = 0$ for null orbits. Setting $L = \epsilon$ in equation (4.4) and squaring yields the Lagrangian in the equatorial plane of the gravitational field exterior to a rotating mass distribution within regions of spherical geometry as

$$\epsilon^2 = \frac{1}{c^2}\left[-\left(1 + \frac{2}{c^2}f(r,\theta)\right)\dot{t}^2\right] + \\ + \frac{1}{c^2}\left[\left(1 + \frac{2}{c^2}f(r,\theta)\right)^{-1}\dot{r}^2 + r^2\dot{\phi}^2\right]. \quad (4.14)$$

Substituting equations (4.8) and (4.10) into equation (4.14) and simplifying yields

$$\dot{r}^2 + \left(1 + \frac{2}{c^2}f(r,\theta)\right)\frac{l^2}{r^2} - \\ - 2\epsilon^2 f(r,\theta) = c^2\epsilon^2 + k^2. \quad (4.15)$$

In most applications of general relativity, we are more interested in the shape of orbits (that is, as a function of the azimuthal angle) than in their time history [1, 14, 17]. Hence, it is instructive to transform equation (4.15) into an equation in terms of the azimuthal angle ϕ. Now, let us consider the following standard transformation

$$r = r(\phi) \quad \text{and} \quad u(\phi) = \frac{1}{r(\phi)}, \quad (4.16)$$

then

$$\dot{r} = -\frac{l}{1+u^2}\frac{du}{d\phi}. \quad (4.17)$$

Imposing the transformation equations (4.16) and (4.17) on (4.15) and simplifying yields

$$\left(\frac{l}{1+u^2}\frac{dt}{d\tau}\right)^2 + \left(1 + \frac{2}{c^2}f(u,\theta)\right)u^2 - \\ - 2\epsilon^2\frac{f(u,\theta)}{l^2} = \frac{c^2\epsilon^2 + k^2}{l^2}. \quad (4.18)$$

Equation (4.18) can be integrated immediately, but it leads to elliptical integrals, which are awkward to handle [14]. We thus differentiate this equation to obtain:

$$\frac{d^2u}{d\phi^2} - 2u\left(1+u^2\right)\frac{du}{d\phi} + u\left(1+u^2\right)^2 \times \\ \times\left(1 + \frac{2}{c^2}f(u,\theta)\right) = \left(\frac{2\epsilon^2}{l^2} - \frac{u^2}{c^2}\right)\left(1+u^2\right)^2\frac{\partial f}{\partial u}. \quad (4.19)$$

For time like orbits, equation (4.19) reduces to;

$$\frac{d^2u}{d\phi^2} - 2u\left(1+u^2\right)\frac{du}{d\phi} + u\left(1+u^2\right)^2 \times \\ \times\left(1 + \frac{2}{c^2}f(u,\theta)\right) = \left(\frac{2}{l^2} - \frac{u^2}{c^2}\right)\left(1+u^2\right)^2\frac{\partial f}{\partial u}. \quad (4.20)$$

This is the planetary equation of motion in the equatorial plane of this gravitational field. It can be solved to obtain the perihelion precision of planetary orbits. This equation has additional terms (resulting from the rotation of the mass distribution), not found in the corresponding equation in Schwarzschild's field. Light rays travel on null geodesics and thus equation (4.19) yields;

$$\frac{d^2u}{d\phi^2} - 2u\left(1+u^2\right)\frac{du}{d\phi} + u\left(1+u^2\right)^2 \times \\ \times\left(1 + \frac{2}{c^2}f(u,\theta)\right) = -\frac{u^2}{c^2}\left(1+u^2\right)^2\frac{\partial f}{\partial u}. \quad (4.21)$$

as the photon equation of motion in the vicinity of the homogeneous rotating mass distribution within a static sphere. The equation contains additional terms not found in the corresponding equation in Schwarzschild's field. In the limit of special relativity, some terms in equation (4.21) vanish and the equation becomes

$$\frac{d^2u}{d\phi^2} - 2u\left(1+u^2\right)\frac{du}{d\phi} + u\left(1+u^2\right)^2 = 0. \quad (4.22)$$

The solution of the special relativistic equation, (4.22), can be used to solve the general relativistic equation, (4.21). This can be done by taking the general solution of equation (4.21) to be a perturbation of the solution of equation (4.22). The immediate consequence of this analysis is that it will produce an expression for the total deflection of light grazing the massive sphere.

5 Conclusion

The equations of motion for test particles in the gravitational field exterior to a homogeneous rotating mass distribution within a static sphere were obtained as equations (3.2), (3.5), (3.7) and (3.8). Expressions for the conservation of energy and angular momentum were obtained as equations (4.8) and (4.10) respectively. The planetary equation of motion and the photon equation of motion in the vicinity of the mass where obtained as equations (4.19) and (4.20). The immediate theoretical, physical and astrophysical consequences of the results obtained in this article are three fold.

Firstly, the planetary equation of motion and the photon equation have additional rotational terms not found in Schwarzschild's gravitational field. These equations are opened up for further research work and astrophysical interpretations.

Secondly, in approximate gravitational fields, the arbitrary function $f(r,\theta)$ can be conveniently equated to the gravitational scalar potential exterior to the body. Thus, in approximate fields, the complete solutions for the derived equations of motion can be constructed.

Thirdly, Einstein's field equations constructed using our metric tensor have only one unknown function, $f(r,\theta)$. Solution to these field equations give explicit expressions for the function, $f(r,\theta)$, which can then be interpreted physically and used in our equations of motion. Thus, our method places Einstein's geometrical gravitational field theory on the same footing with Newton's dynamical gravitational field theory; as our method introduces the dependence of the field on one and only one dependent variable, $f(r,\theta)$, comparable to one and only one gravitational scalar potential function in Newton's theory [12, 13].

Submitted on March 12, 2009 / Accepted on March 24, 2009

References

1. Bergmann P. G. Introduction to the theory of relativity. Prentice Hall, New Delhi, 1987.
2. Einstein A. The foundation of the General Theory of Relativity. *Annalen der Physik*, 1916, Bd. 49, 12–34.
3. Schwarzschild K. Über das Gravitationsfeld eines Massenpunktes nach der Einsteinschen Theorie. *Sitzungsberichte der Königlich Preussischen Akademie der Wissenschaften*, 1916, 189–196 (published in English as: Schwarzschild K. On the gravitational field of a point mass according to Einstein's theory. *Abraham Zelmanov Journal*, 2008, v. 1, 10–19).
4. Finster F., et al. Decay of solutions of the wave equation in the Kerr geometry. *Communications in Mathematical Physics*, 2006, v. 264, 465–503.
5. Anderson L., et al. Assymptotic silence of generic cosmological singularities. *Physical Review Letters*, 2001, v. 94, 51–101.
6. Czerniawski J. What is wrong with Schwarzschild's coordinates. *Concepts of Physics*, 2006, v. 3, 309–320.
7. MacCallum H. Finding and using exact solutions of the Einstein equation. arXiv: 0314.4133.
8. Rendall M. Local and global existence theorems for the Einstein equations. *Living Reviews in Relativity*, 2005; arXiv: 1092.31.
9. Stephani H., et al. Exact solutions of Einstein's field equations. Cambridge Monographs Publ., London, 2003.
10. Friedrich H. On the existence of n-geodesically complete or future complete solutions of Einstein's field equations with smooth asmptotic structure. *Communications in Mathematical Physics*, 1986, v. 107, 587–609.
11. Berger B., et al. Oscillatory approach to the singularity in vacuum spacetimes with T^2 Isometry. *Physical Reviews D*, 2001, v. 64, 6–20.
12. Howusu S.X.K. The 210 astrophysical solutions plus 210 cosmological solutions of Einstein's geometrical gravitational field equations. Jos University Press, Jos, 2007 (also available on http://www.natphilweb.com).
13. Chifu E.N. and Howusu S.X.K. Gravitational radiation and propagation field equation exterior to astrophysically real or hypothetical time varying distributions of mass within regions of spherical geometry. *Physics Essays*, 2009, v. 22, no. 1, 73–77.
14. Weinberg S. Gravitation and cosmology, J. Wiley & Sons, New York, 1972.
15. Arfken G. Mathematical methods for physicists. Academic Press, New York, 1995.
16. Rabounski D. and Borissova L. Reply to the "Certain Conceptual Anomalies in Einstein's Theory of Relativity" and related questions. *Progress in Physics*. 2008, v. 2, 166–168.
17. Dunsby P. An introduction to tensors and relativity. Shiva, Cape Town, 2000.

Experimental Verification of a Classical Model of Gravitation

Pieter Wagener

Department of Physics, NMMU South Campus, Port Elizabeth, South Africa
E-mail: Pieter.Wagener@nmmu.ac.za

A previously proposed model of gravitation is evaluated according to recent tests of higher order gravitational effects such as for gravito-electromagnetic phenomena and the properties of binary pulsars. It is shown that the model complies with all the tests.

1 Introduction

In previous articles [1–3] in this journal we presented a model of gravitation, which also led to a unified model of electromagnetism and the nuclear force. The model is based on a Lagrangian,

$$L = -m_0(c^2 + v^2)\exp R/r, \tag{1}$$

where

m_0 = *gravitational rest mass* of a test body moving at velocity $\mathbf{v}$ in the vicinity of a massive, central body of mass M,
$\gamma = 1/\sqrt{1 - v^2/c^2}$,
$R = 2GM/c^2$ is the Schwarzschild radius of the central body.

The following conservation equations follow:

$$E = mc^2 e^{R/r} = \text{total energy} = \text{constant}, \tag{2}$$

$$\mathbf{L} = e^{R/r}\mathbf{M} = \text{constant}, \tag{3}$$

$$L_z = M_z e^{R/r} = e^{R/r} m_0 r^2 \sin^2\theta\, \dot{\phi}, \tag{4}$$

$$= z\text{-component of } \mathbf{L} = \text{constant},$$

where

$$m = m_0/\gamma^2 \tag{5}$$

and

$$\mathbf{M} = (\mathbf{r} \times m_0\mathbf{v}), \tag{6}$$

is the total angular momentum of the test body.

It was shown that the tests for perihelion precession and the bending of light by a massive body are satisfied by the equations of motion derived from the conservation equations.

The *kinematics* of the system is determined by assuming the local and instantaneous validity of special relativity (SR). This leads to an expression for gravitational redshift,

$$\nu = \nu_0 e^{-R/2r} \ (\nu_0 = \text{constant}), \tag{7}$$

which agrees with observation.

The model is further confirmed by confirmation of its electromagnetic and nuclear results.

Details of all calculations appear in the doctoral thesis of the author [4].

1.1 Lorentz-type force

Applying the associated Euler-Lagrange equations to the Lagrangian gives the following Lorentz-type force:

$$\dot{\mathbf{p}} = \mathbf{E}\, m + m_0\mathbf{v} \times \mathbf{H}, \tag{8}$$

where

$$\mathbf{p} = m_0\dot{\mathbf{r}} = m_0\mathbf{v}, \tag{9}$$

$$\mathbf{E} = -\hat{\mathbf{r}}\,\frac{GM}{r^2}, \tag{10}$$

$$\mathbf{H} = \frac{GM(\mathbf{v} \times \mathbf{r})}{c^2 r^3}. \tag{11}$$

1.2 Metric formulation

The above equations can also be derived from a metric,

$$ds^2 = e^{-R/r}dt^2 - e^{R/r}(dr^2 + r^2 d\theta^2 + r^2\sin^2\theta\, d\phi^2). \tag{12}$$

Comparing this metric with that of GR,

$$ds^2 = \left(1 - \frac{R}{r}\right)dt^2 - \\ - \frac{1}{1 - \frac{R}{r}}\,dr^2 - r^2 d\theta^2 - r^2\sin^2\theta\, d\phi^2, \tag{13}$$

we note that this metric is an approximation to our metric.

2 Higher order gravitational effects

Recent measurements of higher order gravitational effects have placed stricter constraints on the viability of gravitational theories. We consider some of these.

These effects fall in two categories: (i) Measurements by earth satellites and (ii) observations of binary pulsars.

2.1 Measurements by earth satellites

These involve the so-called gravito-electromagnetic effects (GEM) such as frame-dragging, or Coriolis effect, and the geodetic displacement. Surveys of recent research are given by Ruffini and Sigismondi [5], Soffel [6] and Pascual-Sànchez et.al. [7] A list of papers on these effects is given by Bini

and Jantzen [8], but we refer in particular to a survey by Mashoon. [9]

Mashhoon points out that for a complete GEM theory, one requires an analogue of the Lorentz force law. Assuming slowly moving matter ($v \ll c$) he derives a spacetime metric of GR in a GEM form (see (1.4) of reference [9]). Assuming further that measurements are taken far from the source, ($r \gg R$) (see (1.5) of reference [9]), he derives a Lorentz-type force (see (1.11) of reference [9]),

$$\mathbf{F} = -m\mathbf{E} - 2m\frac{\mathbf{v}}{c} \times \mathbf{B}, \tag{14}$$

where m in this case is a constant.

This equation is analogous to (8). The latter equation, however, is an *exact* derivation, whereas that of Mashhoon is an approximate one for weak gravitational fields and for particles moving at slow velocities. This difference can be understood by pointing out that GR, as shown above, is an approximation to our model. This implies that all predictions of GR in this regard will be accommodated by our model.

2.2 Binary pulsars

Binary pulsars provide accurate laboratories for the determination of higher order gravitational effects as tests for the viability of gravitational models. We refer to the surveys by Esposito-Farese [10] and Damour [11, 12].

The Parametric-Post-Newtonian (PPN) formulation provides a formulation whereby the predictions of gravitational models could be verified to second order in R/r. This formulation, initially developed by Eddington [13], was further developed by especially Will and Nordtvedt [14, 15]. According to this formulation the metric coefficients of a general metric, $ds^2 = -g_{00}dt^2 + g_{rr}dr^2 + g_{\theta\theta}r^2 d\theta^2 + g_{\phi\phi}r^2 \sin^2\theta\, d\phi^2$, can be represented by the following expansions (see eqs. 1a and 1b of reference [10]):

$$-g_{00} = 1 - \frac{R}{r} + \beta^{PPN}\frac{1}{2}\left(\frac{R}{r}\right)^2 + O\left(\frac{1}{c^6}\right), \tag{15}$$

$$g_{ij} = \delta_{ij}\left(1 + \gamma^{PPN}\frac{R}{r}\right) + O\left(\frac{1}{c^4}\right). \tag{16}$$

Recent observations place the parameters in the above equations within the limits of [16]:

$$|\beta^{PPN} - 1| < 6\times10^{-4}, \tag{17}$$

and [17]

$$\gamma^{PPN} - 1 = (2.1 \pm 2.3)\times10^{-6}. \tag{18}$$

We note that the coefficients of (12) fall within these limits. This implies that the predictions of our model will agree with observations of binary pulsars, or with other sources of higher order gravitational effects.

3 Other effects

Eqs. (2) and (5) show that gravitational repulsion occurs between bodies when their masses are increased by converting radiation energy into mass. We proposed in ref. [1] that this accounts for the start of the Big Bang and the accelerating expansion of the universe. It should be possible to demonstrate this effect in a laboratory.

Conversely, the conversion of matter into radiation energy ($v \to c$) as $r \to R$ describes the formation of a black hole without the mathematical singularity of GR.

4 Conclusion

The proposed model gives a mathematically and conceptually simple method to verify higher order gravitational effects.

Submitted on February 27, 2009 / Accepted on March 31, 2009

References

1. Wagener P. C. A classical model of gravitation. *Progress in Physics*, 2008, v. 3, 21–23.
2. Wagener P. C. A unified theory of interaction: gravitation and electrodynamics. *Progress in Physics*, 2008, v. 4, 3–9.
3. Wagener P. C. A unified theory of interaction: Gravitation, electrodynamics and the strong force. *Progress in Physics*, 2009, v. 1, 33–35.
4. Wagener P. C. Principles of a theory of general interaction. PhD thesis, University of South Africa, 1987. An updated version will be published as a book during 2009.
5. Ruffini R. J. and Constantino S. Nonlinear gravitodynamics: The Lense-Thirring effect. A documentary introduction to current research. World Scientific Publishing, 2003.
6. Soffel M. H. Relativity in astrometry, celestial mechanics and geodesy. Springer-Verlag, 1989.
7. Pascual-Sànchez J.F., Floria L., San Miguel A. and Vicente R. Reference frames and gravitomagnetism. World Scientific, 2001.
8. Bini D. and Jantzen R.T. A list of references on spacetime splitting and gravitoelectromagnetism. In: Pascual-Sànchez J.F., Floria L., San Miguel A. and Vicente R., editors. Reference frames and gravitomagnetism. World Scientific, 2001, 199–224.
9. Mashhoon B. Gravitoelectromagnetism: a brief review. In: Iorio L. editor. Measuring gravitomagnetism: a challenging enterprise. Nova Publishers, 2007, 29–39; arXiv: gr-qc/0311030.
10. Esposito-Farese G. Binary-pulsar tests of strong-field gravity and gravitational radiation damping. arXiv: gr-qc/0402007.
11. Damour T. Binary systems as test-beds of gravity theories. arXiv: gr-qc/0704.0749.
12. Damour T. Black hole and neutron star binaries: theoretical challenges. arXiv: gr-qc/0705.3109.
13. Eddington A. S. Fundamental theory. Cambridge Univ. Press, Cambridge, 1946, 93–94.

14. Nordvedt Jr. K. and Will C.M. Conservation laws and preferred frames in relativistic gravity. II: experimental evidence to rule out prefered-frame theories of gravity. *Astrophys. J.*, 1972, v. 177, 775–792.

15. Will C. M. Theory and experiment in gravitational physics. Revised edition, Cambridge Univ. Press, Cambridge, 1993.

16. Will C. M. *Living Rev. Rel.*, 2001, v. 4; arXiv: gr-qc/0103036.

17. Bertotti B., Iess I., and Tortora P. A test of General Relativity using radio links with the Cassini Spacecraft. *Nature*, 2003, v. 425, 374–376.

Limits to the Validity of the Einstein Field Equations and General Relativity from the Viewpoint of the Negative-Energy Planck Vacuum State

William C. Daywitt

National Institute for Standards and Technology (retired), Boulder, Colorado, USA
E-mail: wcdaywitt@earthlink.net

It is assumed in what follows that the negative-energy Planck vacuum (see the appendix) is the underlying "space" upon which the spacetime equations of General Relativity operate. That is, General Relativity deals with the spacetime aspects of the Planck vacuum (PV). Thus, as the PV appears continuous only down to a certain length ($l = 5r_*$ or greater, perhaps), there is a limit to which the differential geometry of the general theory is valid, that point being where the "graininess" ($l \sim r_* > 0$) of the vacuum state begins to dominate. This aspect of the continuity problem is obvious; what the following deals with is a demonstration that the Einstein equation is tied to the PV, and that the Schwarzschild line elements derived from this equation may be significantly limited by the nature of that vacuum state.

A spherical object of mass m and radius r exerts a relative curvature force

$$n_r = \frac{mc^2/r}{m_*c^2/r_*} \tag{1}$$

on the negative-energy PV and the spacetime of General Relativity, where m_* and r_* are the Planck particle (PP) mass and Compton radius respectively. For example: a white dwarf of mass 9×10^{32} gm and radius 3×10^{8} cm exerts a curvature force equal to 2.7×10^{45} dyne; while a neutron star of mass 3×10^{33} gm and radius 1×10^{6} cm exerts a force of 2.7×10^{48} dyne. Dividing these forces by the 1.21×10^{49} dyne force in the denominator leads to the n-ratios $n_r = 0.0002$ and $n_r = 0.2$ at the surface of the white dwarf and neutron star respectively. As the free PP curvature force m_*c^2/r_* is assumed to be the maximum such force that can be exerted on spacetime and the PV, the n-ratio is limited to the range $n_r < 1$.

The numerator in the first of the following two expressions for the Einstein field equation derived in the appendix

$$G_{\mu\nu} = \frac{8\pi T_{\mu\nu}}{m_*c^2/r_*} \qquad \text{and} \qquad \frac{G_{\mu\nu}/6}{1/r_*^2} = \frac{T_{\mu\nu}}{\rho_*c^2} \tag{2}$$

is normalized by this maximum curvature force. The second expression ties the Einstein equation to the PPs making up the degenerate PV, where $1/r_*^2$ and ρ_*c^2 are the PPs' Gaussian curvature and mass-energy density respectively. The denominators in the second expression represent the Planck limits for the maximum curvature and the maximum equivalent mass-energy density respectively, both limits corresponding to $n_r = 1$. For larger n_r, the equations of General Relativity, derived for a continuum using differential geometry, break down for the reasons already cited.

The limits on the Einstein equation carry over, of course, to results derived therefrom. A simple example is the case of Schwarzschild's point-mass derivation [1]. Its more general form [2] for a point mass m at $r = 0$ consists of the infinite collection ($n = 1, 2, 3, \cdots$) of Schwarzschild-like equations with continuous, non-singular metrics for $r > 0$:

$$ds^2 = \left(1 - \frac{\alpha}{R_n}\right) c^2 dt^2 - \frac{(r/R_n)^{2n-2}\, dr^2}{1 - \alpha/R_n} - \\ - R_n^2 \left(d\theta^2 + \sin^2\theta\, d\phi^2\right), \tag{3}$$

where

$$\alpha = \frac{2mc^2}{c^4/G} = 2\,\frac{mc^2}{m_*c^2/r_*} \tag{4}$$

and

$$R_n = \left(r^n + \alpha^n\right)^{1/n} = r\left(1 + 2^n n_r^n\right)^{1/n} = \\ = \alpha\left(1 + 1/2^n n_r^n\right)^{1/n}, \tag{5}$$

where n_r is given by (1) with r in this case being the *coordinate* radius from the point mass to the field point of interest. The original Schwarzschild solution [1] corresponds to $n = 3$. Here again, r is restricted to the range $r > r_*$ due to the previous continuity arguments leading to $n_r < 1$.

The plots of the time metric

$$g_{00} = g_{00}(n; n_r) = 1 - \frac{\alpha}{R_n} = 1 - \frac{2n_r}{\left(1 + 2^n n_r^n\right)^{1/n}} \tag{6}$$

as a function of n_r in Figure 1 show its behavior as n increases from 1 to 20. The vertical axis represents g_{00} from 0 to 1 and the horizontal axis n_r over the same range. The limiting case as n increases without limit yields

$$g_{00} = 1 - 2n_r \tag{7}$$

for $n_r \leqslant 0.5$. The same limit leads from (3) to the line element

$$ds^2 = \left(1 - 2n_r\right) c^2 dt^2 - \frac{dr^2}{\left(1 - 2n_r\right)} - \\ - r^2 \left(d\theta^2 + \sin^2\theta\, d\phi^2\right), \tag{8}$$

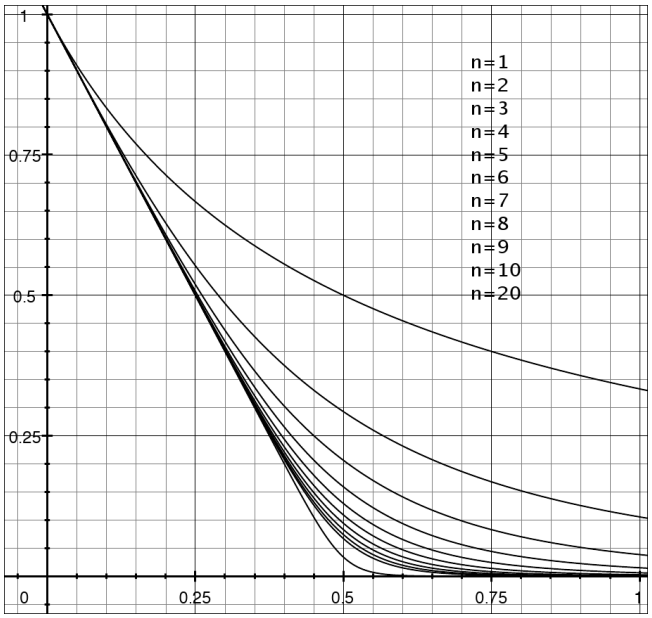

Fig. 1: The graph shows the time metric $g_{00} = g_{00}(n; n_r)$ plotted as a function of the n-ratio n_r for various indices n. Both axes run from 0 to 1. The "dog-leg" in the curves approaches the point (0.5,0) from above ($n_r > 0.5$) as n increases, the limiting case $n \to \infty$ yielding the metric $g_{00} = 1 - 2n_r$ for $n_r \leqslant 0.5$.

for $n_r \leqslant 0.5$. This is the same equation as the standard black-hole/event-horizon line element [3, p.360] except for the reduced range in n_r. Mathematically, the metrics in (3) are non-singular down to any $r > 0$, but we have already seen that this latter inequality should be replaced by $r > r_* > 0$ as $n_r < 1$.

As n_r increases from 0.5, it is assumed that a point is reached prior to $n_r = 1$ where the curvature stress on the PV is sufficient to allow energy to be released from the PV directly into the visible universe. A related viewpoint can be found in a closely similar, field-theoretic context:

> "[This release of energy] is in agreement with observational astrophysics, which in respect of high-energy activity is all of explosive outbursts, as seen in the QSOs, the active galactic nuclei, etc. The profusion of sites where X-ray and γ-ray activity is occurring are in the present [quasi-steady-state] theory sites where the creation of matter is currently taking place" [4, p. 340].

In summary: the obvious restraint on the Einstein field equations is that their time and space differentials be an order of magnitude or so greater than r_*/c and r_* respectively; and that $n_r < 1$, with some thought being given to the application of the equations in the region where $0.5 < n_r < 1$.

Appendix The Planck vacuum

The PV [5] is a uni-polar, omnipresent, degenerate gas of negative-energy PPs which are characterized by the triad (e_*, m_*, r_*), where e_*, m_*, and r_* ($\lambda_*/2\pi$) are the PP charge, mass, and Compton radius respectively. The vacuum is held together by van der Waals forces. The charge e_* is the bare (true) electronic charge common to all charged elementary particles and is related to the observed electronic charge e through the fine structure constant $\alpha = e^2/e_*^2$ which is a manifestation of the PV polarizability. The PP mass and Compton radius are equal to the Planck mass and length respectively. The particle-PV interaction is the source of the gravitational ($G = e_*^2/m_*^2$) and Planck ($\hbar = e_*^2/c$) constants, and the string of Compton relations

$$r_* m_* = \cdots = r_c m = \cdots = e_*^2/c^2 = \hbar/c \qquad \text{(A1)}$$

relating the PV and its PPs to the observed elementary particles, where the charged elementary particles are characterized by the triad (e_*, m, r_c), m and r_c being the mass and Compton radius ($\lambda_c/2\pi$) of the particle (particle spin is not yet included in the theory). The zero-point random motion of the PP charges e_* about their equilibrium positions within the PV, and the PV dynamics, are the source of the quantum vacuum [6] [7]. Neutrinos appear to be phonon packets that exist and propagate within the PV [8].

The Compton relations (A1) follow from the fact that an elementary particle exerts two perturbing forces on the PV, a curvature force mc^2/r and a polarization force e_*^2/r^2:

$$\frac{mc^2}{r} = \frac{e_*^2}{r^2} \qquad \Longrightarrow \qquad r_c = \frac{e_*^2}{mc^2} \qquad \text{(A2)}$$

whose magnitudes are equal at the particle's Compton radius r_c.

Equating the first and third expressions in (A1) leads to $r_* m_* = e_*^2/c^2$. Changing this result from Gaussian to MKS units yields the free-space permittivities

$$\epsilon_0 = \frac{1}{\mu_0 c^2} = \frac{e_*^2}{4\pi r_* m_* c^2} \quad \text{[mks]}, \qquad \text{(A3)}$$

where $\mu_0/4\pi = r_* m_*/e_*^2 = r_c m/e_*^2 = 10^{-7}$ in MKS units. Converting (A3) back into Gaussian units gives

$$\epsilon = \frac{1}{\mu} = \frac{e_*^2}{r_* m_* c^2} = 1 \qquad \text{(A4)}$$

for the permittivities.

A feedback mechanism in the particle-PV interaction leads to the Maxwell equations and the Lorentz transformation [5] [9].

General Relativity describes the spacetime-curvature aspects of the PV. The ultimate curvature force

$$\frac{c^4}{G} = \frac{m_* c^2}{r_*} \qquad \text{(A5)}$$

that can be exerted on spacetime and the PV is due to a free PP. An astrophysical object of mass m exerts a curvature force equal to mc^2/r at a coordinate distance r from the center of the mass. Equation (A5) leads to the ratio

$$\frac{c^4}{8\pi G} = \frac{1}{6}\,\frac{\rho_* c^2}{1/r_*^2}, \qquad \text{(A6)}$$

where $\rho_* \equiv m_*/(4\pi r_*^3/3)$ is the PP mass density and $1/r_*^2$ is its Gaussian curvature. The Einstein equation including the cosmological constant Λ can then be expressed as

$$\frac{(G_{\mu\nu} + \Lambda g_{\mu\nu})/6}{1/r_*^2} = \frac{T_{\mu\nu}}{\rho_* c^2} \qquad \text{(A7)}$$

tying the differential geometry of Einstein to the PPs in the negative-energy PV. In this form both sides of the equation are dimensionless.

Submitted on April 12, 2009 / Accepted on April 28, 2009

References

1. Schwarzschild K. Über das Gravitationsfeld eines Massenpunktes nach der Einsteinschen Theorie. *Sitzungsberichte der Königlich Preussischen Akademie der Wissenschaften*, 1916, 189–196 (published in English as: Schwarzschild K. On the gravitational field of a point mass according to Einstein's theory. *Abraham Zelmanov Journal*, 2008, v. 1, 10–19).
2. Crothers S. J. On the general solution to Einstein's vacuum field and its implications for relativistic degeneracy. *Progress in Physics*, 2005, v. 1, 68.
3. Carroll B. W., Ostlie D. A. An introduction to modern astrophysics. Addison-Wesley, San Francisco — Toronto, 2007.
4. Narlikar J. V. An introduction to cosmology. Third edition, Cambridge Univ. Press, Cambridge, UK, 2002.
5. Daywitt W. C. The planck vacuum. *Progress in Physics*, 2009, v. 1, 20.
6. Daywitt W. C. The source of the quantum vacuum. *Progress in Physics*, 2009, v. 1, 27.
7. Milonni P. W. The quantum vacuum — an introduction to quantum electrodynamics. Academic Press, New York, 1994.
8. Daywitt W. C. The neutrino: evidence of a negative-energy vacuum state. *Progress in Physics*, 2009, v. 2, 3.
9. Pemper R. R. A classical foundation for electrodynamics. Master Dissertation, U. of Texas, El Paso, 1977. Barnes T.G. Physics of the future — a classical unification of physics. Institute for Creation Research, California, 1983, 81.

The Planck Vacuum and the Schwarzschild Metrics

William C. Daywitt

National Institute for Standards and Technology (retired), Boulder, Colorado, USA
E-mail: wcdaywitt@earthlink.net

The Planck vacuum (PV) is assumed to be the source of the visible universe [1, 2]. So under conditions of sufficient stress, there must exist a pathway through which energy from the PV can travel into this universe. Conversely, the passage of energy from the visible universe to the PV must also exist under the same stressful conditions. The following examines two versions of the Schwarzschild metric equation for compatability with this open-pathway idea.

The first version is the general solution to the Einstein field equations [3, 4] for a point mass m at $r = 0$ and consists of the infinite collection ($n = 1, 2, 3, \cdots$) of Schwarzschild-like equations with continuous, non-singular metrics for all $r > 0$:

$$ds^2 = \left(1 - \frac{\alpha}{R_n}\right) c^2 dt^2 - \frac{(r/R_n)^{2n-2}\, dr^2}{1 - \alpha/R_n} - \\ - R_n^2 \left(d\theta^2 + \sin^2\theta\, d\phi^2\right), \tag{1}$$

where

$$\alpha = \frac{2mc^2}{m_* c^2/r_*} = 2rn_r\,, \tag{2}$$

$$R_n = \left(r^n + \alpha^n\right)^{1/n} = r\left(1 + 2^n n_r^n\right)^{1/n} = \\ = \alpha\left(1 + 1/2^n n_r^n\right)^{1/n}, \tag{3}$$

and

$$n_r = \frac{mc^2/r}{m_* c^2/r_*}\,, \tag{4}$$

where r is the *coordinate* radius from the point mass to the field point of interest, and m_* and r_* are the Planck particle mass and Compton radius respectively. The n-ratio n_r is the relative stress the point mass exerts on the PV, its allowable range being $0 < n_r < 1$ which translates into $r > r_*$. The original Schwarzschild line element [5] corresponds to $n = 3$.

The magnitude of the relative coordinate velocity of a photon approaching or leaving the point mass in a radial direction is calculated from the metrics in (1) (by setting $ds = 0$, $d\theta = 0$, $d\phi = 0$) and leads to

$$\beta_n(n_r) = \left|\frac{dr}{c\,dt}\right| = \left(\frac{g_{00}}{-g_{11}}\right)^{1/2} = \\ = \left(1 + 2^n n_r^n\right)^{(1-1/n)} \left(1 - \frac{2n_r}{\left(1 + 2^n n_r^n\right)^{1/n}}\right) \tag{5}$$

whose plot as a function of n_r in Figure 1 shows β_n's behavior as n increases from 1 to 20. The vertical and horizontal axes run from 0 to 1. The limiting case as n increases without limit is

$$\beta_\infty(n_r) = \begin{cases} 1 - 2n_r, & 0 < n_r \leqslant 0.5 \\ 0, & 0.5 \leqslant n_r < 1\,. \end{cases} \tag{6}$$

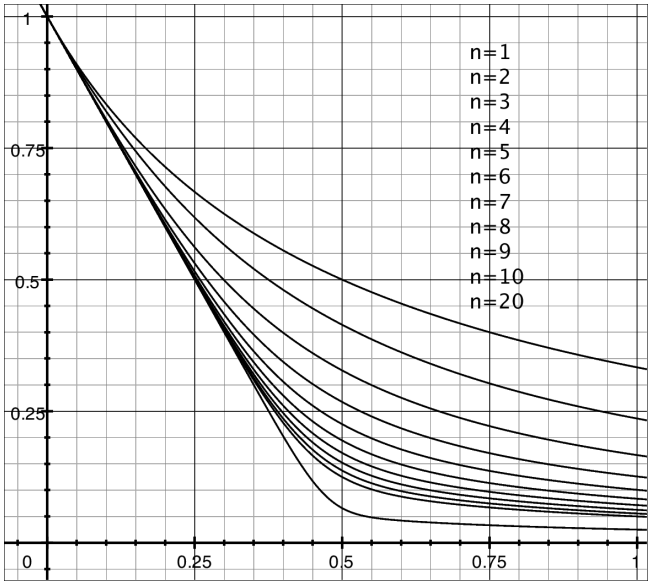

Fig. 1: The graph shows the relative photon velocity $\beta_n(n_r)$ plotted as a function of the n-ratio n_r for various indices n. Both axes run from 0 to 1. The limiting case $n \to \infty$ yields $\beta_n(n_r) = 1 - 2n_r$ for $n_r \leqslant 0.5$.

That is, the photon does not propagate ($\beta_\infty(n_r) = 0$) in the region $0.5 \leqslant n_r < 1$ for the limiting case. So if photon propagation is expected for n_r in this range, i.e., if energy transfer between the stressed PV and the visible universe is assumed, then the "$n = \infty$" solution must be discarded.

The second version of the Schwarzschild line element [6, p. 634]

$$ds^2 = \left(1 - 2n_r\right) c^2 dt^2 - \frac{dr^2}{\left(1 - 2n_r\right)} - \\ - r^2 \left(d\theta^2 + \sin^2\theta\, d\phi^2\right) \tag{7}$$

is the standard black-hole line element universally employed to interpret various astrophysical observations, where $2n_r = 1$ leads to the so-called Schwarzschild radius

$$R_s = \frac{2mc^2}{m_* c^2/r_*} = 2rn_r \tag{8}$$

the interior ($r < R_s$) of which is called the black hole. Within this black hole is the naked singularity at the coordinate radius $r = 0$ where the black-hole mass is assumed to reside—hiding this singularity is the event-horizon sphere with the Schwarzschild radius. It should be noted that this version is the same as the previous version with $n \to \infty$ except that there the coordinate radius is restricted to $r > r_*$ as $n_r < 1$. Equations (1) and (7) are functionally identical if one assumes that $R_n = r$, this being the assumption (for $n = 3$) that led to the standard version of the Schwarzschild equation.

The photon velocity calculated from (7) is the same as (6). That is, there is no energy propagation ($\beta = 0$) in the region $0.5 \leqslant n_r < 1$; so the standard Schwarzschild solution to the Einstein equation is not compatible with the assumed existence of the PV as a source for the visible universe, and thus must be discarded in the PV scenario.

Submitted on April 18, 2009 / Accepted on April 28, 2009

References

1. Daywitt W. C. The Planck vacuum. *Progress in Physics*, 2009, v. 1, 20.
2. Daywitt W. C. The source of the quantum vacuum. *Progress in Physics*, 2009, v. 1, 27.
3. Crothers S. J. On the general solution to Einstein's vacuum field and its implications for relativistic degeneracy. *Progress in Physics*, 2005, v. 1, 68.
4. Daywitt W. C. Limits to the validity of the Einstein field equations and General Relativity from the viewpoint of the negative-energy Planck vacuum state. *Progress in Physics*, 2009, v. 3, 27.
5. Schwarzschild K. Über das Gravitationsfeld eines Massenpunktes nach der Einsteinschen Theorie. *Sitzungsberichte der Königlich Preussischen Akademie der Wissenschaften*, 1916, 189–196 (published in English as: Schwarzschild K. On the gravitational field of a point mass according to Einstein's theory. *Abraham Zelmanov Journal*, 2008, v. 1, 10–19).
6. Carroll B. W., Ostlie D. A. An introduction to modern astrophysics. Addison-Wesley, San Francisco — Toronto, 2007.

Higgsless Glashow's and Quark-Gluon Theories and Gravity without Superstrings

Gunn Alex Quznetsov

Chelyabinsk State University, Chelyabinsk, Ural, Russia
E-mail: gunn@mail.ru, quznets@yahoo.com

This is the probabilistic explanation of some laws of physics (gravitation, red shift, electroweak, confinement, asymptotic freedom phenomenons).

1 Introduction

I do not construct any models because Physics does not need any strange hypotheses. Electroweak, quark-gluon, and gravity phenomenons are explained purely logically from spinor expression of probabilities:

Denote:

$$1_2 := \begin{bmatrix} 1 & 0 \\ 0 & 1 \end{bmatrix}, 0_2 := \begin{bmatrix} 0 & 0 \\ 0 & 0 \end{bmatrix},$$

$$\beta^{[0]} := -\begin{bmatrix} 1_2 & 0_2 \\ 0_2 & 1_2 \end{bmatrix} = -1_4,$$

the Pauli matrices:

$$\sigma_1 = \begin{bmatrix} 0 & 1 \\ 1 & 0 \end{bmatrix}, \sigma_2 = \begin{bmatrix} 0 & -\mathrm{i} \\ \mathrm{i} & 0 \end{bmatrix}, \sigma_3 = \begin{bmatrix} 1 & 0 \\ 0 & -1 \end{bmatrix}.$$

A set $\widetilde{C}$ of complex $n \times n$ matrices is called *a Clifford set of rank* n if the following conditions are fulfilled [1]:
if $\alpha_k \in \widetilde{C}$ and $\alpha_r \in \widetilde{C}$ then $\alpha_k\alpha_r + \alpha_r\alpha_k = 2\delta_{k,r}$;
if $\alpha_k\alpha_r + \alpha_r\alpha_k = 2\delta_{k,r}$ for all elements α_r of set $\widetilde{C}$ then $\alpha_k \in \widetilde{C}$.

If $n = 4$ then a Clifford set either contains 3 (*a Clifford triplet*) or 5 matrices (*a Clifford pentad*).

Here exist only six Clifford pentads [1]: one which I call *light pentad* β:

• *light pentad* β:

$$\beta^{[1]} := \begin{bmatrix} \sigma_1 & 0_2 \\ 0_2 & -\sigma_1 \end{bmatrix}, \quad \beta^{[2]} := \begin{bmatrix} \sigma_2 & 0_2 \\ 0_2 & -\sigma_2 \end{bmatrix}, \quad \beta^{[3]} := \begin{bmatrix} \sigma_3 & 0_2 \\ 0_2 & -\sigma_3 \end{bmatrix}, \tag{1}$$

$$\gamma^{[0]} := \begin{bmatrix} 0_2 & 1_2 \\ 1_2 & 0_2 \end{bmatrix}, \tag{2}$$

$$\beta^{[4]} := \mathrm{i} \cdot \begin{bmatrix} 0_2 & 1_2 \\ -1_2 & 0_2 \end{bmatrix}; \tag{3}$$

three *coloured* pentads:

• *the red pentad* ζ:

$$\zeta^{[1]} := \begin{bmatrix} -\sigma_1 & 0_2 \\ 0_2 & \sigma_1 \end{bmatrix}, \quad \zeta^{[2]} := \begin{bmatrix} \sigma_2 & 0_2 \\ 0_2 & \sigma_2 \end{bmatrix}, \quad \zeta^{[3]} := \begin{bmatrix} -\sigma_3 & 0_2 \\ 0_2 & -\sigma_3 \end{bmatrix},$$

$$\gamma_\zeta^{[0]} := \begin{bmatrix} 0_2 & -\sigma_1 \\ -\sigma_1 & 0_2 \end{bmatrix}, \zeta^{[4]} := \mathrm{i}\begin{bmatrix} 0_2 & \sigma_1 \\ -\sigma_1 & 0_2 \end{bmatrix}; \tag{4}$$

• *the green pentad* η:

$$\eta^{[1]} := \begin{bmatrix} -\sigma_1 & 0_2 \\ 0_2 & -\sigma_1 \end{bmatrix}, \quad \eta^{[2]} := \begin{bmatrix} -\sigma_2 & 0_2 \\ 0_2 & \sigma_2 \end{bmatrix}, \quad \eta^{[3]} := \begin{bmatrix} \sigma_3 & 0_2 \\ 0_2 & \sigma_3 \end{bmatrix},$$

$$\gamma_\eta^{[0]} := \begin{bmatrix} 0_2 & -\sigma_2 \\ -\sigma_2 & 0_2 \end{bmatrix}, \quad \eta^{[4]} := \mathrm{i}\begin{bmatrix} 0_2 & \sigma_2 \\ -\sigma_2 & 0_2 \end{bmatrix}; \tag{5}$$

• *the blue pentad* θ:

$$\theta^{[1]} := \begin{bmatrix} \sigma_1 & 0_2 \\ 0_2 & \sigma_1 \end{bmatrix}, \quad \theta^{[2]} := \begin{bmatrix} -\sigma_2 & 0_2 \\ 0_2 & -\sigma_2 \end{bmatrix}, \quad \theta^{[3]} := \begin{bmatrix} -\sigma_3 & 0_2 \\ 0_2 & \sigma_3 \end{bmatrix},$$

$$\gamma_\theta^{[0]} := \begin{bmatrix} 0_2 & -\sigma_3 \\ -\sigma_3 & 0_2 \end{bmatrix}, \quad \theta^{[4]} := \mathrm{i}\begin{bmatrix} 0_2 & \sigma_3 \\ -\sigma_3 & 0_2 \end{bmatrix}; \tag{6}$$

two *gustatory* pentads (about these pentads in detail, please, see in [2]):

• *the sweet pentad* $\underline{\Delta}$:

$$\underline{\Delta}^{[1]} := \begin{bmatrix} 0_2 & -\sigma_1 \\ -\sigma_1 & 0_2 \end{bmatrix}, \quad \underline{\Delta}^{[2]} := \begin{bmatrix} 0_2 & -\sigma_2 \\ -\sigma_2 & 0_2 \end{bmatrix}, \quad \underline{\Delta}^{[3]} := \begin{bmatrix} 0_2 & -\sigma_3 \\ -\sigma_3 & 0_2 \end{bmatrix},$$

$$\underline{\Delta}^{[0]} := \begin{bmatrix} -1_2 & 0_2 \\ 0_2 & 1_2 \end{bmatrix}, \quad \underline{\Delta}^{[4]} := \mathrm{i}\begin{bmatrix} 0_2 & 1_2 \\ -1_2 & 0_2 \end{bmatrix}.$$

• *the bitter pentad* $\underline{\Gamma}$:

$$\underline{\Gamma}^{[1]} := \mathrm{i}\begin{bmatrix} 0_2 & -\sigma_1 \\ \sigma_1 & 0_2 \end{bmatrix}, \quad \underline{\Gamma}^{[2]} := \mathrm{i}\begin{bmatrix} 0_2 & -\sigma_2 \\ \sigma_2 & 0_2 \end{bmatrix}, \quad \underline{\Gamma}^{[3]} := \mathrm{i}\begin{bmatrix} 0_2 & -\sigma_3 \\ \sigma_3 & 0_2 \end{bmatrix},$$

$$\underline{\Gamma}^{[0]} := \begin{bmatrix} -1_2 & 0_2 \\ 0_2 & 1_2 \end{bmatrix}, \quad \underline{\Gamma}^{[4]} := \begin{bmatrix} 0_2 & 1_2 \\ 1_2 & 0_2 \end{bmatrix}.$$

Denote: if A is a 2×2 matrix then

$$A1_4 := \left[\begin{array}{cc} A & 0_2 \\ 0_2 & A \end{array}\right] \text{ and } 1_4 A := \left[\begin{array}{cc} A & 0_2 \\ 0_2 & A \end{array}\right].$$

And if B is a 4×4 matrix then

$$A+B := A1_4 + B,\ AB := A1_4 B$$

etc.

$$\underline{x} := \langle x_0, \mathbf{x}\rangle := \langle x_0, x_1, x_2, x_3\rangle,$$
$$x_0 := ct,$$

with $\mathtt{c} = 299792458$.

2 Probabilities' movement equations

Let $\rho_{\mathtt{A}}(\underline{x})$ be a probability density [4] of a point event $\mathtt{A}(\underline{x})$. And let real functions

$$u_{\mathtt{A},1}(\underline{x}), u_{\mathtt{A},2}(\underline{x}), u_{\mathtt{A},3}(\underline{x})$$

satisfy conditions

$$u_{\mathtt{A},1}^2 + u_{\mathtt{A},2}^2 + u_{\mathtt{A},3}^2 < \mathtt{c}^2,$$

and if $j_{\mathtt{A},s} := \rho_{\mathtt{A}} u_{\mathtt{A},s}$ then

$$\rho_{\mathtt{A}} \to \rho'_{\mathtt{A}} = \frac{\rho_{\mathtt{A}} - \frac{v}{\mathtt{c}^2} j_{\mathtt{A},k}}{\sqrt{1-\left(\frac{v}{\mathtt{c}}\right)^2}},$$
$$j_{\mathtt{A},k} \to j'_{\mathtt{A},k} = \frac{j_{\mathtt{A},k} - v\rho_{\mathtt{A}}}{\sqrt{1-\left(\frac{v}{\mathtt{c}}\right)^2}},$$
$$j_{\mathtt{A},s} \to j'_{\mathtt{A},s} = j_{\mathtt{A},s} \text{ for } s \neq k$$

for $s \in \{1,2,3\}$ and $k \in \{1,2,3\}$ under the Lorentz transformations:

$$\begin{aligned} t &\to t' = \frac{t - \frac{v}{\mathtt{c}^2} x_k}{\sqrt{1-\frac{v^2}{\mathtt{c}^2}}}, \\ x_k &\to x'_k = \frac{x_k - vt}{\sqrt{1-\frac{v^2}{\mathtt{c}^2}}}, \\ x_s &\to x'_s = x_s, \text{ if } s \neq k. \end{aligned}$$

In that case $\mathbf{u}_{\mathtt{A}}\langle u_{\mathtt{A},1}, u_{\mathtt{A},2}, u_{\mathtt{A},3}\rangle$ is called *a vector of local velocity* of an event $\mathtt{A}$ *probability propagation* and

$$\mathbf{j}_{\mathtt{A}}\langle j_{\mathtt{A},1}, j_{\mathtt{A},2}, j_{\mathtt{A},3}\rangle$$

is called *a current vector* of an event $\mathtt{A}$ probability.

Let us consider the following set of four real equations with eight real unknowns:

$$b^2 \text{ with } b>0, \alpha, \beta, \chi, \theta, \gamma, \upsilon, \lambda:$$

$$\left.\begin{array}{l} b^2 = \rho_{\mathtt{A}} \\ b^2\left(\begin{array}{c}\cos^2(\alpha)\sin(2\beta)\cos(\theta-\gamma)\\ -\sin^2(\alpha)\sin(2\chi)\cos(\upsilon-\lambda)\end{array}\right) = -\frac{j_{\mathtt{A},1}}{\mathtt{c}} \\ b^2\left(\begin{array}{c}\cos^2(\alpha)\sin(2\beta)\sin(\theta-\gamma)\\ -\sin^2(\alpha)\sin(2\chi)\sin(\upsilon-\lambda)\end{array}\right) = -\frac{j_{\mathtt{A},2}}{\mathtt{c}} \\ b^2\left(\begin{array}{c}\cos^2(\alpha)\cos(2\beta)\\ -\sin^2(\alpha)\cos(2\chi)\end{array}\right) = -\frac{j_{\mathtt{A},3}}{\mathtt{c}} \end{array}\right\}. \quad (7)$$

This set has solutions for any $\rho_{\mathtt{A}}$ and $j_{\mathtt{A},k}$. For example, one of these solutions is placed in [4].

If

$$\begin{aligned} \varphi_1 &:= b\cdot\exp(\mathrm{i}\gamma)\cos(\beta)\cos(\alpha), \\ \varphi_2 &:= b\cdot\exp(\mathrm{i}\theta)\sin(\beta)\cos(\alpha), \\ \varphi_3 &:= b\cdot\exp(\mathrm{i}\lambda)\cos(\chi)\sin(\alpha), \\ \varphi_4 &:= b\cdot\exp(\mathrm{i}\upsilon)\sin(\chi)\sin(\alpha) \end{aligned} \quad (8)$$

then

$$\begin{aligned} \rho_{\mathtt{A}} &= \sum_{s=1}^{4} \varphi_s^* \varphi_s, \\ \frac{j_{\mathtt{A},r}}{\mathtt{c}} &= -\sum_{k=1}^{4}\sum_{s=1}^{4} \varphi_s^* \beta_{s,k}^{[r]} \varphi_k \end{aligned} \quad (9)$$

with $r \in \{1,2,3\}$. These functions φ_s are called *functions of event* $\mathtt{A}$ *state*.

If $\rho_{\mathtt{A}}(\underline{x}) = 0$ for all $\underline{x}$ such that $|\underline{x}| > (\pi\mathtt{c}/\mathtt{h})$ with $\mathtt{h} := 6.6260755\cdot 10^{-34}$ then $\varphi_s(\underline{x})$ are Planck's functions [3]. And if

$$\varphi := \left[\begin{array}{c}\varphi_1\\ \varphi_2\\ \varphi_3\\ \varphi_4\end{array}\right]$$

then these functions obey [5] the following equation:

$$\begin{aligned} &\sum_{k=0}^{3} \beta^{[k]}\left(\partial_k + \mathrm{i}\Theta_k + \mathrm{i}\Upsilon_k \gamma^{[5]}\right)\varphi + \\ &+\left(\begin{array}{c} +\mathrm{i}M_0\gamma^{[0]} + \mathrm{i}M_4\beta^{[4]} - \\ -\mathrm{i}M_{\zeta,0}\gamma_\zeta^{[0]} + \mathrm{i}M_{\zeta,4}\zeta^{[4]} - \\ -\mathrm{i}M_{\eta,0}\gamma_\eta^{[0]} - \mathrm{i}M_{\eta,4}\eta^{[4]} + \\ +\mathrm{i}M_{\theta,0}\gamma_\theta^{[0]} + \mathrm{i}M_{\theta,4}\theta^{[4]} \end{array}\right)\varphi = 0 \end{aligned} \quad (10)$$

with real $\Theta_k(\underline{x})$, $\Upsilon_k(\underline{x})$, $M_0(\underline{x})$, $M_4(\underline{x})$, $M_{\zeta,0}(\underline{x})$, $M_{\zeta,4}(\underline{x})$, $M_{\eta,0}(\underline{x})$, $M_{\eta,4}(\underline{x})$, $M_{\theta,0}(\underline{x})$, $M_{\theta,4}(\underline{x})$ and with

$$\gamma^{[5]} := \left[\begin{array}{cc} 1_2 & 0_2 \\ 0_2 & -1_2 \end{array}\right]. \quad (11)$$

2.1 Lepton movement equation

If $M_{\zeta,0}(\underline{x}) = 0$, $M_{\zeta,4}(\underline{x}) = 0$, $M_{\eta,0}(\underline{x}) = 0$, $M_{\eta,4}(\underline{x}) = 0$, $M_{\theta,0}(\underline{x}) = 0$, $M_{\theta,4}(\underline{x}) = 0$ then the following equation is deduced from (10):

$$\left(\begin{array}{c} \beta^{[0]} \left(\frac{1}{c} i\partial_t - \Theta_0 - \Upsilon_0 \gamma^{[5]} \right) \\ + \sum\limits_{\alpha=1}^{3} \beta^{[\alpha]} \left(i\partial_\alpha - \Theta_\alpha - \Upsilon_\alpha \gamma^{[5]} \right) \\ - M_0 \gamma^{[0]} - M_4 \beta^{[4]} \end{array} \right) \widetilde{\varphi} = 0 \qquad (12)$$

I call it *lepton movement equation* [6].

If similar to (9):

$$j_{\mathcal{A},5} := -c \cdot \varphi^{\dagger} \gamma^{[0]} \varphi \text{ and } j_{\mathcal{A},4} := -c \cdot \varphi^{\dagger} \beta^{[4]} \varphi$$

and:

$$u_{\mathcal{A},4} := j_{\mathcal{A},4} / \rho_{\mathcal{A}} \text{ and } u_{\mathcal{A},5} := j_{\mathcal{A},5} / \rho_{\mathcal{A}} \qquad (13)$$

then from (8):

$$-\frac{u_{\mathcal{A},5}}{c} = \sin 2\alpha \left(\begin{array}{c} \sin\beta \sin\chi \cos(-\theta + \upsilon) \\ + \cos\beta \cos\chi \cos(\gamma - \lambda) \end{array} \right),$$

$$-\frac{u_{\mathcal{A},4}}{c} = \sin 2\alpha \left(\begin{array}{c} -\sin\beta \sin\chi \sin(-\theta + \upsilon) \\ + \cos\beta \cos\chi \sin(\gamma - \lambda) \end{array} \right).$$

Hence from (7):

$$u_{\mathcal{A},1}^2 + u_{\mathcal{A},2}^2 + u_{\mathcal{A},3}^2 + u_{\mathcal{A},4}^2 + u_{\mathcal{A},5}^2 = c^2.$$

Thus only all five elements of a Clifford pentad provide an entire set of speed components and, for completeness, yet two "space" coordinates x_5 and x_4 should be added to our three x_1, x_2, x_3. These additional coordinates can be selected so that

$$-\frac{\pi c}{h} \leqslant x_5 \leqslant \frac{\pi c}{h}, \quad -\frac{\pi c}{h} \leqslant x_4 \leqslant \frac{\pi c}{h}.$$

Coordinates x_4 and x_5 are not coordinates of any events. Hence, our devices do not detect them as actual space coordinates.

Let us denote:

$$\widetilde{\varphi}(t, x_1, x_2, x_3, x_5, x_4) := \varphi(t, x_1, x_2, x_3) \times$$
$$\times \left(\exp\left(i \left(x_5 M_0(t, x_1, x_2, x_3) + x_4 M_4(t, x_1, x_2, x_3) \right) \right) \right).$$

In this case a lepton movement equation (12) shape is the following:

$$\left(\sum_{s=0}^{3} \beta^{[s]} \left(i\partial_s - \Theta_s - \Upsilon_s \gamma^{[5]} \right) - \gamma^{[0]} i\partial_5 - \beta^{[4]} i\partial_4 \right) \widetilde{\varphi} = 0$$

This equation can be transformated into the following form [7]:

$$\left(\begin{array}{c} \sum_{s=0}^{3} \beta^{[s]} \left(i\partial_s + F_s + 0.5 g_1 Y B_s \right) \\ -\gamma^{[0]} i\partial_5 - \beta^{[4]} i\partial_4 \end{array} \right) \widetilde{\varphi} = 0 \qquad (14)$$

with real F_s, B_s, a real positive constant g_1, and with *charge matrix* Y:

$$Y := -\left[\begin{array}{cc} 1_2 & 0_2 \\ 0_2 & 2 \cdot 1_2 \end{array} \right]. \qquad (15)$$

If $\chi(t, x_1, x_2, x_3)$ is a real function and:

$$\widetilde{U}(\chi) := \left[\begin{array}{cc} \exp\left(i\frac{\chi}{2} \right) 1_2 & 0_2 \\ 0_2 & \exp(i\chi)\, 1_2 \end{array} \right]. \qquad (16)$$

then equation (14) is invariant under the following transformations [8]:

$$\begin{array}{l} x_4 \to x_4' := x_4 \cos\frac{\chi}{2} - x_5 \sin\frac{\chi}{2}; \\ x_5 \to x_5' := x_5 \cos\frac{\chi}{2} + x_4 \sin\frac{\chi}{2}; \\ x_\mu \to x_\mu' := x_\mu \text{ for } \mu \in \{0, 1, 2, 3\}; \\ \widetilde{\varphi} \to \widetilde{\varphi}' := \widetilde{U} \widetilde{\varphi}, \\ B_\mu \to B_\mu' := B_\mu - \frac{1}{g_1} \partial_\mu \chi, \\ F_\mu \to F_\mu' := \widetilde{U} F_s \widetilde{U}^{\dagger}. \end{array} \qquad (17)$$

Therefore, B_μ are similar to components of the Standard Model gauge field B.

Further $\Im_{\mathbf{J}}$ is the space spanned by the following basis [9]:

$$\mathbf{J} := \left\langle \begin{array}{c} \frac{h}{2\pi c} \exp\left(-i\frac{h}{c}(s_0 x_4) \right) \epsilon_k, \ldots \\ \frac{h}{2\pi c} \exp\left(-i\frac{h}{c}(n_0 x_5) \right) \epsilon_r, \ldots \end{array} \right\rangle \qquad (18)$$

with some integer numbers s_0 and n_0 and with

$$\epsilon_1 := \left[\begin{array}{c} 1 \\ 0 \\ 0 \\ 0 \end{array} \right], \ \epsilon_2 := \left[\begin{array}{c} 0 \\ 1 \\ 0 \\ 0 \end{array} \right], \ \epsilon_3 := \left[\begin{array}{c} 0 \\ 0 \\ 1 \\ 0 \end{array} \right], \ \epsilon_4 := \left[\begin{array}{c} 0 \\ 0 \\ 0 \\ 1 \end{array} \right].$$

Further in this subsection U is any linear transformation of space $\Im_{\mathbf{J}}$ so that for every $\widetilde{\varphi}$: if $\widetilde{\varphi} \in \Im_{\mathbf{J}}$ then:

$$\begin{array}{c} \int\limits_{-\frac{\pi c}{h}}^{\frac{\pi c}{h}} dx_4 \int\limits_{-\frac{\pi c}{h}}^{\frac{\pi c}{h}} dx_5 \cdot (U\widetilde{\varphi})^{\dagger} (U\widetilde{\varphi}) = \rho_{\mathrm{A}}, \\ \int\limits_{-\frac{\pi c}{h}}^{\frac{\pi c}{h}} dx_4 \int\limits_{-\frac{\pi c}{h}}^{\frac{\pi c}{h}} dx_5 \cdot (U\widetilde{\varphi})^{\dagger} \beta^{[s]} (U\widetilde{\varphi}) = -\frac{j_{\mathrm{A},s}}{c} \end{array} \qquad (19)$$

for $s \in \{1, 2, 3\}$.

Matrix U is factorized as the following:

$$U = \exp(i\varsigma)\, \widetilde{U} U^{(-)} U^{(+)}$$

with real ς, with $\widetilde{U}$ from (16), and with

$$U^{(+)} := \begin{bmatrix} 1_2 & 0_2 & 0_2 & 0_2 \\ 0_2 & (u+iv)\,1_2 & 0_2 & (k+is)\,1_2 \\ 0_2 & 0_2 & 1_2 & 0_2 \\ 0_2 & (-k+is)\,1_2 & 0_2 & (u-iv)\,1_2 \end{bmatrix} \quad (20)$$

and

$$U^{(-)} := \begin{bmatrix} (a+ib)\,1_2 & 0_2 & (c+iq)\,1_2 & 0_2 \\ 0_2 & 1_2 & 0_2 & 0_2 \\ (-c+iq)\,1_2 & 0_2 & (a-ib)\,1_2 & 0_2 \\ 0_2 & 0_2 & 0_2 & 1_2 \end{bmatrix} \quad (21)$$

with real a, b, c, q, u, v, k, s.

Matrix $U^{(+)}$ refers to antiparticles (About antiparticles in detail, please, see [10] and about neutrinos - [11]). And transformation $U^{(-)}$ reduces equation (14) to the following shape:

$$\left(\begin{array}{c} \sum_{\mu=0}^{3} \beta^{[\mu]} i \begin{pmatrix} \partial_\mu - i0.5 g_1 B_\mu Y \\ -i\frac{1}{2} g_2 W_\mu - iF_\mu \end{pmatrix} \\ +\gamma^{[0]} i\partial_5 + \beta^{[4]} i\partial_4 \end{array} \right) \widetilde{\varphi} = 0. \quad (22)$$

with a real positive constant g_2 and with

$$W_\mu := \begin{bmatrix} W_{0,\mu}\,1_2 & 0_2 & (W_{1,\mu} - iW_{2,\mu})\,1_2 & 0_2 \\ 0_2 & 0_2 & 0_2 & 0_2 \\ (W_{1,\mu} + iW_{2,\mu})\,1_2 & 0_2 & -W_{0,\mu}\,1_2 & 0_2 \\ 0_2 & 0_2 & 0_2 & 0_2 \end{bmatrix}$$

with real $W_{0,\mu}$, $W_{1,\mu}$ and $W_{2,\mu}$.

Equation (22) is invariant under the following transformation:

$$\varphi \to \varphi' := U\varphi,$$
$$x_4 \to x'_4 := (\ell_\circ + \ell_*)\, a x_4 + (\ell_\circ - \ell_*)\, \sqrt{1-a^2}\, x_5,$$
$$x_5 \to x'_5 := (\ell_\circ + \ell_*)\, a x_5 - (\ell_\circ - \ell_*)\, \sqrt{1-a^2}\, x_4,$$
$$x_\mu \to x'_\mu := x_\mu, \text{ for } \mu \in \{0,1,2,3\},$$
$$B_\mu \to B'_\mu := B_\mu,$$
$$W_\mu \to W'_\mu := U W_\mu U^\dagger - \frac{2i}{g_2} (\partial_\mu U)\, U^\dagger$$

with

$$\ell_\circ := \frac{1}{2\sqrt{(1-a^2)}} \times$$
$$\times \begin{bmatrix} \left(b + \sqrt{(1-a^2)}\right) 1_4 & (q - ic)\,1_4 \\ (q + ic)\,1_4 & \left(\sqrt{(1-a^2)} - b\right) 1_4 \end{bmatrix},$$
$$\ell_* := \frac{1}{2\sqrt{(1-a^2)}} \times$$
$$\times \begin{bmatrix} \left(\sqrt{(1-a^2)} - b\right) 1_4 & (-q + ic)\,1_4 \\ (-q - ic)\,1_4 & \left(b + \sqrt{(1-a^2)}\right) 1_4 \end{bmatrix}.$$

Hence W_μ behaves the same way as components of the weak field W of Standard Model.

Field $W_{0,\mu}$ obeys the following equation [12]:

$$\left(-\frac{1}{c^2}\,\partial_t^2 + \sum_{s=1}^{3} \partial_s^2 \right) W_{0,\mu} =$$
$$= g_2^2 \left(\widetilde{W}_0^2 - \widetilde{W}_1^2 - \widetilde{W}_2^2 - \widetilde{W}_3^2 \right) W_{0,\mu} + \Lambda \quad (23)$$

with

$$\widetilde{W}_\nu := \begin{bmatrix} W_{0,\nu} \\ W_{1,\nu} \\ W_{2,\nu} \end{bmatrix}$$

and Λ is the action of other components of field W on $W_{0,\mu}$.

Equation (23) looks like the Klein-Gordon equation of field $W_{0,\mu}$ with mass

$$m := \frac{h}{c}\, g_2 \sqrt{\widetilde{W}_0^2 - \sum_{s=1}^{3} \widetilde{W}_s^2} \quad (24)$$

and with additional terms of the $W_{0,\mu}$ interactions with other components of $\widetilde{W}$. Fields $W_{1,\mu}$ and $W_{2,\mu}$ have similar equations.

The "mass" (24) is invariant under the Lorentz transformations

$$\widetilde{W}'_0 := \frac{\widetilde{W}_0 - \frac{v}{c}\widetilde{W}_k}{\sqrt{1 - \left(\frac{v}{c}\right)^2}}, \quad \widetilde{W}'_k := \frac{\widetilde{W}_k - \frac{v}{c}\widetilde{W}_0}{\sqrt{1 - \left(\frac{v}{c}\right)^2}},$$

$$\widetilde{W}'_s := \widetilde{W}_s, \text{ if } s \neq k,$$

is invariant under the turns of the $\left\langle \widetilde{W}_1, \widetilde{W}_2, \widetilde{W}_3 \right\rangle$ space

$$\left\{ \begin{array}{l} \widetilde{W}'_r := \widetilde{W}_r \cos\lambda - \widetilde{W}_s \sin\lambda \\ \widetilde{W}'_s := \widetilde{W}_r \sin\lambda + \widetilde{W}_s \cos\lambda \end{array} \right.$$

and invariant under a global weak isospin transformation $U^{(-)}$:

$$W_\nu \to W'_\nu := U^{(-)} W_\nu U^{(-)\dagger},$$

but is not invariant for a local transformation $U^{(-)}$. But local transformations for $W_{0,\mu}$, $W_{1,\mu}$ and $W_{2,\mu}$ are insignificant since all three particles are very short-lived.

The form (24) can vary in space, but locally acts like mass - i.e. it does not allow particles of this field to behave the same way as massless ones.

If

$$Z_\mu := (W_{0,\mu} \cos\alpha - B_\mu \sin\alpha),$$
$$A_\mu := (B_\mu \cos\alpha + W_{0,\mu} \sin\alpha)$$

with

$$\alpha := \arctan \frac{g_1}{g_2}$$

then masses of Z and W fulfill the following ratio:

$$m_Z = \frac{m_W}{\cos\alpha}\,.$$

If

$$\mathrm{e} := \frac{g_1 g_2}{\sqrt{g_1^2 + g_2^2}}\,,$$

and

$$\widehat{Z}_\mu := Z_\mu \frac{1}{\sqrt{g_2^2 + g_1^2}} \times$$

$$\times \begin{bmatrix} \left(g_2^2 + g_1^2\right) 1_2 & 0_2 & 0_2 & 0_2 \\ 0_2 & 2g_1^2 1_2 & 0_2 & 0_2 \\ 0_2 & 0_2 & \left(g_2^2 - g_1^2\right) 1_2 & 0_2 \\ 0_2 & 0_2 & 0_2 & 2g_1^2 1_2 \end{bmatrix},$$

$$\widehat{W}_\mu := g_2 \times$$

$$\times \begin{bmatrix} 0_2 & 0_2 & \left(W_{1,\mu} - \mathrm{i}W_{2,\mu}\right) 1_2 & 0_2 \\ 0_2 & 0_2 & 0_2 & 0_2 \\ \left(W_{1,\mu} + \mathrm{i}W_{2,\mu}\right) 1_2 & 0_2 & 0_2 & 0_2 \\ 0_2 & 0_2 & 0_2 & 0_2 \end{bmatrix},$$

$$\widehat{A}_\mu := A_\mu \begin{bmatrix} 0_2 & 0_2 & 0_2 & 0_2 \\ 0_2 & 1_2 & 0_2 & 0_2 \\ 0_2 & 0_2 & 1_2 & 0_2 \\ 0_2 & 0_2 & 0_2 & 1_2 \end{bmatrix}.$$

then equation (22) has the following form:

$$\begin{pmatrix} \sum_{\mu=0}^{3} \beta^{[\mu]} \mathrm{i} \begin{pmatrix} \partial_\mu + \mathrm{i}\mathrm{e}\widehat{A}_\mu \\ -\mathrm{i}0.5\left(\widehat{Z}_\mu + \widehat{W}_\mu\right) \end{pmatrix} \\ +\gamma^{[0]}\mathrm{i}\partial_5 + \beta^{[4]}\mathrm{i}\partial_4 \end{pmatrix} \widetilde{\varphi} = 0. \quad (25)$$

Here [13] the vector field A_μ is similar to *the electromagnetic potential* and $\left(\widehat{Z}_\mu + \widehat{W}_\mu\right)$ is similar to *the weak potential*.

2.2 Colored equations

The following part of (10) I call *colored movement equation* [3]:

$$\begin{pmatrix} \sum_{k=0}^{3} \beta^{[k]} \left(-\mathrm{i}\partial_k + \Theta_k + \Upsilon_k \gamma^{[5]}\right) - \\ -M_{\zeta,0}\gamma_\zeta^{[0]} + M_{\zeta,4}\zeta^{[4]} + \\ -M_{\eta,0}\gamma_\eta^{[0]} - M_{\eta,4}\eta^{[4]} + \\ +M_{\theta,0}\gamma_\theta^{[0]} + M_{\theta,4}\theta^{[4]} \end{pmatrix} \varphi = 0. \quad (26)$$

Here (4), (5), (6):

$$\gamma_\zeta^{[0]} = -\begin{bmatrix} 0 & 0 & 0 & 1 \\ 0 & 0 & 1 & 0 \\ 0 & 1 & 0 & 0 \\ 1 & 0 & 0 & 0 \end{bmatrix}, \quad \zeta^{[4]} = \begin{bmatrix} 0 & 0 & 0 & \mathrm{i} \\ 0 & 0 & \mathrm{i} & 0 \\ 0 & -\mathrm{i} & 0 & 0 \\ -\mathrm{i} & 0 & 0 & 0 \end{bmatrix}$$

are mass elements of red pentad;

$$\gamma_\eta^{[0]} = \begin{bmatrix} 0 & 0 & 0 & \mathrm{i} \\ 0 & 0 & -\mathrm{i} & 0 \\ 0 & \mathrm{i} & 0 & 0 \\ -\mathrm{i} & 0 & 0 & 0 \end{bmatrix}, \quad \eta^{[4]} = \begin{bmatrix} 0 & 0 & 0 & 1 \\ 0 & 0 & -1 & 0 \\ 0 & -1 & 0 & 0 \\ 1 & 0 & 0 & 0 \end{bmatrix}$$

are mass elements of green pentad;

$$\gamma_\theta^{[0]} = \begin{bmatrix} 0 & 0 & -1 & 0 \\ 0 & 0 & 0 & 1 \\ -1 & 0 & 0 & 0 \\ 0 & 1 & 0 & 0 \end{bmatrix}, \quad \theta^{[4]} = \begin{bmatrix} 0 & 0 & -\mathrm{i} & 0 \\ 0 & 0 & 0 & \mathrm{i} \\ -\mathrm{i} & 0 & 0 & 0 \\ 0 & \mathrm{i} & 0 & 0 \end{bmatrix}$$

are mass elements of blue pentad.

I call:

- $M_{\zeta,0}$, $M_{\zeta,4}$ *red lower and upper mass members*;
- $M_{\eta,0}$, $M_{\eta,4}$ *green lower and upper mass members*;
- $M_{\theta,0}$, $M_{\theta,4}$ *blue lower and upper mass members*.

The mass members of this equation form the following matrix sum:

$$\widehat{M} := \begin{pmatrix} -M_{\zeta,0}\gamma_\zeta^{[0]} + M_{\zeta,4}\zeta^{[4]} - \\ -M_{\eta,0}\gamma_\eta^{[0]} - M_{\eta,4}\eta^{[4]} + \\ +M_{\theta,0}\gamma_\theta^{[0]} + M_{\theta,4}\theta^{[4]} \end{pmatrix} =$$

$$= \begin{bmatrix} 0 & 0 & -M_{\theta,0} & M_{\zeta,\eta,0} \\ 0 & 0 & M^*_{\zeta,\eta,0} & M_{\theta,0} \\ -M_{\theta,0} & M_{\zeta,\eta,0} & 0 & 0 \\ M^*_{\zeta,\eta,0} & M_{\theta,0} & 0 & 0 \end{bmatrix} +$$

$$+\mathrm{i}\begin{bmatrix} 0 & 0 & -M_{\theta,4} & M^*_{\zeta,\eta,4} \\ 0 & 0 & M_{\zeta,\eta,4} & M_{\theta,4} \\ -M_{\theta,4} & -M^*_{\zeta,\eta,4} & 0 & 0 \\ -M_{\zeta,\eta,4} & M_{\theta,4} & 0 & 0 \end{bmatrix}$$

with $M_{\zeta,\eta,0} := M_{\zeta,0} - \mathrm{i}M_{\eta,0}$ and $M_{\zeta,\eta,4} := M_{\zeta,4} - \mathrm{i}M_{\eta,4}$.

Elements of these matrices can be turned by formula of shape [14]:

$$\begin{pmatrix} \cos\frac{\theta}{2} & \mathrm{i}\sin\frac{\theta}{2} \\ \mathrm{i}\sin\frac{\theta}{2} & \cos\frac{\theta}{2} \end{pmatrix} \begin{pmatrix} Z & X - \mathrm{i}Y \\ X + \mathrm{i}Y & -Z \end{pmatrix} \times$$

$$\times \begin{pmatrix} \cos\frac{\theta}{2} & -\mathrm{i}\sin\frac{\theta}{2} \\ -\mathrm{i}\sin\frac{\theta}{2} & \cos\frac{\theta}{2} \end{pmatrix} =$$

$$= \begin{pmatrix} Z\cos\theta - Y\sin\theta & X - \mathrm{i}\begin{pmatrix} Y\cos\theta \\ +Z\sin\theta \end{pmatrix} \\ X + \mathrm{i}\begin{pmatrix} Y\cos\theta \\ +Z\sin\theta \end{pmatrix} & -Z\cos\theta + Y\sin\theta \end{pmatrix}.$$

Hence, if:

$$U_{2,3}(\alpha) := \begin{bmatrix} \cos\alpha & \mathrm{i}\sin\alpha & 0 & 0 \\ \mathrm{i}\sin\alpha & \cos\alpha & 0 & 0 \\ 0 & 0 & \cos\alpha & \mathrm{i}\sin\alpha \\ 0 & 0 & \mathrm{i}\sin\alpha & \cos\alpha \end{bmatrix}$$

and

$$\widehat{M}' := \begin{pmatrix} -M'_{\zeta,0}\gamma^{[0]}_{\zeta} + M'_{\zeta,4}\zeta^{[4]} - \\ -M'_{\eta,0}\gamma^{[0]}_{\eta} - M'_{\eta,4}\eta^{[4]} + \\ +M'_{\theta,0}\gamma^{[0]}_{\theta} + M'_{\theta,4}\theta^{[4]} \end{pmatrix} := U^{-1}_{2,3}(\alpha)\,\widehat{M}U_{2,3}(\alpha)$$

then

$$\begin{aligned} M'_{\zeta,0} &= M_{\zeta,0}\,,\\ M'_{\eta,0} &= M_{\eta,0}\cos 2\alpha + M_{\theta,0}\sin 2\alpha\,,\\ M'_{\theta,0} &= M_{\theta,0}\cos 2\alpha - M_{\eta,0}\sin 2\alpha\,,\\ M'_{\zeta,4} &= M_{\zeta,4}\,,\\ M'_{\eta,4} &= M_{\eta,4}\cos 2\alpha + M_{\theta,4}\sin 2\alpha\,,\\ M'_{\theta,4} &= M_{\theta,4}\cos 2\alpha - M_{\eta,4}\sin 2\alpha\,. \end{aligned}$$

Therefore, matrix $U_{2,3}(\alpha)$ makes an oscillation between green and blue colours.

If α is an arbitrary real function of time-space variables ($\alpha = \alpha(t, x_1, x_2, x_3)$) then the following expression is received from equation (10) under transformation $U_{2,3}(\alpha)$ [3]:

$$\left(\frac{1}{\mathrm{c}}\partial_t + U^{-1}_{2,3}(\alpha)\,\frac{1}{\mathrm{c}}\,\partial_t U_{2,3}(\alpha) + \mathrm{i}\Theta_0 + \mathrm{i}\Upsilon_0\gamma^{[5]}\right)\varphi =$$

$$= \begin{pmatrix} \beta^{[1]}\begin{pmatrix} \partial_1 + U^{-1}_{2,3}(\alpha)\,\partial_1 U_{2,3}(\alpha) \\ +\mathrm{i}\Theta_1 + \mathrm{i}\Upsilon_1\gamma^{[5]} \end{pmatrix} \\ +\beta^{[2]}\begin{pmatrix} \partial'_2 + U^{-1}_{2,3}(\alpha)\,\partial'_2 U_{2,3}(\alpha) \\ +\mathrm{i}\Theta'_2 + \mathrm{i}\Upsilon'_2\gamma^{[5]} \end{pmatrix} \\ +\beta^{[3]}\begin{pmatrix} \partial'_3 + U^{-1}_{2,3}(\alpha)\,\partial'_3 U_{2,3}(\alpha) \\ +\mathrm{i}\Theta'_3 + \mathrm{i}\Upsilon'_3\gamma^{[5]} \end{pmatrix} \\ +\mathrm{i}M_0\gamma^{[0]} + \mathrm{i}M_4\beta^{[4]} + \widehat{M}' \end{pmatrix}\varphi\,.$$

Here

$$\begin{aligned} \Theta'_2 &:= \Theta_2\cos 2\alpha - \Theta_3\sin 2\alpha\,,\\ \Theta'_3 &:= \Theta_2\sin 2\alpha + \Theta_3\cos 2\alpha\,,\\ \Upsilon'_2 &:= \Upsilon_2\cos 2\alpha - \Upsilon_3\sin 2\alpha\,,\\ \Upsilon'_3 &:= \Upsilon_3\cos 2\alpha + \Upsilon_2\sin 2\alpha\,, \end{aligned}$$

and x'_2 and x'_3 are elements of an another coordinate system so that:

$$\begin{aligned} \frac{\partial x_2}{\partial x'_2} &= \cos 2\alpha\,,\\ \frac{\partial x_3}{\partial x'_2} &= -\sin 2\alpha\,,\\ \frac{\partial x_2}{\partial x'_3} &= \sin 2\alpha\,,\\ \frac{\partial x_3}{\partial x'_3} &= \cos 2\alpha\,,\\ \frac{\partial x_0}{\partial x'_2} &= \frac{\partial x_1}{\partial x'_2} = \frac{\partial x_0}{\partial x'_3} = \frac{\partial x_1}{\partial x'_3} = 0\,. \end{aligned}$$

Therefore, the oscillation between blue and green colours curves the space in the x_2, x_3 directions.

Similarly, matrix

$$U_{1,3}(\vartheta) := \begin{bmatrix} \cos\vartheta & \sin\vartheta & 0 & 0 \\ -\sin\vartheta & \cos\vartheta & 0 & 0 \\ 0 & 0 & \cos\vartheta & \sin\vartheta \\ 0 & 0 & -\sin\vartheta & \cos\vartheta \end{bmatrix}$$

with an arbitrary real function $\vartheta(t, x_1, x_2, x_3)$ describes the oscillation between blue and red colours which curves the space in the x_1, x_3 directions. And matrix

$$U_{1,2}(\varsigma) := \begin{bmatrix} e^{-\mathrm{i}\varsigma} & 0 & 0 & 0 \\ 0 & e^{\mathrm{i}\varsigma} & 0 & 0 \\ 0 & 0 & e^{-\mathrm{i}\varsigma} & 0 \\ 0 & 0 & 0 & e^{\mathrm{i}\varsigma} \end{bmatrix}$$

with an arbitrary real function $\varsigma(t, x_1, x_2, x_3)$ describes the oscillation between green and red colours which curves the space in the x_1, x_2 directions.

Now, let

$$U_{0,1}(\sigma) := \begin{bmatrix} \cosh\sigma & -\sinh\sigma & 0 & 0 \\ -\sinh\sigma & \cosh\sigma & 0 & 0 \\ 0 & 0 & \cosh\sigma & \sinh\sigma \\ 0 & 0 & \sinh\sigma & \cosh\sigma \end{bmatrix}.$$

and

$$\widehat{M}'' := \begin{pmatrix} -M''_{\zeta,0}\gamma^{[0]}_{\zeta} + M''_{\zeta,4}\zeta^{[4]} - \\ -M''_{\eta,0}\gamma^{[0]}_{\eta} - M''_{\eta,4}\eta^{[4]} + \\ +M''_{\theta,0}\gamma^{[0]}_{\theta} + M''_{\theta,4}\theta^{[4]} \end{pmatrix} := U^{-1}_{0,1}(\sigma)\,\widehat{M}U_{0,1}(\sigma)$$

then:

$$\begin{aligned} M''_{\zeta,0} &= M_{\zeta,0}\,,\\ M''_{\eta,0} &= \left(M_{\eta,0}\cosh 2\sigma - M_{\theta,4}\sinh 2\sigma\right)\,,\\ M''_{\theta,0} &= M_{\theta,0}\cosh 2\sigma + M_{\eta,4}\sinh 2\sigma\,,\\ M''_{\zeta,4} &= M_{\zeta,4}\,,\\ M''_{\eta,4} &= M_{\eta,4}\cosh 2\sigma + M_{\theta,0}\sinh 2\sigma\,,\\ M''_{\theta,4} &= M_{\theta,4}\cosh 2\sigma - M_{\eta,0}\sinh 2\sigma\,. \end{aligned}$$

Therefore, matrix $U_{0,1}(\sigma)$ makes an oscillation between green and blue colours with an oscillation between upper and lower mass members.

If σ is an arbitrary real function of time-space variables ($\sigma = \sigma(t, x_1, x_2, x_3)$) then the following expression is received from equation (10) under transformation $U_{0,1}(\sigma)$ [3]:

$$\left(\begin{array}{l} \beta^{[0]} \left(\begin{array}{l} \frac{1}{\mathrm{c}} \partial'_t + U^{-1}_{0,1}(\sigma) \frac{1}{\mathrm{c}} \partial'_t U_{0,1}(\sigma) \\ + \mathrm{i}\Theta''_0 + \mathrm{i}\Upsilon''_0 \gamma^{[5]} \end{array} \right) \\ + \beta^{[1]} \left(\begin{array}{l} \partial'_1 + U^{-1}_{0,1}(\sigma) \partial'_1 U_{0,1}(\sigma) \\ + \mathrm{i}\Theta''_1 + \mathrm{i}\Upsilon''_1 \gamma^{[5]} \end{array} \right) \\ + \beta^{[2]} \left(\begin{array}{l} \partial_2 + U^{-1}_{0,1}(\sigma) \partial_2 U_{0,1}(\sigma) \\ + \mathrm{i}\Theta_2 + \mathrm{i}\Upsilon_2 \gamma^{[5]} \end{array} \right) \\ + \beta^{[3]} \left(\begin{array}{l} \partial_3 + U^{-1}_{0,1}(\sigma) \partial_3 U_{0,1}(\sigma) \\ + \mathrm{i}\Theta_3 + \mathrm{i}\Upsilon_3 \gamma^{[5]} \end{array} \right) \\ + \mathrm{i}M_0 \gamma^{[0]} + \mathrm{i}M_4 \beta^{[4]} + \widehat{M}'' \end{array} \right) \varphi = 0$$

with

$$\begin{aligned} \Theta''_0 &:= \Theta_0 \cosh 2\sigma + \Theta_1 \sinh 2\sigma , \\ \Theta''_1 &:= \Theta_1 \cosh 2\sigma + \Theta_0 \sinh 2\sigma , \\ \Upsilon''_0 &:= \Upsilon_0 \cosh 2\sigma + \Upsilon_1 \sinh 2\sigma , \\ \Upsilon''_1 &:= \Upsilon_1 \cosh 2\sigma + \Upsilon_0 \sinh 2\sigma \end{aligned}$$

and t' and x'_1 are elements of an another coordinate system so that:

$$\left. \begin{array}{l} \dfrac{\partial x_1}{\partial x'_1} = \cosh 2\sigma \\ \dfrac{\partial t}{\partial x'_1} = \dfrac{1}{\mathrm{c}} \sinh 2\sigma \\ \dfrac{\partial x_1}{\partial t'} = \mathrm{c} \sinh 2\sigma \\ \dfrac{\partial t}{\partial t'} = \cosh 2\sigma \\ \dfrac{\partial x_2}{\partial t'} = \dfrac{\partial x_3}{\partial t'} = \dfrac{\partial x_2}{\partial x'_1} = \dfrac{\partial x_3}{\partial x'_1} = 0 \end{array} \right\} . \qquad (27)$$

Therefore, the oscillation between blue and green colours with the oscillation between upper and lower mass members curves the space in the t, x_1 directions.

Similarly, matrix

$$U_{0,2}(\phi) := \begin{bmatrix} \cosh\phi & \mathrm{i}\sinh\phi & 0 & 0 \\ -\mathrm{i}\sinh\phi & \cosh\phi & 0 & 0 \\ 0 & 0 & \cosh\phi & -\mathrm{i}\sinh\phi \\ 0 & 0 & \mathrm{i}\sinh\phi & \cosh\phi \end{bmatrix}$$

with an arbitrary real function $\phi(t, x_1, x_2, x_3)$ describes the oscillation between blue and red colours with the oscillation between upper and lower mass members curves the space in the t, x_2 directions. And matrix

$$U_{0,3}(\iota) := \begin{bmatrix} e^{\iota} & 0 & 0 & 0 \\ 0 & e^{-\iota} & 0 & 0 \\ 0 & 0 & e^{-\iota} & 0 \\ 0 & 0 & 0 & e^{\iota} \end{bmatrix}$$

with an arbitrary real function $\iota(t, x_1, x_2, x_3)$ describes the oscillation between green and red colours with the oscillation between upper and lower mass members curves the space in the t, x_3 directions.

From (27):

$$\begin{aligned} \frac{\partial x_1}{\partial t'} &= \mathrm{c} \sinh 2\sigma , \\ \frac{\partial t}{\partial t'} &= \cosh 2\sigma . \end{aligned}$$

Because

$$\begin{aligned} \sinh 2\sigma &= \frac{v}{\sqrt{1 - \frac{v^2}{\mathrm{c}^2}}} , \\ \cosh 2\sigma &= \frac{1}{\sqrt{1 - \frac{v^2}{\mathrm{c}^2}}} \end{aligned}$$

where v is a velocity of system $\{t', x'_1\}$ as respects system $\{t, x_1\}$ then

$$v = \tanh 2\sigma .$$

Let

$$2\sigma := \omega(x_1) \frac{t}{x_1}$$

with

$$\omega(x_1) := \frac{\lambda}{|x_1|} ,$$

where λ is a real constant bearing positive numerical value.

In that case

$$v(t, x_1) = \tanh\left(\omega(x_1) \frac{t}{x_1} \right)$$

and if g is an acceleration of system $\{t', x'_1\}$ as respects system $\{t, x_1\}$ then

$$g(t, x_1) = \frac{\partial v}{\partial t} = \frac{\omega(x_1)}{x_1 \cosh^2\left(\omega(x_1) \frac{t}{x_1} \right)} .$$

Figure 1 shows the dependency of a system $\{t', x'_1\}$ velocity $v(t, x_1)$ on x_1 in system $\{t, x_1\}$.

This velocity in point A is not equal to one in point B. Hence, an oscillator, placed in B has a nonzero velocity in respects an observer placed in point A. Therefore, from the Lorentz transformations this oscillator frequency for observer placed in point A is less than own frequency of this oscillator (*red shift*).

Figure 2 shows the dependency of a system $\{t', x'_1\}$ acceleration $g(t, x_1)$ on x_1 in system $\{t, x_1\}$.

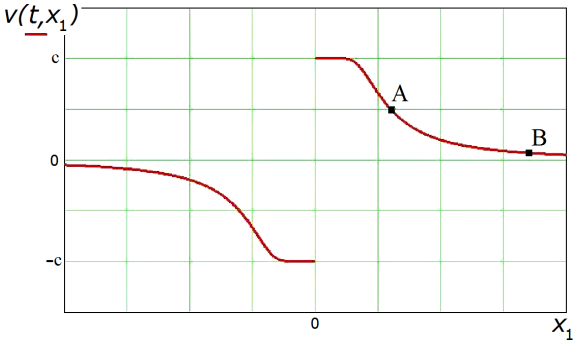

Fig. 1: Dependency of $v(t, x_1)$ from x_1 [3].

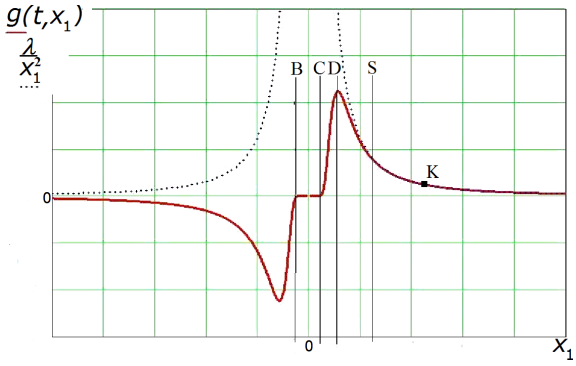

Fig. 2: Dependency of $g(t, x_1)$ from x_1 [3].

If an object immovable in system $\{t, x_1\}$ is placed in point K then in system $\{t', x_1'\}$ this object must move to the left with acceleration g and $g \simeq \lambda / x_1^2$.

I call:

- interval from S to ∞: *Newton Gravity Zone*,
- interval from B to C: *Asymptotic Freedom Zone*,
- and interval from C to D: *Confinement Force Zone*.

Now let

$$\widetilde{U}(\chi) := \begin{bmatrix} e^{i\chi} & 0 & 0 & 0 \\ 0 & e^{i\chi} & 0 & 0 \\ 0 & 0 & e^{2i\chi} & 0 \\ 0 & 0 & 0 & e^{2i\chi} \end{bmatrix}$$

and

$$\widehat{M'} := \begin{pmatrix} -M'_{\zeta,0}\gamma_\zeta^{[0]} + M'_{\zeta,4}\zeta^{[4]} - \\ -M'_{\eta,0}\gamma_\eta^{[0]} - M'_{\eta,4}\eta^{[4]} + \\ +M'_{\theta,0}\gamma_\theta^{[0]} + M'_{\theta,4}\theta^{[4]} \end{pmatrix} := \widetilde{U}^{-1}(\chi)\,\widehat{M}\widetilde{U}(\chi)$$

then:

$$\begin{aligned} M'_{\zeta,0} &= (M_{\zeta,0}\cos\chi - M_{\zeta,4}\sin\chi), \\ M'_{\zeta,4} &= (M_{\zeta,4}\cos\chi + M_{\zeta,0}\sin\chi), \\ M'_{\eta,4} &= (M_{\eta,4}\cos\chi - M_{\eta,0}\sin\chi), \\ M'_{\eta,0} &= (M_{\eta,0}\cos\chi + M_{\eta,4}\sin\chi), \\ M'_{\theta,0} &= (M_{\theta,0}\cos\chi + M_{\theta,4}\sin\chi), \\ M'_{\theta,4} &= (M_{\theta,4}\cos\chi - M_{\theta,0}\sin\chi). \end{aligned}$$

Therefore, matrix $\widetilde{U}(\chi)$ makes an oscillation between upper and lower mass members.

If χ is an arbitrary real function of time-space variables ($\chi = \chi(t, x_1, x_2, x_3)$) then the following expression is received from equation (26) under transformation $\widetilde{U}(\chi)$ [3]:

$$\left(\frac{1}{c}\partial_t + \frac{1}{c}\widetilde{U}^{-1}(\chi)\left(\partial_t\widetilde{U}(\chi)\right) + i\Theta_0 + i\Upsilon_0\gamma^{[5]}\right)\varphi =$$
$$= \left(\begin{array}{c} \sum_{k=1}^{3}\beta^{[k]}\left(\begin{array}{c}\partial_k + \widetilde{U}^{-1}(\chi)\left(\partial_k\widetilde{U}(\chi)\right) \\ + i\Theta_k + i\Upsilon_k\gamma^{[5]}\end{array}\right) + \\ + \widetilde{U}^{-1}(\chi)\,\widehat{M}\widetilde{U}(\chi)\end{array}\right)\varphi.$$

Now let:

$$\widehat{U}(\kappa) := \begin{bmatrix} e^{\kappa} & 0 & 0 & 0 \\ 0 & e^{\kappa} & 0 & 0 \\ 0 & 0 & e^{2\kappa} & 0 \\ 0 & 0 & 0 & e^{2\kappa} \end{bmatrix}$$

and

$$\widehat{M'} := \begin{pmatrix} -M'_{\zeta,0}\gamma_\zeta^{[0]} + M'_{\zeta,4}\zeta^{[4]} - \\ -M'_{\eta,0}\gamma_\eta^{[0]} - M'_{\eta,4}\eta^{[4]} + \\ +M'_{\theta,0}\gamma_\theta^{[0]} + M'_{\theta,4}\theta^{[4]} \end{pmatrix} := \widehat{U}^{-1}(\kappa)\,\widehat{M}\widehat{U}(\kappa)$$

then:

$$\begin{aligned} M'_{\theta,0} &= (M_{\theta,0}\cosh\kappa - iM_{\theta,4}\sinh\kappa), \\ M'_{\theta,4} &= (M_{\theta,4}\cosh\kappa + iM_{\theta,0}\sinh\kappa), \\ M'_{\eta,0} &= (M_{\eta,0}\cosh\kappa - iM_{\eta,4}\sinh\kappa), \\ M'_{\eta,4} &= (M_{\eta,4}\cosh\kappa + iM_{\eta,0}\sinh\kappa), \\ M'_{\zeta,0} &= (M_{\zeta,0}\cosh\kappa + iM_{\zeta,4}\sinh\kappa), \\ M'_{\zeta,4} &= (M_{\zeta,4}\cosh\kappa - iM_{\zeta,0}\sinh\kappa). \end{aligned}$$

Therefore, matrix $\widehat{U}(\kappa)$ makes an oscillation between upper and lower mass members, too.

If κ is an arbitrary real function of time-space variables ($\kappa = \kappa(t, x_1, x_2, x_3)$) then the following expression is received from equation (26) under transformation $\widehat{U}(\kappa)$ [3]:

$$\left(\frac{1}{c}\partial_t + \widehat{U}^{-1}(\kappa)\left(\frac{1}{c}\partial_t\widehat{U}(\kappa)\right) + i\Theta_0 + i\Upsilon_0\gamma^{[5]}\right)\varphi =$$
$$= \left(\begin{array}{c} \sum_{s=1}^{3}\beta^{[s]}\left(\begin{array}{c}\partial_s + \widehat{U}^{-1}(\kappa)\left(\partial_s\widehat{U}(\kappa)\right) \\ + i\Theta_s + i\Upsilon_s\gamma^{[5]}\end{array}\right) \\ + \widehat{U}^{-1}(\kappa)\,\widehat{M}\widehat{U}(\kappa)\end{array}\right)\varphi.$$

Denote: $U_{0,1} := U_1$, $U_{2,3} := U_2$, $U_{1,3} := U_3$, $U_{0,2} := U_4$, $U_{1,2} := U_5$, $U_{0,3} := U_6$, $\widehat{U} := U_7$, $\widetilde{U} := U_8$.

In that case for every natural k ($1 \leqslant k \leqslant 8$) there a 4×4 constant complex matrix Λ_k exists [3] so that:

$$U_k^{-1}(\beta)\,\partial_s U_k(\beta) = \Lambda_k \partial_s \beta$$

and if $r \neq k$ then for every natural r ($1 \leqslant r \leqslant 8$) there real functions $a_s^{k,r}(\alpha)$ exist so that:

$$U_k^{-1}(\alpha)\,\Lambda_r U_k(\alpha) = \sum_{s=1}^{8} a_s^{k,r}(\alpha) \cdot \Lambda_s.$$

Hence, if $\grave{U}$ is the following set:

$$\grave{U} := \left\{ U_{0,1}, U_{2,3}, U_{1,3}, U_{0,2}, U_{1,2}, U_{0,3}, \widehat{U}, \widetilde{U} \right\}$$

then for every product U of $\grave{U}$'s elements real functions $G_s^r(t, x_1, x_2, x_3)$ exist so that

$$U^{-1}(\partial_s U) = \frac{g_3}{2} \sum_{r=1}^{8} \Lambda_r G_s^r$$

with some real constant g_3 (similar to 8 gluons).

3 Conclusion

Therefore, higgsless electroweak and quark-gluon theories and gravity without superstrings can be deduced from properties of probability.

Submitted on April 14, 2009 / Accepted on April 29, 2009

References

1. For instance, Madelung E. Die Mathematischen Hilfsmittel des Physikers Springer Verlag, 1957, p. 29.
2. Quznetsov G. Logical foundation of theoretical physics. Nova Sci. Publ., NY, 2006, p. 107
3. Quznetsov G. *Progress in Physics*, 2009, v. 2, 96–106
4. Quznetsov G. Probabilistic treatment of gauge theories. In series *Contemporary Fundamental Physics*, Nova Sci. Publ., NY, 2007, pp. 29, 40–41.
5. Ibidem, p. 61.
6. Ibidem, p. 62.
7. Ibidem, p. 63.
8. Ibidem, pp. 64–68.
9. Ibidem, pp. 96–100.
10. Ibidem, pp. 91–94.
11. Ibidem, pp. 100–117.
12. Ibidem, p. 127.
13. Ibidem, pp. 130–131.
14. For instance, Ziman J. M. Elements of advanced quantum theory. Cambridge University Press, 1969, formula (6.59).

A Heuristic Model for the Active Galactic Nucleus Based on the Planck Vacuum Theory

William C. Daywitt

National Institute for Standards and Technology (retired), Boulder, Colorado, USA
E-mail: wcdaywitt@earthlink.net

The standard explanation for an active galactic nucleus (AGN) is a "central engine" consisting of a hot accretion disk surrounding a supermassive black hole [1, p. 32]. Energy is generated by the gravitational infall of material which is heated to high temperatures in this dissipative accretion disk. What follows is an alternative model for the AGN based on the Planck vacuum (PV) theory [2, Appendix], where both the energy of the AGN and its variable luminosity are explained in terms of a variable photon flux emanating from the PV.

The Einstein field equation

$$\frac{G_{\mu\nu}/6}{1/r_*^2} = \frac{T_{\mu\nu}}{\rho_* c^2} \tag{1}$$

is probably invalid in much of the region of interest ($0.5 < n_r < 1$) to the AGN modeling process, especially as n_r gets closer to unity [2]. Ignoring this concern, though, there is a non-black-hole Schwarzschild line element for an extended mass [3, 4] available for consideration. Unfortunately, this incompressible-fluid model is incompatible with the PV theory (see Appendix B). The following calculations provide a rough heuristic way around these modeling problems.

The expression to be used to estimate the mass of an AGN can be derived from the relation between a spherical mass m and its mass density ρ_0

$$m = \frac{4\pi r^3}{3}\,\rho_0 = \frac{8\pi}{6}\,\rho_0 r^3 \tag{2}$$

where $r\,(\leqslant r_0)$ is the radius of the sphere and ρ_0 is assumed to be constant. This can be expressed as

$$S_r = \frac{mc^2}{r} = \frac{8\pi}{6}\,\frac{\rho_0 c^2}{1/r^2} \tag{3}$$

in terms of the curvature stress S_r exerted on the PV at the mass' surface. The maximum stress S_* that can be exerted on the PV is given by the first ratio in

$$S_* = \frac{m_* c^2}{r_*} = \frac{8\pi}{6}\,\frac{\rho_* c^2}{1/r_*^2} \tag{4}$$

which can be transformed to the second ratio by recognizing $\rho_* = m_*/(4\pi r_*^3/3)$ as the mass density of the individual PPs making up the degenerate PV. Dividing equation (3) by (4) leads to

$$\frac{n_r(1/r^2)}{1/r_*^2} = \frac{\rho_0 c^2}{\rho_* c^2} \tag{5}$$

where the n-ratio

$$n_r = \frac{S_r}{S_*} = \frac{mc^2/r}{m_* c^2/r_*} < 1 \tag{6}$$

is the relative stress exerted by m. The curvature stress in (3) is infinite if r is allowed to vanish, but the PV theory restricts r to $r > r_*$ [2]. The surface of the AGN is at $r = r_0$ where $m = m_0$.

As an aside, it is interesting to note that the result in (5) can be made to resemble the Einstein equation in (1)

$$\frac{G_{00}/6}{1/r_*^2} = \frac{T_{00}}{\rho_* c^2} \tag{7}$$

by defining $G_{00} \equiv 6n_r(1/r^2)$ and $T_{00} \equiv \rho_0 c^2$. That G_{00} is proportional to the n-ratio n_r demonstrates in a simple way that the Einstein equation is physically related to stresses in the PV.

The time varying luminosity of an AGN can be used to estimate the AGN's radius. A simplified calculation for a typical AGN [5, p.1110] leads to the radius $r_0 = 1.1\times10^{14}$cm. From (5) with $r = r_0$, this radius can be related to the AGN mass density ρ_0 via

$$\frac{\rho_0}{\rho_*} = n_0\left(\frac{r_*}{r_0}\right)^2 \tag{8}$$

where $n_0 = (m_0 c^2/r_0)/(m_* c^2/r_*)$. From previous investigations [2, 6], a reasonable n-ratio to assume for the AGN might be $n_0 = 0.5$, leading from (8) to

$$\frac{\rho_0}{\rho_*} = 0.5\left(\frac{1.62\times10^{-33}}{1.1\times10^{14}}\right)^2 = 1.1\times10^{-94} \tag{9}$$

for the relative mass density. Then the absolute density is

$$\begin{aligned}\rho_0 &= 1.1\times10^{-94}\rho_* = \\ &= 1.1\times10^{-94}\,1.22\times10^{93} = 0.13\,[\mathrm{gm/cm^3}]\end{aligned} \tag{10}$$

which yields

$$m_0 = \frac{4\pi r_0^3\,\rho_0}{3} = \\ = \frac{4\pi(1.1\times10^{14})^3(0.13)}{3} = 7.2\times10^{41}[\mathrm{gm}] \tag{11}$$

for the mass of the AGN.

The standard calculation uses the black-hole/mass-accretion paradigm to determine the AGN mass and leads to the estimate $m_0 > 6.6\times10^{41}$gm for the typical calculation referenced above. This result compares favorably with the 7.2×10^{41}gm estimate in (11) and yields the n-ratio $n_r = 0.44$.

Currently there is no generally accepted theory for the time variability in the luminosity of an AGN [1, 7]. As mentioned above, there is also no PV-acceptable line element to be used in the AGN modeling. As a substitute, the line elements for the generalized Schwarzschild solution of a point mass will be used to address the luminosity variability. Furthermore, because the differential geometry of the General theory is certainly not applicable for $r < r_* = 1.62\times10^{-33}$ [2], the point-mass solution will be treated as a model for a "hole" of radius r_* that leads from the visible universe into the PV.

If it assumed that the luminosity of the AGN is due to a large photon flux from the PV, through the "hole", and into the visible universe, then the corresponding luminosity will be proportional to the *coordinate* velocity of this flux. If it is further assumed that the flux excites material that has collected between the coordinate radii corresponding to the n-ratios $n_r = 0.5$ and $n_r = 1$, then both the variable luminosity and its uniformity at the surface of the AGN can be explained by the model, the uniformity resulting from the compact nature of the variable-flux source at the surface $r = r_*$. (The distortion of the PV by the collection of material between 0.5 and 1 is ignored in the rough model being pursued.)

The general solution [8, 9] to the Einstein field equations leading to the Schwarzschild line elements mentioned above is given in Appendix A. The magnitude of the relative coordinate velocity of a photon approaching or leaving the area of the point mass in a radial direction can be calculated from this solution as ($n = 1, 2, 3, \ldots$)

$$\beta_n(n_r) = \left|\frac{dr}{c\,dt}\right| = \left(\frac{g_{00}}{-g_{11}}\right)^{1/2} = \\ = \left(1+2^n n_r^n\right)^{(1-1/n)}\left(1-\frac{2n_r}{\left(1+2^n n_r^n\right)^{1/n}}\right) \tag{12}$$

whose plot as a function of n_r in Figure 1 shows β_n's behavior for $n = 3, 10, 20$. The vertical and horizontal axes run from 0 to 1. The approximate n-ratios for various astrophysical bodies are labeled on the $n = 3$ curve and include white dwarfs, neutron stars, and AGNs. The free Planck particle is labeled PP.

The existence of multiple solutions ($n = 1, 2, 3, \ldots$) in the spacetime geometry suggests a dynamic condition implying the possibility of a variable n or a composite solution "oscillating" between various values of n. For example, consider a solution oscillating between the $n = 10$ and $n = 20$ indices in the figure, where the relative flux velocities at $n_r = 0.5$ are 0.125 and 0.066 respectively. Since the luminosity is proportional to these flux velocities, the variation in luminosity changes by a factor of $0.125/0.066 \sim 2$ over the period of the oscillation. Again, as the source of the flux is the compact "hole" leading from the PV, the surface of the AGN is uniformly brightened by the subsequent flux scattered by the material intervening between the "hole" and the AGN surface at $n_r = 0.5$ where from (6)

$$r_0 = \frac{2m_0c^2}{m_*c^2/r_*} \tag{13}$$

as $m = m_0$ at $r = r_0$.

"Earlier studies of galaxies and their central black holes in the nearby Universe revealed an intriguing linkage between the masses of the black holes and of the central 'bulges' of stars and gas in the galaxies.The ratio of the black hole and the bulge mass is nearly the same for a wide range of galactic sizes and ages. For central black holes from a million to many billions of times the mass of our sun, the black hole's mass is about one one-thousandth of the mass of the surrounding galactic bludge. ... This constant ratio indicates that the black hole and the bulge affect each others' growth in some sort of interactive relationship. ... The big question has been whether one grows before the other or if they grow together, maintaining their mass ratio throughout the entire process." [10] Recent measurements suggest that the constant ratio seen in nearby galaxies may not hold in the early more distant galaxies. The black holes in these young galaxies are much more massive compared to the bulges in the nearby galaxies, implying that the black holes started growing first.

The astrophysical measurements described in the preceding paragraph in terms of black holes could just as well be described by the PV model of the present paper, suggesting that the PV is the source of the energy and variability of the AGN and probably the primary gases (electrons and protons) of its galactic bulge.

Acknowledgment

The author takes pleasure in thanking a friend, Gerry Simonson, for bringing reference [10] to the author's attention.

Appendix A Crothers point mass

The general solution [6,8,9] to the Einstein field equations for a point mass m at $r = 0$ consists of the infinite collection ($n = 1, 2, 3, \ldots$) of Schwarzschild-like equations with continuous, non-singular met-

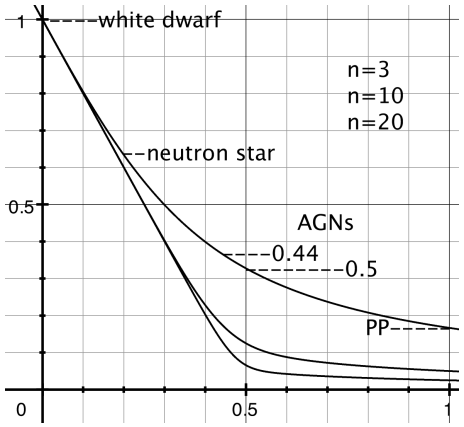

Fig. 1: The graph shows the relative coordinate velocity $\beta_n(n_r)$ plotted as a function of the n-ratio n_r for various indices n. Both axes run from 0 to 1. The approximate n-ratios corresponding to various astrophysical bodies are labeled on the $n = 3$ curve and include white dwarfs ($n_r \sim 0.0002$), neutron stars (~ 0.2), and AGNs (the 0.44 value calculated from the black-hole model and the 0.5 assumed by the PV model). The free Planck particle is represented by PP (1). The intersections of the $n = 10$ and $n = 20$ curves with the 0.5 ordinate result in the relative velocities $\beta_{10}(0.5) = 0.125$ and $\beta_{20}(0.5) = 0.066$ respectively.

rics for $r > 0$:

$$ds^2 = g_{00}\, c^2 dt^2 + g_{11}\, dr^2 - R_n^2 \left(d\theta^2 + \sin^2\theta\, d\phi^2\right) \tag{A1}$$

where

$$g_{00} = (1 - \alpha/R_n) \qquad \text{and} \qquad g_{11} = -\frac{(r/R_n)^{2n-2}}{g_{00}} \tag{A2}$$

$$\alpha = \frac{2mc^2}{m_* c^2/r_*} = 2r n_r \tag{A3}$$

$$R_n = \left(r^n + \alpha^n\right)^{1/n} = r(1 + 2^n n_r^n)^{1/n} = \\ = \alpha(1 + 1/2^n n_r^n)^{1/n} \tag{A4}$$

and

$$0 < n_r \left(= \frac{mc^2/r}{m_* c^2/r_*}\right) < 1 \tag{A5}$$

where r is the *coordinate* radius from the point mass to the field point of interest, and m_* and r_* are the PP mass and Compton radius respectively.

The metrics in (A2) yield

$$g_{00} = 1 - \frac{2n_r}{(1 + 2^n n_r^n)^{1/n}} \longrightarrow 1 \tag{A6}$$

$$-g_{11} = \frac{(1 + 2^n n_r^n)^{(2-2n)/n}}{g_{00}} \longrightarrow 1 \tag{A7}$$

with

$$R_n = r(1 + 2^n n_r^n)^{1/n} \longrightarrow r \tag{A8}$$

where the arrows lead to the far-field results for $n_r \to 0$. As expected, the n-ratio n_r in these equations is the sole variable that expresses the relative distortion of the PV due to the mass at $r = 0$.

Appendix B Incompressible fluid

Outside a spherical mass of incompressible fluid (or any static mass of the same shape), the Schwarzschild line elements [3, 4] are the same as (A1) and (A2) except that for the fluid model

$$\alpha = \left(\frac{3}{\kappa\rho_0 c^2}\right)^{1/2} \sin^3\chi_0 \tag{B1}$$

where $\kappa = 8\pi G/c^4 = 6(1/r_*^2)/\rho_* c^2$ [2]

$$R_n = (r^n + \epsilon^n)^{1/n} \tag{B2}$$

$$\sin\chi_0 = \left(\frac{\kappa\rho_0 c^2}{3}\right)^{1/2} (r_0^3 + \rho)^{1/3} \tag{B3}$$

and $\epsilon = \epsilon(\rho_0, \chi_0)$ and $\rho = \rho(\rho_0, \chi_0)$ are constants, where ρ_0 represents the constant density of the fluid. The ratios in (B1) and (B3) can be expressed as

$$\frac{3}{\kappa\rho_0 c^2} = \frac{\rho_* r_*^2}{2\rho_0} \tag{B4}$$

where $\rho_* \left(= m_*/(4\pi r_*^3/3)\right)$ is the PP mass density.

Dividing (B1) by (B2) and using (B3) leads to

$$\frac{\alpha}{R_n} = \left(\frac{\kappa\rho_0 c^2}{3}\right) \frac{r_0^3(1 + \rho/r_0^3)}{r(1 + \epsilon^n/r^n)^{1/n}}\,. \tag{B5}$$

Inserting (B4) into (B5) then gives

$$\frac{\alpha}{R_n} = 2n_r \frac{1 + \rho/r_0^3}{(1 + \epsilon^n/r^n)^{1/n}} \tag{B6}$$

after some manipulation, where the n-ratio

$$n_r = \frac{m_0 c^2/r}{m_* c^2/r_*}\,. \tag{B7}$$

Here m_0 is defined in terms of the fluid density ρ_0 and the coordinate radius r_0, where $m_0 = (4\pi r_0^3/3)\rho_0$. The radius r_0 corresponds to the coordinate radius r_a in equation (32) of reference [4].

As pointed out in Appendix A, α/R_n (which is related to the PV distortion *exterior* to the mass) should be solely a function of the variable n_r as n_r is the only relative stress the static spherical mass as a whole can exert on the exterior vacuum. Consequently the variable r can only appear within the variable n_r. Therefor the denominator in (B6), and thus the incompressible-fluid model, are incompatible with the PV model.

Submitted on May 06, 2009 / Accepted on May 11, 2009

References

1. Peterson B.M. An introduction to active galactic nuclei. Cambridge Univ. Press, Cambridge UK, 1997.
2. Daywitt W.C. Limits to the validity of the Einstein field equations and General Relativity from the viewpoint of the negative-energy Planck vacuum state. *Progress in Physics*, 2009, v. 3, 27.
3. Crothers S.J. On the vacuum field of a sphere of incompressible fluid. *Progress in Physics*, 2005, v. 12, 76.

4. Schwarzschild K. Über das Gravitationsfeld einer Kugel aus incompressiebler Flüssigkeit nach der Einsteinschen Theorie. *Sitzungsberichte der Königlich Preussischen Akademie der Wissenschaften*, 1916, 424–435 (published in English as: Schwarzschild K. On the gravitational field of a sphere of incompressible liquid, according to Einstein's theory. *Abraham Zelmanov Journal*, 2008, v. 1, 20–32).
5. Carroll B.W., Ostlie D.A. An introduction to modern astrophysics. Addison-Wesley, San Francisco — Toronto, 2007.
6. Daywitt W.C. The Planck vacuum and the Schwarzschild metrics. *Progress in Physics*, 2009, v. 3, 30.
7. Kembhavi A.K., Narlikar J.V. Quasars and active galactic nuclei — an introduction. Cambridge Univ. Press, Cambridge UK, 1999.
8. Crothers S.J. On the general solution to Einstein's vacuum field and its implications for relativistic degeneracy. *Progress in Physics*, 2005, v. 1, 68.
9. Schwarzschild K. Über das Gravitationsfeld eines Massenpunktes nach der Einsteinschen Theorie. *Sitzungsberichte der Königlich Preussischen Akademie der Wissenschaften*, 1916, 189–196 (published in English as: Schwarzschild K. On the gravitational field of a point mass according to Einstein's theory. *Abraham Zelmanov Journal*, 2008, v. 1, 10–19).
10. National Radio Astronomy Observatory: Black holes lead galaxy growth, new research shows. Socorro, NM 87801, USA, Jan. 6, 2009.

Solution of Einstein's Geometrical Gravitational Field Equations Exterior to Astrophysically Real or Hypothetical Time Varying Distributions of Mass within Regions of Spherical Geometry

Chifu Ebenezer Ndikilar* and Samuel Xede Kofi Howusu†

*Physics Department, Gombe State University, P.M.B. 127, Gombe, Gombe State, Nigeria
E-mail: ebenechifu@yahoo.com

†Physics Department, Kogi State University, Anyighba, Kogi State, Nigeria
E-mail: sxkhowusu@yahoo.co.uk

Here, we present a profound and complete analytical solution to Einstein's gravitational field equations exterior to astrophysically real or hypothetical time varying distributions of mass or pressure within regions of spherical geometry. The single arbitrary function f in our proposed exterior metric tensor and constructed field equations makes our method unique, mathematically less combersome and astrophysically satisfactory. The obtained solution of Einstein's gravitational field equations tends out to be a generalization of Newton's gravitational scalar potential exterior to the spherical mass or pressure distribution under consideration.

1 Introduction

After the publication of Einstein's geometrical gravitational field equations in 1915, the search for their exact and analytical solutions for all the gravitational fields in nature began [1]. In recent publications [2–4], we have presented a standard generalization of Schwarzschild's metric to obtain the mathematically most simple and astrophysically most satisfactory metric tensors exterior to various mass distributions within regions of spherical geometry. Our method of generating metric tensors for gravitational fields is unique as it introduces the dependence of the field on one and only one dependent function f and thus the geometrical field equations for a gravitational field exterior to any astrophysically real or hypothetical massive spherical body has only one unknown f.

In this article, the equation satisfied by the function f in the gravitational field produced at an external point by a time varying spherical mass distribution situated in empty space is considered and an analytical solution for it proposed. A possible astrophysical example of such a distribution is when one considers the vacuum gravitational field produced by a spherically symmetric star in which the material in the star experiences radial displacement or explosion.

2 Gravitational radiation and propagation field equation exterior to a time varying spherical mass distribution

The covariant metric tensor exterior to a homogeneous time varying distribution of mass within regions of spherical geometry [2] is

$$g_{00} = 1 + \frac{2}{c^2} f(t,r)\,, \tag{2.1}$$

$$g_{11} = -\left[1 + \frac{2}{c^2} f(t,r)\right]^{-1}, \tag{2.2}$$

$$g_{22} = -r^2, \tag{2.3}$$

$$g_{33} = -r^2 \sin^2\theta\,, \tag{2.4}$$

$$g_{\mu\nu} = 0;\ \text{otherwise.} \tag{2.5}$$

The corresponding contravariant metric tensor for this field, is then constructed trivially using the Quotient Theorem of tensor analysis and used to compute the affine coefficients, given explicitly as

$$\Gamma^0_{00} = \frac{1}{c^3}\left[1 + \frac{2}{c^2} f(t,r)\right]^{-1} \frac{\partial f(t,r)}{\partial t}\,, \tag{2.6}$$

$$\Gamma^0_{01} \equiv \Gamma^0_{10} = \frac{1}{c^2}\left[1 + \frac{2}{c^2} f(t,r)\right]^{-1} \frac{\partial f(t,r)}{\partial r}\,, \tag{2.7}$$

$$\Gamma^0_{11} = -\frac{1}{c^3}\left[1 + \frac{2}{c^2} f(t,r)\right]^{-3} \frac{\partial f(t,r)}{\partial t}\,, \tag{2.8}$$

$$\Gamma^1_{00} = \frac{1}{c^2}\left[1 + \frac{2}{c^2} f(t,r)\right] \frac{\partial f(t,r)}{\partial r}\,, \tag{2.9}$$

$$\Gamma^1_{01} \equiv \Gamma^1_{10} = -\frac{1}{c^3}\left[1 + \frac{2}{c^2} f(t,r)\right]^{-1} \frac{\partial f(t,r)}{\partial t}\,, \tag{2.10}$$

$$\Gamma^1_{11} = -\frac{1}{c^2}\left[1 + \frac{2}{c^2} f(t,r)\right]^{-1} \frac{\partial f(t,r)}{\partial r}\,, \tag{2.11}$$

$$\Gamma^1_{22} = -r\left[1 + \frac{2}{c^2} f(t,r)\right], \tag{2.12}$$

$$\Gamma^1_{33} = -r\sin^2\theta\left[1 + \frac{2}{c^2} f(t,r)\right], \tag{2.13}$$

$$R_{00} = \frac{4}{c^6}\left[1+\frac{2}{c^2}f(t,r)\right]^{-2}\left(\frac{\partial f}{\partial t}\right)^2 - \frac{1}{c^4}\left[1+\frac{2}{c^2}f(t,r)\right]^{-1}\frac{\partial^2 f}{\partial t^2} - \\ - \frac{1}{c^2}\left[1+\frac{2}{c^2}f(t,r)\right]\frac{\partial^2 f}{\partial r^2} - \frac{2}{rc^2}\left(1+\frac{2}{c^2}f(t,r)\right)\frac{\partial f}{\partial r} \tag{2.18}$$

$$R_{11} = -\frac{4}{c^6}\left[1+\frac{2}{c^2}f(t,r)\right]^{-4}\left(\frac{\partial f}{\partial t}\right)^2 + \frac{1}{c^4}\left[1+\frac{2}{c^2}f(t,r)\right]^{-3}\frac{\partial^2 f}{\partial t^2} + \\ + \frac{1}{c^2}\left[1+\frac{2}{c^2}f(t,r)\right]^{-1}\frac{\partial^2 f}{\partial r^2} + \frac{2}{rc^2}\left[1+\frac{2}{c^2}f(t,r)\right]^{-1}\frac{\partial f}{\partial r} \tag{2.19}$$

$$R_{22} = \frac{2}{c^2}\left[1+\frac{2}{c^2}f(t,r)\right] \tag{2.20}$$

$$R_{33} = \frac{2}{c^2}\sin^2\theta\left(r\frac{\partial f}{\partial r}+f(t,r)\right) \tag{2.21}$$

$$R_{\alpha\beta} = 0;\ \text{otherwise} \tag{2.22}$$

$$R = \frac{8}{c^6}\left[1+\frac{2}{c^2}f(t,r)\right]^{-3}\left(\frac{\partial f}{\partial t}\right)^2 - \frac{2}{c^4}\left[1+\frac{2}{c^2}f(t,r)\right]^{-2}\frac{\partial^2 f}{\partial t^2} - \frac{2}{c^2}\frac{\partial^2 f}{\partial r^2} - \frac{8}{rc^2}\frac{\partial f}{\partial r} - \frac{4f(t,r)}{r^2c^2} \tag{2.23}$$

$$\nabla^2 f(t,r) + \frac{\partial}{\partial t}\left\{\frac{1}{c^2}\left[1+\frac{2}{c^2}f(t,r)\right]^{-2}\frac{\partial f(t,r)}{\partial t}\right\} = 0 \tag{2.25}$$

$$\nabla^2 f(t,r) + \frac{1}{c^2}\left[1+\frac{2}{c^2}f(t,r)\right]^{-2}\frac{\partial^2 f(t,r)}{\partial t^2} - \frac{4}{c^4}\left[1+\frac{2}{c^2}f(t,r)\right]^{-3}\left(\frac{\partial f(t,r)}{\partial t}\right)^2 = 0 \tag{2.26}$$

$$\Gamma^2_{12} \equiv \Gamma^2_{21} \equiv \Gamma^3_{13} \equiv \Gamma^3_{31} = r^{-1}, \tag{2.14}$$

$$\Gamma^2_{33} = -\frac{1}{2}\sin 2\theta\,, \tag{2.15}$$

$$\Gamma^3_{23} \equiv \Gamma^3_{32} = \cot\theta\,, \tag{2.16}$$

$$\Gamma^\alpha_{\beta\gamma} = \quad 0;\ \text{otherwise}. \tag{2.17}$$

The Riemann-Christoffel or curvature tensor for the gravitational field is then constructed and the Ricci tensor obtained from it as (2.18)–(2.22).

From the Ricci tensor, we construct the curvature scalar R as (2.23).

Now, with the Ricci tensor and the curvature scalar, Einstein's gravitational field equations for a region exterior to a time varying spherical mass distribution is eminent. The field equations are given generally as

$$R_{\alpha\beta} - \frac{1}{2}Rg_{\alpha\beta} = 0\,. \tag{2.24}$$

Substituting the expressions for the Ricci tensor, curvature scalar and the covariant metric tensor; the R_{22} and R_{33} equations reduce identically to zero. The R_{00} and R_{11} field equations reduce identically to the single equation (2.25), or equivalently (2.26).

It is interesting and instructive to note that to the order of c^0, the geometrical wave equation (2.26) reduces to

$$\nabla^2 f(t,r) + \frac{\partial^2 f(t,r)}{\partial t^2} = 0\,. \tag{2.27}$$

Equation (2.27) admits a wave solution with a phase velocity v given as

$$v = i\ \mathrm{m\,s^{-1}}, \tag{2.28}$$

where $i = \sqrt{-1}$. Thus, such a wave exists only in imagination and is not physically or astrophysically real.

It is also worth noting that, to the order of c^2, the geometrical wave equation (2.26) reduces, in the limit of weak gravitational fields, to

$$\nabla^2 f(t,r) + \frac{1}{c^2}\frac{\partial^2 f(t,r)}{\partial t^2} = 0 \tag{2.29}$$

and equation (2.28) is the wave equation of a wave propagating with an imaginary speed *ic* in vacuum.

We now, present a profound and complete analytical solution to the field equation (2.26).

$$\frac{\partial^2}{\partial r^2} f(t,r) + \frac{2}{r}\frac{\partial}{\partial r} f(t,r) - \frac{1}{c^2}\frac{\partial}{\partial t}\left\{\left[1 - \frac{4}{c^2} f(t,r) + \frac{12}{c^4} f^2(t,r) + \ldots\right]\frac{\partial}{\partial t} f(t,r)\right\} = 0 \tag{3.1}$$

$$\frac{\partial^2}{\partial r^2} f(t,r) + \frac{2}{r}\frac{\partial}{\partial r} f(t,r) - \frac{1}{c^2}\frac{\partial^2}{\partial t^2} f(t,r) + \frac{4}{c^4} f(t,r)\frac{\partial^2}{\partial t^2} f(t,r) + \frac{4}{c^4}\left[\frac{\partial}{\partial t} f(t,r)\right]^2 + \ldots = 0 \tag{3.2}$$

$$\frac{\partial^2}{\partial r^2} f(t,r) = \sum_{n=0}^{\infty}\left[R_n''(r) - \frac{2ni\omega}{c} R_n'(r) + \frac{n^2 i^2 \omega^2}{c^2} R_n(r)\right] \exp ni\omega\left(t - \frac{r}{c}\right) \tag{3.4}$$

$$\frac{2}{r}\frac{\partial}{\partial r} f(t,r) = \sum_{n=0}^{\infty}\frac{2}{r}\left(R_n'(r) - \frac{ni\omega}{r}\right) \exp ni\omega\left(t - \frac{r}{c}\right) \tag{3.5}$$

$$\frac{1}{c^2}\frac{\partial^2}{\partial t^2} f(t,r) = \frac{1}{c^2}\sum_{n=0}^{\infty} n^2 i^2 \omega^2 R_n \exp\ ni\omega\left(t - \frac{r}{c}\right) \tag{3.6}$$

$$\begin{aligned} f(t,r)\frac{\partial^2 f(t,r)}{\partial t^2} = {} & i^2\omega^2 R_0 R_1 \exp i\omega\left(t - \frac{r}{c}\right) + \left[2^2 i^2 \omega^2 R_0 R_2 + i\omega^2 R_1^2\right] \exp 2i\omega\left(t - \frac{r}{c}\right) + \\ & + \left[3^2 i^2 \omega^2 R_0 R_3 + 2^2 i^2 \omega^2 R_1 R_2 + i^2 \omega^2 R_1 R_2\right] \exp 3i\omega\left(t - \frac{r}{c}\right) + \ldots \end{aligned} \tag{3.7}$$

$$\left(\frac{\partial}{\partial t} f(t,r)\right)^2 = \left[i\omega R_1(r) \exp i\omega\left(t - \frac{r}{c}\right) + 2i\omega R_2(r) \exp 2i\omega\left(t - \frac{r}{c}\right) + \ldots\right]^2 \tag{3.8}$$

$$R_2''(r) + 2\left(\frac{1}{r} - \frac{2i\omega}{c}\right) R_2'(r) - \frac{4}{c}\left(\frac{i\omega}{r} + \frac{4\omega}{c^3} R_0\right) R_2(r) - \frac{8\omega^2}{c^4} R_1^2(r) = 0\,. \tag{3.13}$$

3 Formulation of analytical solution to Einstein's geometrical gravitational field equation

The field equation for the gravitational field exterior to a time varying mass distribution within regions of spherical geometry are found to be given equally as equation (2.25) or (2.26).

For small gravitational fields (weak fields), the geometrical wave equation (1.1) reduces to (3.1) or equally (3.2).

We now seek a possible solution of equation (3.2) in the form

$$f(t,r) = \sum_{n=0}^{\infty} R_n(r)\ \exp\ ni\omega\left(t - \frac{r}{c}\right), \tag{3.3}$$

where R_n are functions of r only. Thus, by evaluating the first and second partial derivatives of our proposed solution for $f(t,r)$ in equation (3.3); it can be trivially shown that the separate terms of our expanded field equation (3.2) can be written as (3.4), (3.5), (3.6), (3.7), and (3.8), where the primes on the function R denote differentiation with respect to r. Now, substituting equations (3.4) to (3.8) into our field equation (3.2) and equating coefficients on both sides yields the following:

Equating coefficients of $\exp(0)$ gives

$$R_0'' + \frac{2}{r} R_0' = 0\,. \tag{3.9}$$

Thus, we can conveniently choose the best astrophysical solution for equation (3.9) as

$$R_0(r) = -\frac{k}{r} \tag{3.10}$$

where $k = GM_0$; by deduction from Schwarzschild's metric and Newton's theory of gravitation; with G being the universal gravitational constant and M_0 the total mass of the spherical body. Thus at this level, we note that the field equation yields a value for the arbitrary function f in our field equal to that in Schwarzschild's field. This is profound and interesting indeed as the link between our solution, Schwarzschild's solution and Newton's dynamical theory of gravitation becomes quite clear and obvious.

Equating coefficients of $\exp i\omega\left(t - \frac{r}{c}\right)$ gives

$$\begin{aligned} & R_1''(r) + 2\left(\frac{1}{r} - \frac{i\omega}{c}\right) R_1' + \\ & \quad + \frac{2\omega}{c}\left(-\frac{i}{r} - \frac{2\omega}{c^3} R_0\right) R_1 = 0\,. \end{aligned} \tag{3.11}$$

This is our exact differential equation for R_1 and it determines R_1 in terms of R_0. Thus, the solution admits an exact wave solution which reduces in the order of c^0 to:

$$f(t,r) \approx -\frac{k}{r} \exp i\omega\left(t - \frac{r}{c}\right). \tag{3.12}$$

Equating coefficients of $\exp 2i\omega\left(t - \frac{r}{c}\right)$ gives (3.13).

This is our exact equation for $R_2(r)$ in terms of $R_0(r)$ and $R_1(r)$. Similarly, all the other unknown functions $R_n(r)$, $n > 2$ are determined in terms of $R_0(r)$ by the other recurrence differential equations. Hence we obtain our unique astrophysically most satisfactory exterior solution of order c^4.

4 Conclusion

Interestingly, we note that the terms of our unique series solution (3.10), (3.11), (3.12) and (3.13) converge everywhere in the exterior space-time. Similarly, all the solutions of the other recurrence differential equations will also converge everywhere in the exterior space-time.

Instructively, we realize that our solution has a unique link to the pure Newtonian gravitational scalar potential for the gravitational field and thus puts Einstein's geometrical gravitational field on same footing with the Newtonian dynamical theory. This method introduces the dependence of geometrical gravitational field on one and only one dependent function f, comparable to one and only one gravitational scalar potential in Newton's dynamical theory of gravitation [4].

Hence, we have obtained a complete solution of Einstein's field equations in this gravitational field. Our metric tensor, which is the fundamental parameter in this field is thus completely defined.The door is thus open for the complete study of the motion of test particles and photons in this gravitational field introduced in the articles [5] and [6].

Submitted on April 29, 2009 / Accepted on May 12, 2009

References

1. Weinberg S. Gravitation and cosmology. J. Wiley, New York, 1972, p. 175–188.
2. Howusu S.X.K. The 210 astrophysical solutions plus 210 cosmological solutions of Einstein's geometrical gravitational field equations. Jos University Press, Jos, 2007.
3. Chifu E.N. and Howusu S.X.K. Einstein's equation of motion for a photon in fields exterior to astrophysically real or imaginary spherical mass distributions who's tensor field varies with azimuthal angle only. *Journal of the Nigerian Association of Mathematical Physics*, 2008, v. 13, 363–366.
4. Chifu E.N., Howusu S.X.K. and Lumbi L.W. Relativistic mechanics in gravitational fields exterior to rotating homogeneous mass distributions within regions of spherical geometry. *Progress in Physics*, 2009, v. 3, 18–23.
5. Chifu E.N., Howusu S.X.K. and Usman A. Motion of photons in time dependent spherical gravitational fields. *Journal of Physics Students*, 2008, v. 2(4), L10–L14.
6. Chifu E.N., Usman A. and Meludu O.C. Motion of particles of non-zero rest masses exterior to a spherical mass distribution with a time dependent potential field. *Pacific Journal of Science and Technology*, 2008, v. 9(2), 351–356.

Orbits in Homogeneous Oblate Spheroidal Gravitational Space-Time

Chifu Ebenezer Ndikilar*, Adams Usman†, and Osita C. Meludu†

*Physics Department, Gombe State University, P.M.B. 127, Gombe, Gombe State, Nigeria
E-mail: ebenechifu@yahoo.com

†Physics Department, Federal University of Technology, Yola, Adamawa State, Nigeria
E-mail: aausman@yahoo.co.uk, omeludu@yahoo.co.uk

The generalized Lagrangian in general relativistic homogeneous oblate spheroidal gravitational fields is constructed and used to study orbits exterior to homogenous oblate spheroids. Expressions for the conservation of energy and angular momentum for this gravitational field are obtained. The planetary equation of motion and the equation of motion of a photon in the vicinity of an oblate spheroid are derived. These equations have additional terms not found in Schwarzschild's space time.

1 Introduction

It is well known experimentally that the Sun and planets in the solar system are more precisely oblate spheroidal in geometry [1–6]. The oblate spheroidal geometries of these bodies have corresponding effects on their gravitational fields and hence the motion of test particles and photons in these fields.

It is also well known that satellite orbits around the Earth are governed by not only the simple inverse distance squared gravitational fields due to perfect spherical geometry. They are also governed by second harmonics (pole of order 3) as well as fourth harmonics (pole of order 5) of gravitational scalar potential not due to perfect spherical geometry. Therefore, towards the more precise explanation and prediction of satellite orbits around the Earth, Stern [3] and Garfinkel [4] introduced the method of quadratures for approximating the second harmonics of the gravitational scalar potential of the Earth due to its spheroidal Earth. This method was improved by O'Keefe [5]. Then in 1960, Vinti [6] suggested a general mathematical form of the gravitational scalar potential of the spheroidal Earth and how to estimate some of the parameters in it for use in the study of satellite orbits. Recently [1], an expression for the scalar potential exterior to a homogeneous oblate spheroidal body was derived. Most recently, Ioannis and Michael [3] proposed the Sagnac interferometric technique as a way of detecting corrections to the Newton's gravitational scalar potential exterior to an oblate spheroid.

In this article, we formulate the metric tensor for the gravitational field exterior to massive homogeneous oblate spheroidal bodies as a direct extension of Schwarzschild's metric. This metric tensor is then used to study orbits in homogeneous oblate spheroidal space time.

2 Metric tensor exterior to a homogeneous oblate spheroid

The invariant world line element in the exterior region of all possible static spherical distributions of mass is given [1, 7] as

$$c^2 d\tau^2 = c^2 \left[1 + \frac{2f(r,\theta,\phi)}{c^2}\right] dt^2 - \\ - \left[1 + \frac{2f(r,\theta,\phi)}{c^2}\right]^{-1} dr^2 - r^2 d\theta^2 - r^2 \sin^2\theta \, d\phi^2 \quad (2.1)$$

where $f(r,\theta,\phi)$ is a generalized arbitrary function determined by the distribution of mass or pressure and possess all the symmetries of the mass distribution. It is a well known fact of general relativity that $f(r,\theta,\phi)$ is approximately equal to Newton's gravitational scalar potential in the space-time exterior to the mass or pressure distributions within regions of spherical geometry [1, 7]. For a static homogeneous spherical body ("Schwarzschild's body") the arbitrary function takes the form $f(r)$.

Now, let "Schwarzschild's body" be transformed, by deformation, into an oblate spheroidal body in such a way that its density and total mass remain the same and its surface parameter is given in oblate spheroidal coordinates [1] as

$$\xi = \xi_0 \,;\ \text{constant}. \quad (2.2)$$

The general relativistic field equation exterior to a homogeneous static oblate spheroidal body is tensorially equivalent to that of a static homogeneous spherical body ("Schwarzschild's body") [1, 7] hence, is related by the transformation from spherical to oblate spheroidal coordinates. Therefore, to get the corresponding invariant world line element in the exterior region of a static homogeneous oblate spheroidal mass, we first replace the arbitrary function in Schwarzschild's field, $f(r)$ by the corresponding arbitrary function exterior to static homogenous oblate spheroidal bodies, $f(\eta,\xi)$. Thus, the function $f(\eta,\xi)$ is approximately equal to the gravitational potential exterior to a homogeneous spheroid. The gravitational scalar potential exterior to a homogeneous static oblate spheroid [1] is given as

$$f(\eta,\xi) = B_0 Q_0(-i\xi) P_0(\eta) + B_2 Q_2(-i\xi) P_2(\eta) \quad (2.3)$$

$$g_{00} = \left(1 + \frac{2}{c^2} f(\eta, \xi)\right) \tag{2.10}$$

$$g_{11} = -\frac{a^2}{1+\xi^2-\eta^2}\left[\eta^2\left(1+\frac{2}{c^2}f(\eta,\xi)\right)^{-1} + \frac{\xi^2(1+\xi^2)}{(1-\eta^2)}\right] \tag{2.11}$$

$$g_{12} \equiv g_{21} = -\frac{a^2\eta\xi}{1+\xi^2-\eta^2}\left[1-\left(1+\frac{2}{c^2}f(\eta,\xi)\right)^{-1}\right] \tag{2.12}$$

$$g_{22} = -\frac{a^2}{1+\xi^2-\eta^2}\left[\xi^2\left(1+\frac{2}{c^2}f(\eta,\xi)\right)^{-1} + \frac{\eta^2(1-\eta^2)}{(1+\xi^2)}\right] \tag{2.13}$$

$$g_{33} = -a^2(1+\xi^2)(1-\eta^2) \tag{2.14}$$

$$g_{\mu\nu} = 0; \text{ otherwise} \tag{2.15}$$

$$g^{00} = \left[1 + \frac{2}{c^2} f(\eta, \xi)\right]^{-1} \tag{2.16}$$

$$g^{11} = \frac{-\left(1-\eta^2\right)\left(1+\xi^2-\eta^2\right)\left[\eta^2\left(1-\eta^2\right)+\xi^2\left(1+\xi^2\right)\left(1+\frac{2}{c^2}f(\eta,\xi)\right)^{-1}\right]}{a^2\left(1+\frac{2}{c^2}f(\eta,\xi)\right)^{-1}\left[\eta^2(1-\eta^2)+\xi^2(1+\xi^2)\right]^2} \tag{2.17}$$

$$g^{12} \equiv g^{21} = \frac{-\eta\xi\left(1-\eta^2\right)\left(1+\xi^2\right)\left(1+\xi^2-\eta^2\right)\left[1-\left(1+\frac{2}{c^2}f(\eta,\xi)\right)^{-1}\right]}{a^2\left(1+\frac{2}{c^2}f(\eta,\xi)\right)^{-1}\left[\eta^2(1-\eta^2)+\xi^2(1+\xi^2)\right]^2} \tag{2.18}$$

$$g^{22} = \frac{-\left(1+\xi^2\right)\left(1+\xi^2-\eta^2\right)\left[\xi^2\left(1+\xi^2\right)+\eta^2\left(1-\eta^2\right)\left(1+\frac{2}{c^2}f(\eta,\xi)\right)^{-1}\right]}{a^2\left(1+\frac{2}{c^2}f(\eta,\xi)\right)^{-1}\left[\eta^2(1-\eta^2)+\xi^2(1+\xi^2)\right]^2} \tag{2.19}$$

$$g^{33} = -\left[a^2\left(1+\xi^2\right)\left(1-\eta^2\right)\right]^{-1} \tag{2.20}$$

$$g^{\mu\nu} = 0; \text{ otherwise} \tag{2.21}$$

where Q_O and Q_2 are the Legendre functions linearly independent to the Legendre polynomials P_0 and P_2 respectively. B_0 and B_2 are constants.

Secondly, we transform coordinates from spherical to oblate spheroidal coordinates;

$$(ct, r, \theta, \phi) \to (ct, \eta, \xi, \phi) \tag{2.4}$$

on the right hand side of equation (2.1).

From the relation between spherical polar coordinates and Cartesian coordinates as well as the relation between oblate spheroidal coordinates and Cartesian coordinates [8] it can be shown trivially that

$$r(\eta, \xi, \phi) = a(1+\xi^2-\eta^2)^{\frac{1}{2}} \tag{2.5}$$

and

$$\theta(\eta, \xi, \phi) = \cos^{-1}\left[\frac{\eta\xi}{(1+\xi^2-\eta^2)^{\frac{1}{2}}}\right] \tag{2.6}$$

where a is a constant parameter. Therefore,

$$dr = a(1+\xi^2-\eta^2)^{-\frac{1}{2}}(\xi d\xi - \eta d\eta) \tag{2.7}$$

and

$$d\theta = -\frac{\xi(1+\xi^2)^{\frac{1}{2}}}{(1-\eta^2)^{\frac{1}{2}}(1+\xi^2-\eta^2)}\,d\eta - \\ -\frac{\eta(1-\eta^2)^{\frac{1}{2}}}{(1+\xi^2)^{\frac{1}{2}}(1+\xi^2-\eta^2)}\,d\xi\,. \tag{2.8}$$

Also,

$$\sin^2\theta = \frac{(1+\xi^2)(1-\eta^2)}{(1+\xi^2-\eta^2)}\,. \tag{2.9}$$

Substituting equations (2.5), (2.7), (2.8) and (2.9) into equation (2.1) and simplifying yields the following components of the covariant metric tensor in the region exterior to a

$$L = \frac{1}{c}\left(-g_{00}\left(\frac{dt}{d\tau}\right)^2 - g_{11}\left(\frac{d\eta}{d\tau}\right)^2 - 2g_{12}\left(\frac{d\eta}{d\tau}\right)\left(\frac{d\xi}{d\tau}\right) - g_{22}\left(\frac{d\xi}{d\tau}\right)^2 - g_{33}\left(\frac{d\phi}{d\tau}\right)^2\right)^{\frac{1}{2}} \tag{3.1}$$

$$L = \frac{1}{c}\left[-\left(1+\frac{2}{c^2}f(\eta,\xi)\right)\dot{t}^2 - \frac{a^2\xi^2}{1+\xi^2}\left(1+\frac{2}{c^2}f(\eta,\xi)\right)^{-1}\dot{\xi}^2 + a^2(1+\xi^2)\dot{\phi}^2\right]^{\frac{1}{2}} \tag{3.2}$$

static homogeneous oblate spheroid in oblate spheroidal coordinates (2.10)–(2.15).

The covariant metric tensor, equations (2.10) to (2.15) is the most fundamental geometric parameter required to study general relativistic mechanics in static homogeneous oblate spheroidal gravitational fields. The covariant metric tensor obtained above for gravitational fields exterior to oblate spheroidal masses has two additional non-zero components g_{12} and g_{21} not found in Schwarzschild field [7]. Thus, the extension from Schwarzschild field to homogeneous oblate spheroidal gravitational fields has produced two additional non-zero tensor components and hence this metric tensor field is unique. This confirms the assertion that oblate spheroidal gravitational fields are more complex than spherical fields and hence general relativistic mechanics in this field is more involved [6].

The contravariant metric tensor for this gravitational field is found to be given explicitly as (2.16)–(2.21).

It can be shown that the coefficients of affine connection for the gravitational field exterior to a homogenous oblate spheroidal mass are given in terms of the metric tensors for the gravitational field as

$$\Gamma^0_{01} \equiv \Gamma^0_{10} = \frac{1}{2}\,g^{00}g_{00,1}\,, \tag{2.22}$$

$$\Gamma^0_{02} \equiv \Gamma^0_{20} = \frac{1}{2}\,g^{00}g_{00,2}\,, \tag{2.23}$$

$$\Gamma^1_{00} = -\frac{1}{2}\,g^{11}g_{00,1} - \frac{1}{2}\,g^{12}g_{00,2}\,, \tag{2.24}$$

$$\Gamma^1_{11} = \frac{1}{2}\,g^{11}g_{11,1} + \frac{1}{2}\,g^{12}\left(2g_{12,1} - g_{11,2}\right)\,, \tag{2.25}$$

$$\Gamma^1_{12} \equiv \Gamma^1_{21} = \frac{1}{2}\,g^{11}g_{11,2} + \frac{1}{2}\,g^{12}g_{22,1}\,, \tag{2.26}$$

$$\Gamma^1_{22} = \frac{1}{2}\,g^{11}\left(2g_{12,2} - g_{22,1}\right) + \frac{1}{2}\,g^{12}g_{22,2}\,, \tag{2.27}$$

$$\Gamma^1_{33} = -\frac{1}{2}\,g^{11}g_{33,1} - \frac{1}{2}\,g^{12}g_{33,2}\,, \tag{2.28}$$

$$\Gamma^2_{00} = -\frac{1}{2}\,g^{21}g_{00,1} - \frac{1}{2}\,g^{22}g_{00,2}\,, \tag{2.29}$$

$$\Gamma^2_{11} = \frac{1}{2}\,g^{21}g_{11,1} + \frac{1}{2}\,g^{22}\left(2g_{12,1} - g_{11,2}\right)\,, \tag{2.30}$$

$$\Gamma^2_{12} \equiv \Gamma^2_{21} = \frac{1}{2}\,g^{21}g_{11,2} + \frac{1}{2}\,g^{22}g_{22,1}\,, \tag{2.31}$$

$$\Gamma^2_{22} = \frac{1}{2}\,g^{21}\left(2g_{12,2} - g_{22,1}\right) + \frac{1}{2}\,g^{22}g_{22,2}\,, \tag{2.32}$$

$$\Gamma^2_{33} = -\frac{1}{2}\,g^{21}g_{33,1} - \frac{1}{2}\,g^{22}g_{33,2}\,, \tag{2.33}$$

$$\Gamma^3_{13} \equiv \Gamma^3_{31} = \frac{1}{2}\,g^{33}g_{33,1}\,, \tag{2.34}$$

$$\Gamma^3_{23} \equiv \Gamma^3_{32} = \frac{1}{2}\,g^{33}g_{33,2}\,, \tag{2.35}$$

$$\Gamma^\delta_{\alpha\beta} = 0;\ \text{otherwise}, \tag{2.36}$$

where comma as in usual notation denotes partial differentiation with respect to $\eta(1)$ and $\xi(2)$.

3 Conservation of total energy and angular momentum

Many physical theories start by specifying the Lagrangian from which everything flows. We would adopt the same attitude with gravitational fields exterior to homogenous oblate spheroidal masses. The Lagrangian in the space time exterior to our mass or pressure distribution is defined explicitly in oblate spheroidal coordinates using the metric tensor as (3.1) [7, 9], where τ is the proper time.

For orbits confined to the equatorial plane of a homogenous oblate spheroidal mass [1, 8]; $\eta \equiv 0$ (or $d\eta \equiv 0$) and substituting the explicit expressions for the components of metric tensor in the equatorial plane yields (3.2), where the dot denotes differentiation with respect to proper time.

It is well known that the gravitational field is a conservative field. The Euler-Lagrange equations for a conservative system in which the potential energy is independent of the generalized velocities is written as [7, 9];

$$\frac{\partial L}{\partial x^\alpha} = \frac{d}{d\tau}\left(\frac{\partial L}{\partial \dot{x}^\alpha}\right) \tag{3.3}$$

but

$$\frac{\partial L}{\partial x^0} \equiv \frac{\partial L}{\partial t} = 0 \tag{3.4}$$

and thus from equation (3.3), we deduce that

$$\frac{\partial L}{\partial \dot{t}} = \text{constant}. \tag{3.5}$$

From equation (3.3), it can be shown using equation (3.5) that

$$\left(1+\frac{2}{c^2}\,f(\eta,\xi)\right)\dot{t} = k, \quad \dot{k} = 0 \tag{3.6}$$

where k is a constant. This is the law of conservation of energy in the equatorial plane of the gravitational field exterior to an oblate spheroidal mass [7, 9].

The law of conservation of total energy, equation (3.6) can also be obtained by constructing the coefficients of affine connection for this gravitational field and evaluating the time equation of motion for particles of non-zero rest masses. The general relativistic equation of motion for particles of non-zero rest masses in a gravitational field are given by

$$\frac{d^2x^\mu}{d\tau^2} + \Gamma^\mu_{\nu\lambda}\left(\frac{dx^\nu}{d\tau}\right)\left(\frac{dx^\lambda}{d\tau}\right) = 0 \tag{3.7}$$

where $\Gamma^\mu_{\nu\lambda}$ are the coefficients of affine connection for the gravitational field.

Setting $\mu = 0$ in equation (3.7) and substituting the explicit expressions for the affine connections Γ^0_{01} and Γ^0_{02} gives

$$\ddot{t} + \frac{2}{c^2}\left(1 + \frac{2}{c^2}f(\eta,\xi)\right)^{-1} \times \times \left(\dot{\eta}\frac{\partial f(\eta,\xi)}{\partial \eta} + \dot{\xi}\frac{\partial f((\eta,\xi))}{\partial \xi}\right)\dot{t} = 0\,. \tag{3.8}$$

Integrating equation (3.8) yields

$$\dot{t} = k\left(1 + \frac{2}{c^2}f(\eta,\xi)\right)^{-1} \tag{3.9}$$

where k is a constant of integration. Thus, the two methods yield same results.

Also, the Lagrangian for this gravitational field is invariant to azimuthal angular rotation and hence angular momentum is conserved, thus;

$$\frac{\partial L}{\partial \phi} = 0 \tag{3.10}$$

and from Lagrange's equation of motion,

$$\left(1 + \xi^2\right)\dot{\phi} = l, \quad \dot{l} = 0 \tag{3.11}$$

where l is a constant. This is the law of conservation of angular momentum in the equatorial plane of the gravitational field exterior to a static homogeneous oblate spheroidal body.

This expression can also be obtained by solving the azimuthal equation of motion for particles of non-zero rest masses in this gravitational field. Setting $\mu = 3$ in equation (3.7) and substituting the relevant affine connection coefficients gives the azimuthal equation of motion as

$$\frac{d}{d\tau}\left(\ln\dot{\phi}\right) + \frac{d}{d\tau}\left(\ln\left(1-\eta^2\right)\right) + + \frac{d}{d\tau}\left(\ln\left(1+\xi^2\right)\right) = 0\,. \tag{3.12}$$

Thus, by integrating equation (3.12), it can be shown that the azimuthal equation of motion for our gravitational field is given as

$$\dot{\phi} = \frac{l}{\left(1-\eta^2\right)\left(1+\xi^2\right)}\,, \tag{3.13}$$

where l is a constant of motion. l physically corresponds to the angular momentum and hence equation (3.13) is the Law of Conservation of angular momentum in this gravitational field [7, 9]. It does not depend on the gravitational potential and is of same form as that obtained in Schwarzschild's Field and Newton's dynamical theory of gravitation [7, 9]. Note that equation (3.13) reduces to equation (3.11) if the particles are confined to move in the equatorial plane of the oblate spheroidal mass.

4 Orbits in homogeneous oblate spheroidal gravitational fields

It is well known [7, 9] that the Lagrangian $L = \epsilon$, with $\epsilon = 1$ for time like orbits and $\epsilon = 0$ for null orbits. Setting $L = \epsilon$ in equation (3.2), substituting equations (3.6) and (3.11) and simplifying yields;

$$\frac{a^2\xi^2}{\left(1+\xi^2\right)}\dot{\xi}^2 + \frac{a^2l^2}{\left(1+\xi^2\right)}\left(1 + \frac{2}{c^2}f(\eta,\xi)\right) - - 2\epsilon^2 f(\eta,\xi) = c^2\epsilon^2 + 1\,. \tag{4.1}$$

In most applications of general relativity, we are more interested in the shape of orbits (that is, as a function of the azimuthal angle) than in their time history [7]. Hence, it is instructive to transform equation (4.1) into an equation in terms of the azimuthal angle ϕ. Now, let us consider the following transformation;

$$\xi = \xi(\phi) \text{ and } u(\phi) = \frac{1}{\xi(\phi)}\,, \tag{4.2}$$

thus,

$$\dot{\xi} = -\frac{l}{1+u^2}\frac{du}{d\phi}\,. \tag{4.3}$$

Now, imposing equations (4.2) and (4.3) on equation (4.1) and simplifying yields (4.4). Differentiating equation (4.4) gives (4.5).

For time like orbits $(\epsilon = 1)$, equation (4.5) reduces to (4.6).

This is the planetary equation of motion in this gravitational field. It can be solved to obtain the perihelion precision of planetary orbits. It has additional terms (resulting from the oblateness of the body), not found in the corresponding equation in Schwarzschild's field [7].

Light rays travel on null geodesics $(\epsilon = 0)$ and hence equation (4.5) becomes (4.7).

In the limit of special relativity, some terms in equation (4.7) vanish and the equation becomes (4.8).

Equation (4.7) is the photon equation of motion in the vicinity of a static massive homogenous oblate spheroidal body. The equation contains additional terms not found in the corresponding equation in Schwarzschild's field. The solution of the special relativistic case, equation (4.8) can be used to solve the general relativistic equation, (4.7). This can

$$\frac{1}{\left(1+u^2\right)^3}\left(\frac{du}{d\phi}\right)^2+\frac{u^2}{1+u^2}\left(1+\frac{2}{c^2}f(u)\right)-\frac{2\epsilon^2 f(u)}{a^2l^2}=\frac{c^2\epsilon^2+1}{a^2l^2}\,. \tag{4.4}$$

$$\frac{d^2u}{d\phi^2}-3u\left(1+u^2\right)\frac{du}{d\phi}+\frac{\left(u+u^2\right)}{2}\left(u^2-u+2\right)\left(1+\frac{2}{c^2}f(u)\right)=\left(\frac{1+u^2}{acl}\right)^2\left(a^2c^2l^2-\epsilon^2-\epsilon^2u^2\right)\frac{d}{du}f(u)\,. \tag{4.5}$$

$$\frac{d^2u}{d\phi^2}-3u\left(1+u^2\right)\frac{du}{d\phi}+\frac{\left(u+u^2\right)}{2}\left(u^2-u+2\right)\left(1+\frac{2}{c^2}f(u)\right)=\left(\frac{1+u^2}{acl}\right)^2\left(a^2c^2u^2-1-u^2\right)\frac{d}{du}f(u)\,. \tag{4.6}$$

$$\frac{d^2u}{d\phi^2}-3u\left(1+u^2\right)\frac{du}{d\phi}+\frac{\left(u+u^2\right)}{2}\left(u^2-u+2\right)\left(1+\frac{2}{c^2}f(u)\right)=\frac{u^2}{c^2}\left(1+u^2\right)^2\frac{d}{du}f(u)\,. \tag{4.7}$$

$$\frac{d^2u}{d\phi^2}-3u\left(1+u^2\right)\frac{du}{d\phi}+\frac{\left(u+u^2\right)}{2}\left(u^2-u+2\right)=0\,. \tag{4.8}$$

be done by taking the general solution of equation (4.7) to be a perturbation of the solution of equation (4.8). The immediate consequence of this analysis is that it will produce an expression for the total deflection of light grazing a massive oblate spheroidal body such as the Sun and the Earth.

5 Remarks and conclusion

The immediate consequences of the results obtained in this article are:

1. The equations derived are closer to reality than those in Schwarzschild's gravitational field. In Schwarzschild's space time, the Sun is assumed to be a static perfect sphere. The Sun has been proven to be oblate spheroidal in shape and our analysis agrees perfectly with this shape;
2. The planetary equation of motion and the photon equation of motion have additional spheroidal terms not found in Schwarzschild's field. This equations are opened up for further research work and astrophysical interpretation.
3. In approximate oblate spheroidal gravitational fields, the arbitrary function $f(\eta,\xi)$ can be conveniently equated to the gravitational scalar potential exterior to an oblate spheroid [7]. Thus for these fields, the complete solutions for our equations of motion can be constructed;
4. Einstein's field equations constructed using our metric tensor has only one unknown, $f(\eta,\xi)$. A solution of these field equations will give explicit expressions for the function, $f(\eta,\xi)$ which can then be used in our equations of motion.

Submitted on April 29, 2009 / Accepted on May 12, 2009

References

1. Howusu S.X.K. The 210 astrophysical solutions plus 210 cosmological solutions of Einstein's geometrical gravitational field equations. Jos University Press, Jos, 2007.
2. Haranas I.I. and Harney M. Detection of the relativistic corrections to the gravitational potential using a Sagnac interferometer. *Progress in Physics*, 2008, v. 3, 3–8.
3. Stern T.E. Theory of satellite orbits. *Astronomical Journal*, 1957, v. 62, 96.
4. Garfinkel B. Problem of quadratures. *Astronomical Journal*, 1958, v. 63, 88.
5. O'Keefe J.A, Ann E., and Kenneth S.R. The gravitational field of the Earth. *Astronomical Journal*, 1959, v. 64, 245.
6. Vinti J.P. New approach in the theory of satellite orbits. *Physical Review Letters*, 1960, v. 3(1), 8.
7. Chifu E.N., Howusu S.X.K. and Lumbi L.W. Relativistic mechanics in gravitational fields exterior to rotating homogeneous mass distributions within regions of spherical geometry. *Progress in Physics*, 2009, v. 3, 18–23.
8. Arfken G. Mathematical methods for physicists. 5th edition, Academic Press, New York, 1995.
9. Peter K.S.D. An introduction to tensors and relativity. Cape Town, 2000, 51–110.

Primes, Geometry and Condensed Matter

Riadh H. Al Rabeh
University of Basra, Basra, Iraq
E-mail: alrabeh_rh@yahoo.com

Fascination with primes dates back to the Greeks and before. Primes are named by some "the elementary particles of arithmetic" as every nonprime integer is made of a unique set of primes. In this article we point to new connections between primes, geometry and physics which show that primes could be called "the elementary particles of physics" too. This study considers the problem of closely packing similar circles/spheres in 2D/3D space. This is in effect a discretization process of space and the allowable number in a pack is found to lead to some unexpected cases of prime configurations which is independent of the size of the constituents. We next suggest that a non-prime can be considered geometrically as a symmetric collection that is separable (factorable) into similar parts- six is two threes or three twos for example. A collection that has no such symmetry is a prime. As a result, a physical prime aggregate is more difficult to split symmetrically resulting in an inherent stability. This "number/physical" stability idea applies to bigger collections made from smaller (prime) units leading to larger stable prime structures in a limitless scaling up process. The distribution of primes among numbers can be understood better using the packing ideas described here and we further suggest that differing numbers (and values) of distinct prime factors making a nonprime collection is an important factor in determining the probability and method of possible and subsequent disintegration. Disintegration is bound by energy conservation and is closely related to symmetry by Noether theorems. Thinking of condensed matter as the packing of identical elements, we examine plots of the masses of chemical elements of the periodic table, and also those of the elementary particles of physics, and show that prime packing rules seem to play a role in the make up of matter. The plots show convincingly that the growth of prime numbers and that of the masses of chemical elements and of elementary particles do follow the same trend indeed.

1 Introduction

Primes have been a source of fascination for a long time- as far back as the Greeks and much before. One reason for this fascination is the fact that every non-prime is the product of a unique set of prime numbers, hence the name *elementary particles of arithmetic*, and that although primes are distributed seemingly randomly among other integers, they do have regular not fully understood patterns (see [1] for example). The literature is rich in theories on primes but one could say that none-to-date have managed to make the strong connection between primes and physics that is intuitively felt by many. One recent attempt in this direction is [2], wherein possible connections between the atomic structure and the zeros of the Zeta function — closely connected to primes — are investigated. We quote from this reference, "Why the periodicity of zeros from the Riemann-Zeta function would match the spacing of energy levels in high-Z nuclei still remains a mystery".

In the present work we attempt to relate primes to both geometry and physics. We start with the packing of circles in a plane (or balls on a plane)- all of the same size, and pose a question; *In a plane, what is the condition for packing an integral number of identical circles to form a larger circle- such that both the diameter and circumference of the larger circle contain an integral numbers of the small circle*? The problem is essentially the same when the 2D circles are replaced with balls on a tray. A surprising result here is the appearance of only two prime numbers 2 and 3 in the answer and *only one of them is nontrivial- the number 3*. This gives such numbers a fundamental and natural importance in geometry. We may view this number as a "discretization number of the continuous $3D$ spaces". We further study this matter and shed light (using balls to represent integers) on bounds on the growth of primes- namely the well known logarithmic law in the theory of primes. Still further, we coin the notion that distinct prime factors in the packing of composite collections/grouping can have a profound influence on the behaviour of such collections and the manner they react with other collections built of some different or similar prime factors. As many physics models of condensed matter assume identical elements for simple matter (photons, boson and fermion statistics and the MIT bag model [3, 6] are examples) we examine the applicability of our packing rules in such case and conclude that condensed matter do seem to follow the packing rules discussed here.

2 Theory

Consider the case of close packing of circles on a plane so as to make a bigger circle (Figure 1). The ratio of the radius of the large circle to that of the small circle is; $R/r = 1+1/\sin t$,

1	**7**	**13**	**19**	25	**31**	**37**	**43**	49	55	**61**	**67**	**73**	**79**	85	91	**97**...
2	8	14	20	26	32	38	44	50	56	62	68	74	80	86	92	98...
3	9	15	21	27	33	39	45	51	57	63	69	75	81	87	93	99...
4	10	16	22	28	34	40	46	52	58	64	70	76	82	88	94	100...
5	**11**	**17**	**23**	**29**	35	**41**	**47**	**53**	**59**	65	**71**	77	**83**	**89**	95	**101**...
6	12	18	24	30	36	42	48	54	60	66	72	78	84	90	96	102...

Table 1: Integers arranged in columns of six.

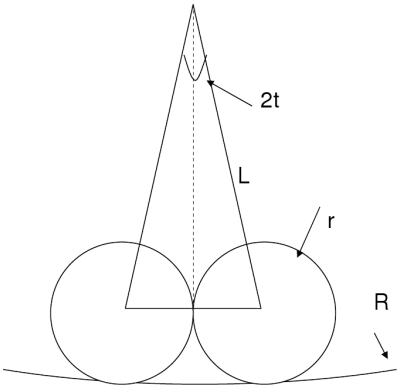

Fig. 1: Close packing of an integral number of circles/balls on a plane have one nontrivial solution- 6 balls, plus one at the centre (see also Figure 2). Here in Fig. 1: $L\sin t = r$; $t = \pi/n$; $R = L + r$; $R/r = 1 + 1/\sin t$. For integral ratio R/r, t must be $\pi/2$ or $\pi/6$ and $L/r = 2, 3$.

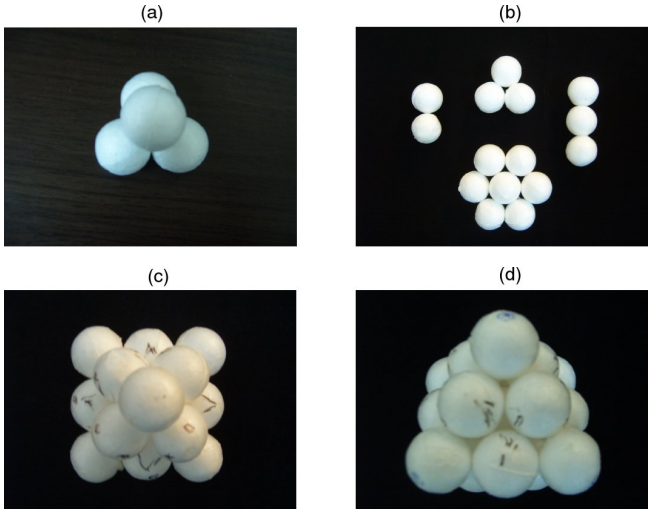

Fig. 2: Packing of 2, 3, 4, 7 & 19 (=7+(3+3)+(3+3)) balls in 3D (a, b). The 19 ball case possesses six side and eight side symmetries (c, d).

where t is half the angle between radial lines through the centers of any two adjacent circles. For this number to be an integer, the quantity $(1/\sin t)$ must be an integer and hence the angle t must be either 30 or 90 degrees. Thus R/r should be either three or two (see Figure 2b). That is; the diameter can be either two or three circles wide. The number 3 is nontrivial, and gives six circles touching each other, and all in turn tangent to a seventh circle at the centre.

Clearly the arrangement of balls on a plane does follow exactly the same pattern leading to six balls touching in pairs and surrounding a seventh ball (touching all other six) at the center. This result is unique and is independent of the size of the balls involved. It is rather remarkable as it gives the number 6 a special stature in the physics of our 3D space, parallel to that of the number π in geometry. Such stature must have been realized in the past by thinkers as far back as the Babylonian times and the divine stature given to such a number in the cultures of many early civilizations- six working days in a week and one for rest is one example, the six prongs of the star of David and the seven days of creation as well as counting in dozens might have also been inspired by the same. Before this, the Bees have discovered the same fact and started building their six sided honey combs accordingly.

Consider now the set of prime numbers. It is known that every prime can be written as $6n \pm 1$, where n is an integer. *That is* the number six is a generator of all primes. Further, we note that whereas the number six is divisible into 2 (threes) or 3 (twos), an addition of one unit raises the number to seven- a prime and not divisible into any smaller symmetric entities. Put differently, an object composed of six elements can easily break into smaller symmetrical parts, whereas an object made of 7 is more stable and not easily breakable into symmetric parts. We know from physics that symmetry in interactions is demanded by many conservation laws. In fact symmetry and conservation are tightly linked by Noether theorems- such that symmetry can always be translated to a conservation law and vice versa. When we have a group of highly symmetric identical items, the addition of one at the centre of the collection can make it a prime.

Now if we arrange natural numbers in columns of six as shown in Table 1, we see clearly that all primes fall along two lines- top line for the $6n + 1$ type and the bottom line for the case of $6n - 1$ type primes (text in bold). If these are balls arranged physically on discs six each and on top of each other, the two lines will appear diametrically opposite on a long cylinder. Thus there are two favourite lines along which all primes fall in a clear display of a sign of the close connection between primes geometry and physics.

We see then that the connection between primes and geometry is an outcome of how the plane and the space lend themselves to discretization, when we pair such blocks with

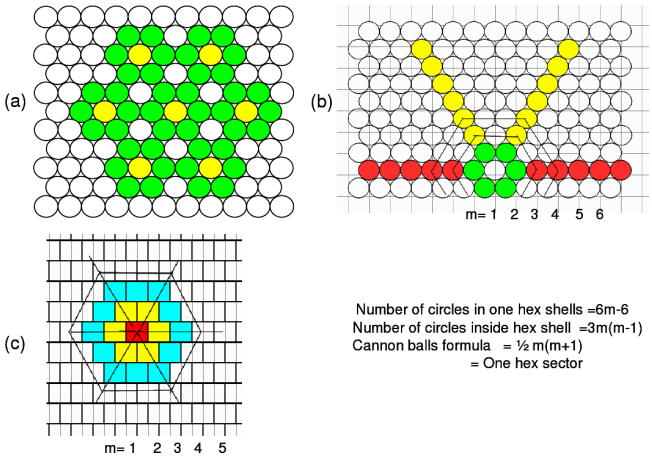

Fig. 3: (a) Scaling up using small blocks of seven to make larger blocks of seven; (b) Tight packing of circles naturally resulting in hex objects made of hex layers. The number of circles in each layer strip increases in steps of 6. Note that each hex sector has cannon balls (or conical) packing structure; (c) Easy to construct (square) brick structure to formally replace circles.

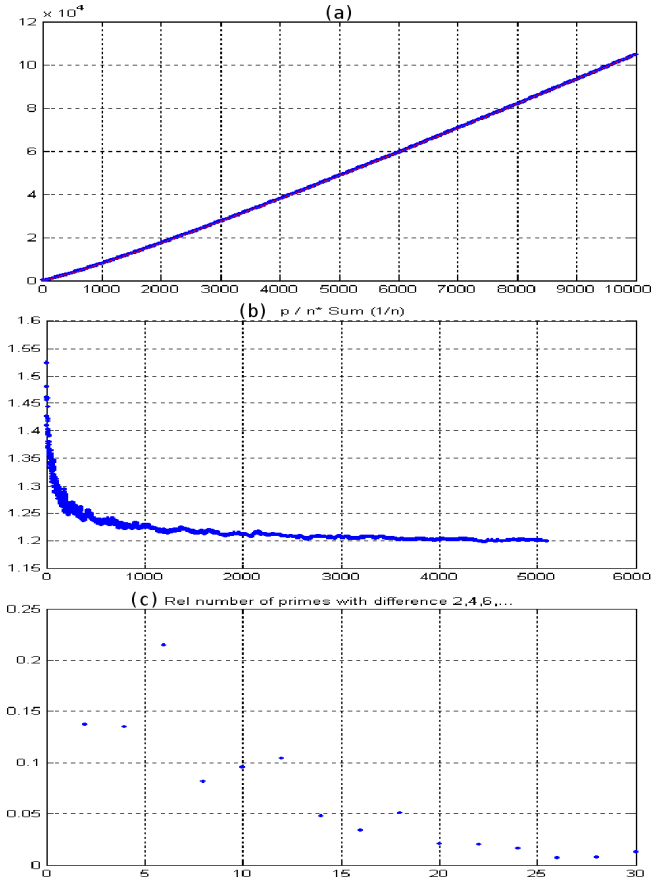

Fig. 4: (a) Two overlapping plots of the first 104 primes: (1, 2, 3, 5, $\cdots$, 104729) compared to fitting plot (–), $y = (\ln \pi) \cdot n \cdot \ln n$ (n = serial positions of prime numbers) (.); (b) Ratio of a prime (p) to $n \sum 1/n$; (c) Relative number of primes with differences of 2, 4, 6, $\cdots$ 30. Peaks occur at differences of 6, 12, 18, 24, 30.

the set of positive integers. We may note also that the density of $6n-1$ and $6n+1$ type primes is the same with respect to the integers. Moreover, if we take the difference between prime pairs, the distribution of the difference peaks at 6 and all multiples of it, but diminishes as the difference increases (Figure 4c).

In a violent interaction between two prime groups, one or more of the groups could momentarily loose a member or more leaving a non-prime group which then become less stable and divisible into symmetric parts according to the factors making the collection. Clearly in this case, the few none primes neighbouring a prime also become important, and would contribute to the rules of break-up, to the type of products and to the energy required in each case.

Our packing endeavour can continue beyond 7 to make larger 3D objects (Figure 2). A stable new arrangement can result from the addition of 6 balls- 3 on each side (top and bottom) making an object of 13 balls- a new prime figure. Further 6 balls can be put symmetrically secured on top and bottom to give an object of 19 balls. This last case in addition to being a prime collection has an interesting shape feature. It has six and eight face symmetries and fairly smooth faces as shown in Figures 2(c, d), which could give rise to two different groups of 19 ball formations. Further addition of 6's is possible, but the resulting object appears less strong. To go a different direction, we can instead consider every 7, 13 or 19 ball objects as the new building unit and use it to form further new collections of objects of prime grouping. Clearly this can be continued in an endless scaling up process (Figure 3b). Scaling is a prominent phenomenon in physical structures. Fig. 3b shows that, in a plane, our packing problem and also that of the packing of cannon-balls [5] are only subsets of the general densest packing problem and thus it truly is a discretization process of space. We note also that circles can be replaced with squares placed in a brick like structure provided we only think of the centres of these squares.

In the process of adding new rings of circles to form larger objects, both prime and nonprime numbers are met. A prime is formed every time we have highly symmetric combination with one to be added or subtracted to it to break the symmetry and produce a prime. If we consider the number of circles added in each ring in the case of circular geometry (the same applies to hex geometry with small modification), the radius of a ring is given by $mr+m$, where m is the number of layers and r is the radius of one small circle set to unity. The number of circles in each ring is estimated by the integer part of $2\pi m$. For the next ring we substitute $(m+1)$ for m in the above expressions and obtain $2\pi(m+1)$ for a ring. The *relative* increase in the number of circles is the difference between these two divided by the circumference which gives $1/m$. The relative (or probable) number of primes for m-th ring should be taken to come from the contribution of all the items in the ring and this is proportional to $\sum 1/m$ for large m. The actual number of primes is an integral of this given by $m \sum 1/m$

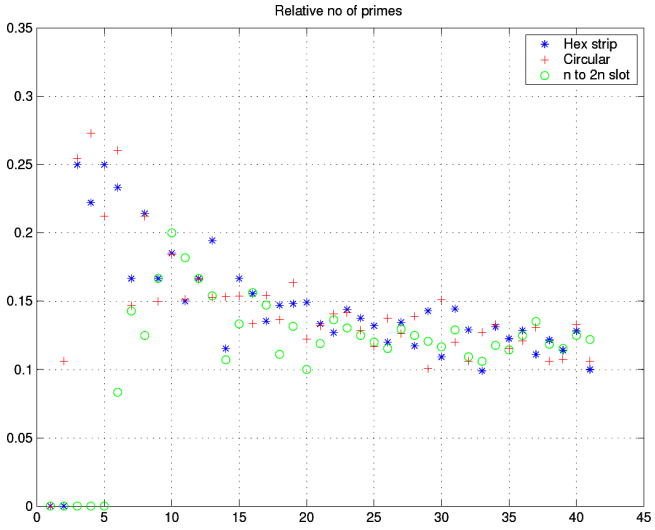

Fig. 5: Relative number of primes in (50000 integer sample): Hex strips $m : m+1$ (*); Circular rings $m : m+1$, m is the number of rings of circles around the centre (+); Interval $n : 2n$, n is the serial number of a prime (○).

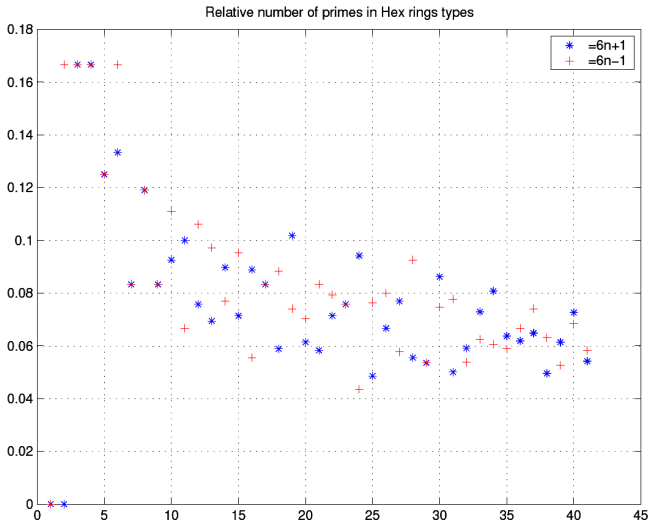

Fig. 6: Relative number of primes in hex strips (see Figure 3b); primes of the form $6n+1$ (*); primes of the form $6n-1$, n is the number of prims around the centre (+).

since both the radius of a circular strip and the number of circles in that strip are proportional to m. Fig. 5 gives the relative number of primes in one strip and the trend is of the form $a/\log m$, thus confirming the reasoning used above.

Figure 4b gives a plot of the ratio $p/(n\sum 1/n)$ where p is the value of the n-th prime for some 50000 primes sample which, for large n, equals the number of integers/circles in the whole area. Since $\sum 1/n \sim \ln(n)$ for large n, we see that this ratio tends to a constant in agreement with the results of the prime number theory (see [1] for example).

Further, there are few results from the theory of primes that can also be interpreted in support of the above arguments. For example the well known conjectures suggesting that there is always a prime between m and $2m$ and also between m^2 and $(m+1)^2$ [7] can respectively be taken to correspond to the symmetrical duplication of an area and to the ring regions between two concentric circles must contain at least one prime. That is if the original area or sector can produce a prime, then duplicating it symmetrically or adding one more sector to it will produce at least one prime. The number of primes in each of the above cases and that of a hex region are of course more than one and the results from a sample of (1–50000) integers are plotted in Figure 5. The data is generated using a simple Excel-Basic program shown below;

```
%Open excel > Tools > micro > Basic Editor > paste and run
subroutine prime( )
kk=0:
% search divisibility up to square root
for ii=1 to 1e6: z=1: iis=int(sqr(ii+1)+1):
% test divisibility
for jj=2 to iis: if ii-int(ii/jj)*jj=0 then z=0: next jj:
% write result in excel sheet
if z=1 then kk=kk+1: if z=1 then cells(kk,1)=ii: next ii:
end sub:
```

Concentric circles can be drawn on top of the hexagons shown in Figure 3, and the number of smaller circles tangent to the large circles then occur in a regular and symmetrical way when the number of circular layers is a prime. Some attempt was made by one researcher to explain this by forming and solving the associated Diophantine equations. It is noted here that potential energy and forces are determined by radial distances- that is the radii of the large circles. Also it is known that the solution of sets of Diophantine equations is a generator of primes.

None prime numbers can be written in a unique set of primes. Thus for any number P we have;

$$P = p_1^a\, p_2^b\, p_3^c \cdots \quad \text{and}$$
$$\log P = a\log p_1 + b\log p_2 + c\log p_3 \cdots$$

where a, b, c are integral powers of the prime factors $p_1\ p_2 \cdots p_n$. Ref. [8] have observed that this relation is equivalent to energy conservation connecting the energy of one large object to the energy of its constituents- where energy is to be associated with $(\log P)$. Further, if the values of a, b, c are unity, the group would only have one energy state (structure), and could be the equivalent of fermions in behaviour. When the exponents are not unity (integer > 1), the group would behave as bosons and would be able to exist in multiple equivalent energy states corresponding to the different combination values of the exponents. Note that $\log p$ would correspond to the derivative of the prime formula $(n\log n)$ for large n accept for a negative sign.

Still in physics, we note that the size of the nucleus of chemical elements is proportional to the number of nucleons [3, 6] inside it. Since many of the physical and statistical models of the nucleus assume identical constituents, we may think of testing the possibility of condensed matter fol-

I – Elementary particles;	II – Particle mass/electron mass;				III – Nearest primes					
I-	e	μ	π^0	$\pi^{\pm}$	$K^{\pm}$	K^0	η	ρ	ω	K^*
II-	1	206.7	264.7	274.5	966.7	974.5	1074.5	1506.8	1532.3	1745.5
III-	1	211	263	277	967	977	1069	1511	1531	1747
I-	p	n	η'	φ	Λ	Σ^+	Σ^0	Σ^-	Δ	Ξ^0
II-	1836.2	1838.7	1873.9	1996.1	2183.2	2327.5	2333.6	2343.1	2410.9	2573.2
III-	1831	1831	1877	2003	2179	2333	2339	2347	2417	2579
I-	Ξ^-	Σ^*	Ξ^*	Ω^-	τ	D^0	$D^{\pm}$	$F^{\pm}$	D^*	Λ_c^-
II-	2585.7	2710.4	3000	3272	3491.2	3649.7	3657.5	3857.1	3933.4	4463.8
III-	2591	2713	3001	3271	3491	3643	3671	3863	3931	4463

Table 2: Relative masses of well known elementary particles and their nearest primes.

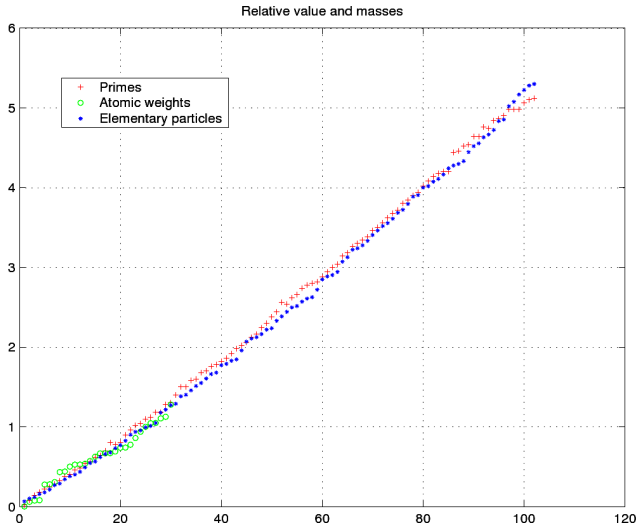

Fig. 7: Three normalized plots in ascending order of the relative atomic weight of 102 elements (+); 30 elementary particles (○); the first 102 prime numbers (*), starting with number 7. Each group is divided by entry number 25 of the group.

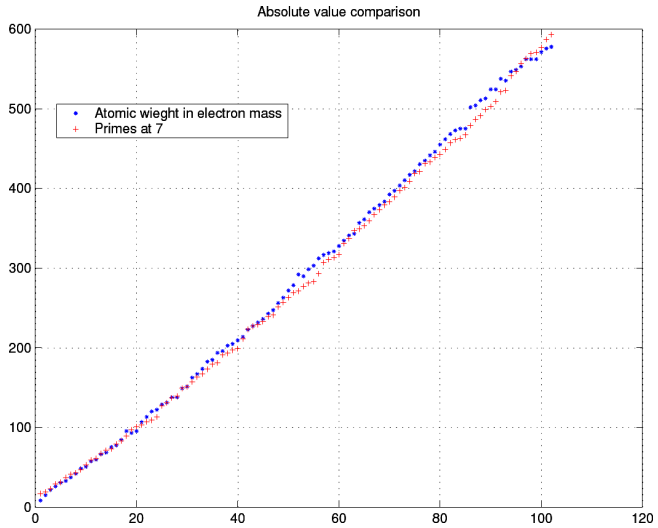

Fig. 8: Absolute-value comparison of the masses of chemical elements and primes. Primes starting from 7 (+) and relative masses of the chemical elements of the periodic table in units of Electron mass divided by (137×6) (*).

lowing the prime packing patterns as a result. We may also repeat the same for the masses of the *elementary particles* of physics which have hitherto defied many efforts to put a sense in the interpretation of their mass spectrum. To do this we shall arrange the various chemical elements of the periodic table (102 in total) and most of the elementary particles (30 in totals) in an ascending order of their masses (disregarding any other chemical property). We shall divide the masses of the chemical elements by the mass of the element say, number 25, in the list of ascending mass- which is Manganese (mass 55 protons) in order to get a relative value picture. The same is done with the group of elementary particles and these are divided by the mass of particle number 25 in the list namely the (Tau) particle (mass 1784 in MeV/c^2 units). Actual units do not matter here as we are only considering ratios. We then compare these with the list of primes arranged in ascending order too. Table 2 contains the data for the case of elementary particles. Masses of the chemical elements can be taken from any periodic table. The nearest prime figures in the table are for information and not used in the plots. In Figure 8 an absolute value comparison for the elements is shown. The primes starts at 7 and the masses of the elements (in electron mass) are divided by 137×6 in order to get the two curves matching at the two ends.

For better fitting, the prime number series had to be started at number 7, not 1 as one might normally do. Comparison results are given in Figures 7 and 8. The trends are strikingly similar. The type of agreement must be a strong indication that the same packing rules are prevailing in all the cases.

3 Concluding remarks

We noticed that primes are closely connected to geometry and physics and this is dictated by the very properties of discrete space geometry like you can closely pack on a plane only seven balls to form a circle. This result and that of the cannon ball packing problem are found to be subsets of the dense packing problem. One clear link between primes and geom-

etry comes from the fact that all primes are generated by the formula $6n \pm 1$. When integers are associated with balls, this formula can be represented in the form of a long cylinder with primes lying along two opposite generator of the cylindrical surface.

Highly energetic particles bound together dynamically are more likely to have circular/spherical structures, and thus can follow the packing arrangements discussed in this article. It may be said now that the source of discreteness frequently observed in the energy levels of atoms and the correspondence between energy levels and prime numbers are only manifestations of this fact. The number of elements (balls) in each circular area or spherical leaf in the building up of a collection is proportional to n^2. The energy of each would naturally be proportional n^2 too. Each constituent will thus carry $1/n^2$ of the energy and the jump of one constituent from one level to the other gives an energy change of $(1/n_1^2 - 1/n_2^2)$ as in the Ballmer series. The Bohr model for the atom relies on an integral number of wavelengths around a circumference, which in this case can be interpreted as integral number of balls, which makes the present model more realistic and easier to digest. The Bohr model was originally intended for the electrons, but later studies took this to concern the whole nucleus [8].

If the packing picture is carried down to the level of very elementary particles, we could speculate that the 2 and 3 circle solutions of the packing problem correspond to the 2 and 3 quarks constituent evidence found in experimental work and stated in the quark theory of elementary particles. Fast particles crossing the nucleus are normally used to probe the nucleus. The 6 pack with 3 balls along any diameter could very well be responsible for the conclusions of such measurements.

The plots of the mass growth (packing) of chemical elements and elementary particles (and hence all massive bodies), as shown here, follow very closely the rules of packing of spheres and also those of the prime numbers. Prime numbers or prime collections appear when it is not possible to divide a collection into symmetric (equal) parts and are hence more stable in structure. This makes the growth of primes to be naturally tied to the growth in the masses of condensed matter in its different phases. We also note that the prime character of a number is an independent property- more of an abstract physical property, and it is not a function of the base of the number system in use or the physical case that number might represent.

The eight fold rules frequently found in the behaviour pattern of chemical elements and elementary particles [4, 8] may now be suspected to be a consequence of the packing rules of similar spheres in space. We might even suggest that the successes of the Bohr Theory for the atom, the Ballmer series formula for energy levels and indeed the Schrödinger equation itself in predicting discrete behaviour in atoms and other entities, might be mainly due to the discretization of space implied in their formulations. In fact while Schrödinger equation has many solutions, those deemed correct have to obey the integrability condition which is essentially a discretization (normalization) of space condition. We mention also that in the solutions of Schrödinger equation, the main interest when finding a solution (the wave function) is the resulting number of discrete states along any radial or circumferential direction and not the actual form (function) of the solution. Not forgetting also that the most fruitful solutions of Schrödinger equation are those in circular no-Cartesian coordinates anyway.

4 Recommendations

More work is needed to reach more concrete, verifiable and useful results. Such work might investigate the origin of the various properties that distinguish groups of elementary particles like strangeness, charm etc in relation to the possible geometric shape/packing of their constituents. The circles and spheres in the present investigation are not referring to a static picture, but one formed by very fast moving particles that generated such shapes as a result of their own dynamic rules. Detailed position-energy calculations of various arrangements, as done on crystals for example, could be done here to pin point the reasons behind an elementary particle to become stable or unstable in the presence of external disturbances, and also the explanation of the various probabilities associated with different break-up scenarios of unstable particles.

Acknowledgement

The author acknowledges very fruitful discussions with Dr. J. Hemp (Oxford). Most of the literature and information used are obtained through the generous contribution of their authors by allowing their free consultation on the open domain. This work was stimulated first by an article by J. Gilson of QMC, attempting to discover the origin of the fine structure constant 137 (approximately a prime number by itself) using algebraic expressions and geometry. The present quest did not get there and the matter will be left for the next inline.

Submitted on May 07, 2009 / Accepted on May 14, 2009

References

1. Wells D. Prime numbers. Whiley, 2005.
2. Harney M. *Progress in Physics*, 2008, v. 1.
3. Finn A. Fundamental university physics. Quantum and statistical physics. Addison-Wesley, 1968.
4. Bohr N. *Nature*, March 24, 1921.
5. Hales T. C. *Notices of the AMS*, 2000, v. 47(4).
6. Griffiths D. Introduction to elementary particles. Wiley, 2004.
7. Hassani M. arXiv: math/0607096.
8. Sugamoto A. *OCHA-PP-277*, arXiv: 0810.4434.

Dual Phase Lag Heat Conduction and Thermoelastic Properties of a Semi-Infinite Medium Induced by Ultrashort Pulsed Laser

Ibrahim A. Abdallah

Department of Mathematics, Helwan University, Ain Helwan, 11795, Egypt
E-mail: iaawavelets@yahoo.com

In this work the uncopled thermoelastic model based on the Dual Phase Lag (DPL) heat conduction equation is used to investigate the thermoelastic properties of a semi-infinite medium induced by a homogeneously illuminating ultrashort pulsed laser heating. The exact solution for the temperature, the displacement and the stresses distributions obtained analytically using the separation of variables method (SVM) hybrid with the source term structure. The results are tested numerically for Cu as a target and presented graphically. The obtained results indicate that at very small time duration disturbance by the pulsed laser the behavior of the temperature, stress and the displacement distribution have wave like behaviour with finite speed.

1 Introduction

Heat transport and thermal stresses response of the medium at small scales becomes recently in the spot of interest due to application in micro-electronics [1] and biology [2, 3] and due to its wide applications in welding, cutting, drilling surface hardening, machining of brittle materials. Because of the unique capability of very high precision control of the ultrashort pulsed laser it is interesting to investigate the thermoelastic properties of the medium due to the ultrashort pulsed laser heating. The different models of thermoelasticity theory based on the equation of heat convection and the elasticity equations. The main categories of these models are the coupled thermoelasticity theory formulated by abd-2-04 [4], and the coupled thermoelasticity theory with one relaxation time [5], the two-temperature theory of thermoelasticity [6], the uncoupled classical linear theory of thermoelasticity based on Fourier'a law [7], the uncoupled thermoelasticity theory based on the Maxwell-Cattaneo modification of heat convection to include one time lag between heat flux and the temperature gradient [8, 9].

The coupled and uncoupled models have been used to solve some problems on the macroscale where the length and time scales are relatively large. The technological needs of a high precision control of the ultrashort pulsed laser applications processes at the microscales ($< 10^{-12}$ s), with high heating rates processes are not compatible with the Fourier's model of heat conduction because it implies to an infinite speed for heat propagation and infinite thermal flux on the boundaries. To overcome the deficiencies of Fourier's law in describing high rate heating processes the concept of wave nature of heat convection had been introduced [10]. Tzou [11, 12] had introduced another modification to Fourier law, by inventing two time lags, Dual Phase Lag (DPL), between the heat flux and the temperature gradient namely the heat flux time lag and the temperature gradient time lag. Therefore he had used the dual phase lag heat convection equation with the energy conservation law to obtain the dual phase lag model for heat convection.

The purpose of the present work is to study the induced thermoelastic waves in a homogeneous isotropic semi-infinite medium caused by an ultrashort pulsed laser heating exponentially decay, based on the dual phase lag modification of Fourier's law. The problem is formulated in the dimensionless form and then solved analytically by inventing a new sort of the separation of variables hybridized by the source structure function. The stress, the displacement and the temperature solutions are obtained and tested by a numerical study using the parameters of Cu as a target. The results performed and presented graphically and concluding remarks are given.

2 Problem formulation

In this investigation I considered a homogeneous isotropic semi-infinite medium with mass density ρ, specific heat c_E, thermal conductivity k, and thermal diffusivity $\alpha = \frac{k}{\rho c_E}$. The medium occupy the half space region $z \geqslant 0$ considering the Cartesian coordinates (x, y, z). the medium is assumed to be traction free, initially at uniform temperature T_0, and subjected to heating process by a ultrashort pulsed laser heat source its structure function; $g(z,t) = \frac{I_0(1-R)}{t_p \phi \sqrt{\pi}} e^{-\frac{z}{\varphi}} e^{-\left|\frac{t-t_p}{t_p}\right|}$, at the surface $z = 0$ as in Fig. 1. where the constants characterize this laser pulse are: I_0, the laser intensity, R the reflectivity of the irradiated surface of the medium, ϕ the absorption depth, and t_p the laser pulse duration. The Cartesian coordinates (x, y, z) are considered and z-axis pointing vertically into the medium. Therefore the governing equations are: The equation of motion in the absence of body forces

$$\sigma_{ji,j} = \rho \ddot{u}_i \qquad i, j = x, y, z\,, \tag{1}$$

where σ_{ij} is the stress tensor components, $u_i = (0, 0, w)$ are the displacement vector components. The constitutive rela-

tion

$$\sigma_{ij} = \left[\lambda\, div\, u_i - \gamma(T - T_0)\right]\delta_{ij} + 2\mu e_{ij} \tag{2}$$

by which the stress components are

$$\begin{aligned} &\sigma_{xx} = \sigma_{yy} = \lambda w_z - \gamma(T - T_0) \\ &\sigma_{zz} = (\lambda + 2\mu) w_z - \gamma(T - T_0) \\ &\sigma_{xy} = 0, \qquad \sigma_{xz} = 0, \qquad \sigma_{yz} = 0\,. \end{aligned} \tag{3}$$

The volume dilation e takes the form

$$e = e_{xx} + e_{yy} + e_{zz} = \frac{\partial w}{\partial z}\,. \tag{4}$$

Where the strain-displacement components e_{ij}, read;

$$\begin{aligned} &e_{ij} = \frac{1}{2}\left(u_{i,j} + u_{j,i}\right) \qquad i, j = x, y, z\,, \\ &e_{zz} = \frac{\partial w}{\partial z}\,, \quad e_{xx} = e_{yy} = e_{xy} = e_{xz} = e_{yz} = 0\,, \end{aligned} \tag{5}$$

substituting from the constitutive relation into the equation of motion using the equation of motion we get:

• The displacement equation

$$(\lambda + 2\mu)\, w_{zz} - \gamma(T - T_0)_z = \rho\, \ddot{w}\,; \tag{6}$$

• The energy conservation

$$-\rho\, c_E \dot{T} = q_z\,. \tag{7}$$

Since the response of the medium to external heating effect comes later after the pulsed laser heating interacts with the medium surface then there is a time lag, and by using the dual phase lag modification of the Fourier's law as invented by Tzou;

$$\begin{aligned} &q(z, t + \tau_q) = -\,k\, T_z(z, t + \tau_T)\,, \\ &q + \tau_q \dot{q} = -\,k\, T_z - k\, \tau_T \dot{T}_z\,. \end{aligned} \tag{8}$$

Then the energy transport equation of hyperbolic type can be obtained by substituting in the energy conservation law and considering the laser heat source

$$\frac{\tau_q}{\alpha}\ddot{T} + \frac{1}{\alpha}\dot{T} = T_{zz} + \tau_T \dot{T}_{zz} - \frac{1}{\rho c_E}\, g(z, t) - \tau_q\, \dot{g}(z, t)\,. \tag{9}$$

This equation shows that the dual lagging should be considered for the processes whose characteristic time are scale comparable to τ_q and τ_T. It describes a heat propagation with finite speed. where τ_q is represents the effect of thermal inertia, it is the delay in heat flux and the associated conduction through the medium, and τ_T is represents the delay in the temperature gradient across the medium during which conduction occurs through its microstructure. For $\tau_T = 0$ one obtain the Maxwell-Cattaneo model, and Fourier law obtained if $\tau_T = \tau_q = 0$.

The boundary conditions are;

$$\begin{aligned} &-k\, T_z(z, t) = g(z, t)\,,\ w = 0\,,\ \sigma_{zz} = 0, \ \text{at}\ z = 0\,, \\ &\sigma_{zz} = 0, \quad w = 0\,, \quad T = 0\,, \quad \text{as} \quad z \to \infty\,. \end{aligned} \tag{10}$$

Introducing the dimensionless transformations $z^* = \frac{z}{\sqrt{\alpha\tau_q}}$, $w^* = \frac{w}{\sqrt{\alpha\tau_q}}$, $\sigma_{ij}^* = \frac{\sigma_{ij}}{\mu}$, $t^* = \frac{t}{\tau_q}$, $t_p^* = \frac{t_p}{\tau_q}$, $\varphi^* = \frac{\varphi}{\sqrt{\alpha\tau_q}}$, $\tau^* = \frac{\tau_T}{\tau_q}$, $\theta_0\theta^* = T - T_0$, $\lambda_1^* = \frac{\lambda}{\mu}$, $\lambda_2^* = \frac{\lambda+2\mu}{\mu}$, $\gamma_0 = \frac{\gamma\theta_0}{\mu}$, $\theta_0 = \frac{I_0(1-R)}{k}\sqrt{\frac{\alpha}{\pi\tau_q}}$, substituting in the governing equations and in boundary conditions of the problem by the above dimensionless transformations and then omitting the $(^*)$ from the resulting equations we obtain the dimensionless set of the governing equations and boundary conditions:

• The dimensionless temperature equation

$$\ddot{\theta} + \dot{\theta} = \theta_{zz} + \tau\dot{\theta}_{zz} + \left(\frac{1 - t_p}{t_p^2\,\varphi}\right) e^{-\frac{z}{\varphi}} e^{-\left|\frac{t-2t_p}{t_p}\right|}\,; \tag{11}$$

• The dimensionless displacement equation

$$w_{zz} - B^2\ddot{w} = G\,\theta_z\,, \tag{12}$$

where $B^2 = \frac{\rho\alpha}{\tau_q t_p^2(\lambda+2\mu)}$ and $G = \frac{\gamma_0\theta_0}{(\lambda+2\mu)}$;

• The dimensionless stresses equations

$$\begin{aligned} &\sigma_{zz} = \lambda_2 w_z - \gamma_0\,\theta\,, \\ &\sigma_{xx} = \sigma_{yy} = \lambda_1 w_z - \gamma_0\,\theta\,; \end{aligned} \tag{13}$$

• Dimensionless boundary conditions

$$\begin{aligned} &w = 0\,, \quad \sigma_{zz} = 0\,, \quad \text{at} \quad z = 0\,, \\ &\theta_z(z, t) = -\frac{1}{k\sqrt{\alpha\tau_q}}\, e^{-\left|\frac{t-2t_p}{t_p}\right|}, \quad \text{at} \quad z = 0\,, \\ &\sigma_{zz} = 0\,, \quad w = 0\,, \quad T = 0\,, \quad \text{as} \quad z \to \infty\,. \end{aligned} \tag{14}$$

3 Solution of the problem

In this section I introduced the hybrid separation of variables method (HSVM) to get the solution of equations (11) and (12). Using this method one can construct the analytic solution for some type of nonhomogeneous partial differential equations (or system). Its idea based on using the structure of the nonhomogeneous term to invent the form of separation of variables. Therefore the PDE (or system) will reduced to ODE (or system) which can be solved. To illustrate the (HSVM) we use it to solve the problem in this paper. Introducing the following separation of variables based on the structure of the source function, which represents the inhomogeneous term,

$$\theta(z, t) = Z(z)\, e^{-\left|\frac{t-2t_p}{t_p}\right|}, \quad w(z, t) = W(z)\, e^{-\left|\frac{t-2t_p}{t_p}\right|} \tag{15}$$

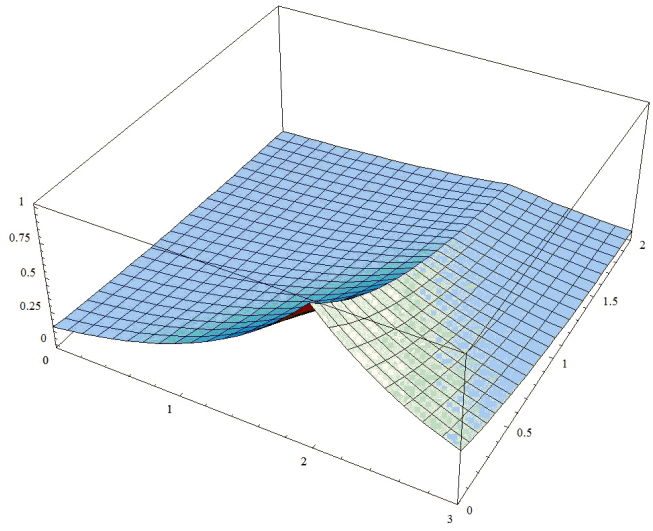

Fig. 1: The strcture function of the ultrashort pulsed laser of exponentially decay.

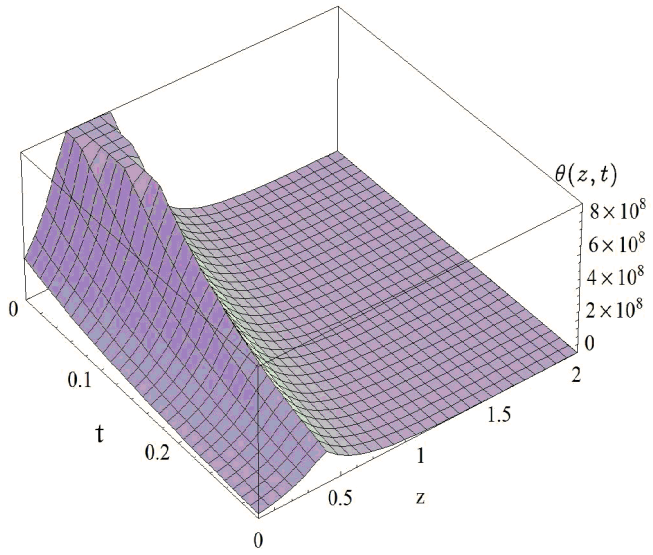

Fig. 2: The dimensionless temperature distribution.

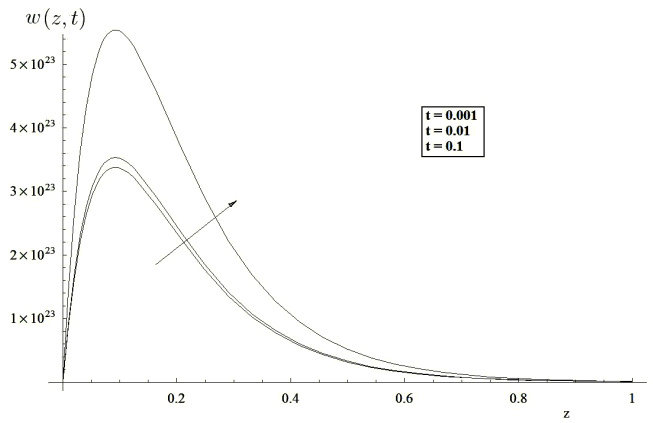

Fig. 3: The dimensionless w-displacement distribution.

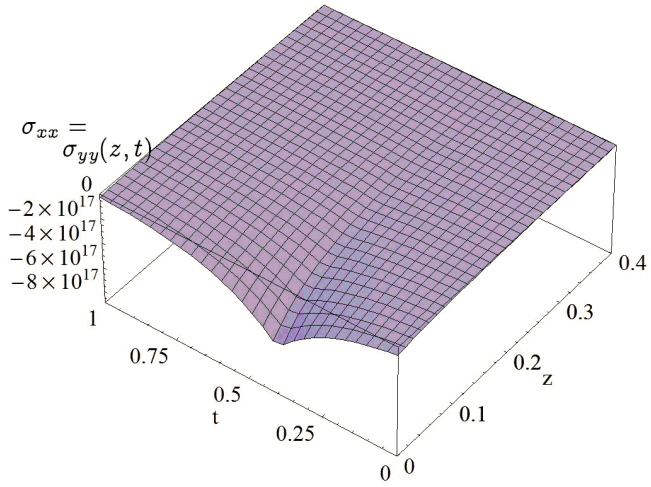

Fig. 4: The dimensionless stresses $\sigma_{xx} = \sigma_{yy}$ distributions.

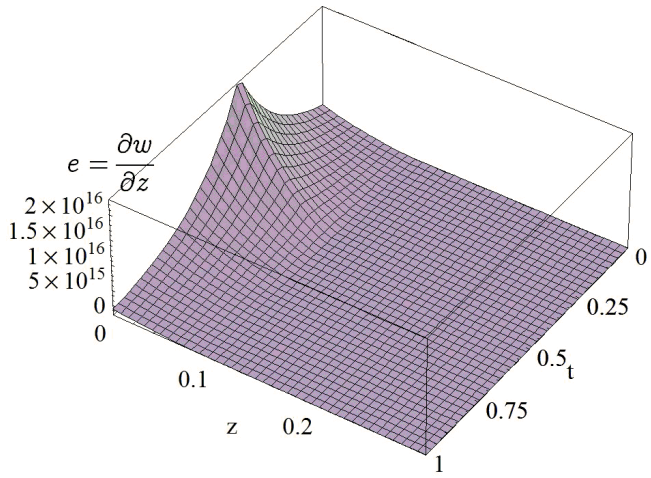

Fig. 5: The dimensionless volume dilation e.

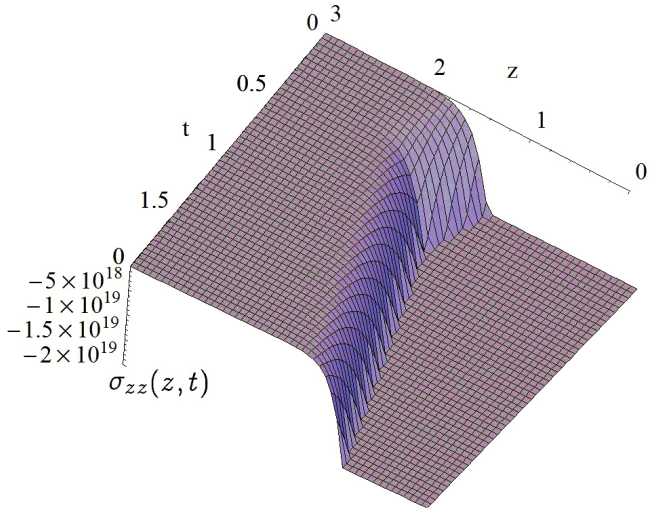

Fig. 6: The dimensionless stresses σ_{zz} distributions.

the equations (11) and (12) will be reduced to a separable form and can be solved directly and therefore using the dimensionless boundary conditions we obtain:

• The solution of the dimensionless temperature equation

$$\theta(z,t) = \left[\vartheta_1 e^{-Az} + \vartheta_2 e^{-\frac{z}{\varphi}}\right] e^{-\left|\frac{t-2t_p}{t_p}\right|}; \qquad (16)$$

where $A^2 = \frac{(1-t_p)}{t_p(t_p-\tau)}$, $H = \frac{(t_p-1)}{t_p\varphi}$,
$\vartheta_1 = \left[\frac{1}{At_p\varphi\sqrt{\alpha\tau_p}} - \frac{H}{A\varphi(\frac{1}{\varphi^2}-A^2)}\right]$, $\vartheta_2 = \frac{H}{(\frac{1}{\varphi^2}-A^2)}$;

• The solution of the dimensionless displacement equation

$$w(z,t) = \left[W_1 e^{-Bz} + W_2 e^{-Az} + W_3 e^{-\frac{z}{\varphi}}\right] e^{-\left|\frac{t-2t_p}{t_p}\right|}, \quad (17)$$

where $W_1 = \left[\frac{GA\vartheta_1}{(A^2-\frac{B^2}{t_p^2})} + \frac{G\vartheta_2}{\varphi(A^2-\frac{B^2}{t_p^2})}\right]$, $W_2 = -\frac{GA\vartheta_1}{(A^2-\frac{B^2}{t_p^2})}$,
$W_3 = -\frac{G\vartheta_2}{\varphi(\frac{1}{\varphi^2}-\frac{B^2}{t_p^2})}$;

• The solution of the dimensionless stresses equation

$$\sigma_{xx} = \sigma_{yy} = -e^{-\left|\frac{t-2t_p}{t_p}\right|}\left[\gamma_0\left(\vartheta_1 e^{-Az} + \vartheta_2 e^{-\frac{z}{\varphi}}\right) + \right.$$
$$\left. + \lambda_1\left(W_1 B e^{-Bz} + W_2 A e^{-Az} + W_3\frac{1}{\varphi}e^{-\frac{z}{\varphi}}\right)\right], \qquad (18)$$

$$\sigma_{zz} = -e^{-\left|\frac{t-2t_p}{t_p}\right|}\left[\gamma_0(\vartheta_1 e^{-Az} + \vartheta_2 e^{-\frac{z}{\varphi}}) + \right.$$
$$\left. + \lambda_2\left(W_1 B e^{-Bz} + W_2 A e^{-Az} + W_3\frac{1}{\varphi}e^{-\frac{z}{\varphi}}\right)\right], \qquad (19)$$

where $\lambda = 7.76\times10^{10}$ kg/m sec^2,
$\rho = 8954$ Kg/m^3, $\mu = 3.86\times10^{10}$ kg/m sec^2,
$\alpha_t = 1.78\times10^{-5}$, $c_E = 383.1$ J/kgK, $t_p = 0.1$ sec,
$k = 386$ W/mK, $\lambda + 2\mu = 1.548\times10^{11}$ kg/m sec^2,
$\tau_q = 0.7\times10^{-12}$ sec, $\tau_\theta = 89\times10^{-12}$ sec,
$\varphi = 0.2$ m, $\gamma = (3\lambda + 2\mu)\alpha_t = 5.518\times10^6$ kg/m sec^2,
$\beta = 2\times10^{13}$, $\delta = 1.7\times10^{-6}$, $A = \beta\tau_q = 14$,
$I_1 = I_0(1-R) = 1\times10^{13}$ W/m^2.

4 Discussion and conclusion

In this paper the thermoelastic waves in a homogeneous isotropic semi-infinite medium caused by an ultrashort pulsed laser heating having exponentially decay, based on the dual phase lag modification of Fourier's law have been investigated. The problem formulated in the dimensionless form and then solved analytically for the temperature, the stress, and the displacement by inventing a new sort of the hybridized separation of variables by the source structure function. The obtained analytical solutions are tested numerically using for Cu as a target medium.

The results are presented graphically. The obtained results indicated that due to the very high power of the laser pulse at the surface in a very short duration the temperature distribution possessing a wave nature with finite speed as in Fig. 2. The medium responses to the laser heating by increasing change in the displacement distribution with increasing time duration as in Fig. 3. The thermoelastic characteristics (stresses components $\sigma_{xx} = \sigma_{yy}$ and volume dilation $e = \frac{\partial w}{\partial z}$) of the medium possess wave nature as in Fig. 4 and Fig. 5. Fig. 6. depicts that the stress component σ_{zz} have wave nature with wave front has its maximum at the average of the laser pulse duration. By these results it is expected that the dual phase lag heat conduction model will serve to be more realistic to handle practically the laser problems with very high heat flux and/or ultrashort time heating duration.

Submitted on May 06, 2009 / Accepted on May 15, 2009

References

1. Kulish V.V., Lage J.L., Komarov P.L., and Raad P.E., *ASME J. Heat Transfer*, 2001, v. 123(6), 1133–1138.
2. Kuo-Chi Liu and Han-Taw Chen. *Int. J. Heat and Mass Transfer*, 2009, v. 52, 1185–1192.
3. Zhou J., Chen J.K., Zhang Y. *Computers in Biology and Medicine*, 2009, v. 39, 286–293.
4. abd-2-04 M. *J. Appl. Phys.*, 1956, v. 27, 240–253.
5. Lord H. and Shulman Y. *J. Mech. Phys. Solid.*, 1967, v. 15, 299–309.
6. Youssef H.M. and Al Lehaibi A. Eman. *I. J. of Sol. and Struct.*, 2007, v. 44, 1550–1562.
7. Chadwick 1.P. Thermoelasticity: the dynamic theory. In: *Prog. in Sol. Mech.*, v. I, Hill R. and Sneddon I.N. (eds.), North-Holland, Amsterdam, 1960, 263–328.
8. Abdallah A.I. *Progress in Physics*, 2009, v. 2, 12–17.
9. Andrea P.R., Patrizia B., Luigi M., and Agostino G.B. *Int. J. Heat and Mass Trans.*, 2008, v. 51, 5327–5332.
10. Özisik M.N. and Tzou D.Y. *ASME J. of Heat Transfer*, 1994, v. 116, 526–535.
11. Tzou D.Y. *ASME J. of Heat Transfer*, 1995, v. 117, 8–16.
12. Tzou D.Y. Macro-to-micro scale heat transfer: the lagging behavior. Taylor and Francis, Washington (DC), 1997.

The Missing Measurements of the Gravitational Constant

Maurizio Michelini
ENEA — Casaccia Research Centre, Rome, Italy
E-mail: m_michelini@alice.it

G measurements are made with torsion balance in "vacuum" to the aim of eliminating the air convection disturbances. Nevertheless, the accuracy of the measured values appears unsatisfying. In 2000 J. Luo and Z. K. Hu first denounced the presence of some unknown systematic error in high vacuum G measurements. In this work a new systematic effect is analyzed which arises in calm air from the non-zero balance of the overall momentum discharged by the air molecules on the test mass. This effect is negligible at vacuum pressures higher than a millibar. However in the interval between the millibar and the nanobar the disturbing force is not negligible and becomes comparable to the gravitational force when the chamber pressure drops to about 10^{-5} bar. At the epoch of Heyl's benchmark measurement at 1–2 millibar (1927), the technology of high vacuum pumps was developed, but this chance was not utilized without declaring the reason. The recent G measurements use high vacuum techniques up to 10^{-10} and 10^{-11} bar, but the effect of the air meatus is not always negligible. We wonder whether the measurements in the interval between the millibar and the nanobar have been made. As a matter of fact, we were not able to find the related papers in the literature. A physical explanation of the denounced unknown systematic error appears useful also in this respect.

1 Introduction

Everyone knows the simple experience of two flat microscopy glasses which cannot be separated from each other when their surfaces touch. Obviously this effect is due to the pressure of the air whose molecules penetrate with difficulty between the corrugations of the polished surfaces generating within the small meatus a considerable air depression. The mean free path of the air molecules at normal pressure is about 10^{-7} metres, that is of the same order of magnitude of the polished surface corrugations. In general, the molecules are not able to freely penetrate within a meatus whose thickness is reduced to about 1 mean free path. When we consider the meatus facing the test mass of a gravitational torsion balance placed in a vacuum chamber, the very little air depression within the meatus originates a disturbing force on the test mass, which adds to the gravitational force. This disturbing force is negligible at normal pressure, but when the pressure within the vacuum chamber is reduced beyond the millibar (for instance to avoid other disturbances due to air convection or to minimize the air friction on the oscillating pendulum) the meatus optical thickness further reduces, so as to attain the above condition about 1 mean free path. It appears opportune to investigate this phenomenon to obtain a semi-quantitative prediction of the disturbing drawing force arising on the gravitational balance. This research takes into account the results of some experimenters which denounced the presence of some unknown systematic effect in the G measurements.

2 Historical background

The torsion balance apparatus was first used by Cavendish in 1798 in a very simple form which permitted him to reach an unexpected accuracy. In the following two centuries the torsion balance was used by several experimenters which substantially improved the technique, but the level of accuracy did not show a dramatic enhancement. Several methods were devised in the XXth century to measure G. In a Conference organized by C. C. Speake and T. J. Quinn [1] at London in 1998 — two centuries after Cavendish — a variety of papers described the methods of measurement and their potential accuracy related to the disturbances and systematic errors. In Table 1 we report the most accurate values presented at the Conference [$G \times 10^{-11}$ kg/m^{3}s^2]:

Author	Method	G	Accur. (ppm)
PTB	torsion balance	6.7154	68
MSL	torsion balance (a)	6.6659	90
MSL	idem (re-evaluation)	6.6742	90
MSL	torsion balance (b)	6.6746	134
BIPM	torsion-streap bal.	6.683	1700
JILA	absolute gravimeter	6.6873	1400
Zurich	beam balance	6.6749	210
Wuppertal	double-pendulum	6.6735	240
Moscow	torsion pendulum	6.6729	75

Table 1: Measurements of G, according to [1].

Among the methods described there are: a torsion balance where the gravitational torque is balanced by an electrostatic torque produced by an electrometer; a torsion-strip balance where the fibre is substituted by a strip; a dynamic method based on a rotating torsion pendulum with angular acceleration feedback; a free fall method where the determination of G depends on changes in acceleration of the falling object, etc. Notwithstanding the technological improvement, up to now the gravitational constant is the less accurately known among the physical constants. The uncertainty has been recognized to depend on various experimental factors. To eliminate the air thermal convection on the test mass, in 1897 K. F. Braun made a torsion balance measurement after extracting the air from the ampule. The level of vacuum ob-

tained with his technique is not known. In 1905 W. Gaede invented the rotary pumps reaching the void level of 10^{-6} bar. Subsequently Gaede developed the molecular drag pumps (1915) using Hg vapour. In 1923 the mercury was substituted by refined or synthetic oil, which enabled to reach void levels around 10^{-9} bar.

In 1927 Heyl [2] made a benchmark measurement with a heavy torsion balance to the aim of establishing a firm value of G. Although the high vacuum technology was available, he adopted a chamber pressure equal to 1–2 millibar. The molecule mean free path at 1 millibar is about 10^{-4} metres, a quantity much smaller than the thickness of the meatus. From our present investigation it appears that the air pressure effect does not alter the accuracy of the classical G measurements performed at pressures higher than some millibars. But this fact was unknown at the epoch. In any case the choice of high vacuum was compelling against the air convection disturbance. After 1958 the development of turbomolecular pumps and the improved molecular drag pumps made available an ultra-high-vacuum up to 10^{-13} bar. Also this spectacular jumping was apparently disregarded by the G experimenters. In 1987 G. T. Gillies published an Index of measurements [3] containing over 200 experiments, which does not report vacuum pressures between the millibar and the nanobar. At the end of ninety the unsatisfying values of G became publicly discussed.

3 First report of a new unknown systematic error

A status of the recent G measurements was published in 2000 by J. Luo and Z. K. Hu [4] in which the presence of some unknown systematic effect was first denounced: "This situation, with a disagreement far in excess to the estimate, suggests the presence of unknown systematic problems".

In 2003 R. Kritzer [5] concluded that "the large spread in G measurements compared to small error estimates, indicates that there are large systematic errors in various results".

Among the last experiments, some of them used new sophisticated methods with technologies coupled to very low pressures within the test chamber. This fact shows a new attention to the problems of possible unknown air effects.

J. H. Gundlach and S. M. Merkowitz [6] made a measurement where a flat pendulum is suspended by a torsion fiber without torque since the accelerated rotation of the attracting masses equals the gravitational acceleration of the pendulum.

To minimize the air dynamic effect, the pressure was lowered to 10^{-7} Torr ($p_0 \approx 10^{-10}$ bar). At this pressure the classical mean free path $l = m/\sigma\,\delta_0$ within a large homogeneous medium is of the order of 1000 metres. Hence within the vacuum chamber the lack of flux homogeneity is everywhere present.

Another accurate measurement was performed in 2002 by M. L. Gershteyn et al. [7] in which the pendulum feels a unique drawing mass fixed at different distances from the test mass. The change of the oscillation period determines G. To minimize the air disturbance, the pressure in the vacuum chamber was lowered to 10^{-6} Pascal (i.e. $p_0 = 10^{-11}$ bar). The reason for such a dramatic lowering is not discussed. The authors revealed the presence of a variation of G with the orientation (regard to the fixed stars) amounting to 0.054%. Incidentally, the anisotropy of G is predicted by the gravitational-inertial theory discussed in [8].

In 2004 a new torsion balance configuration with four attracting spheres located within the vacuum chamber ($p_0 = = 1.5\times10^{-10}$ bar) was described by Z. K. Hu and J. Luo [9]. The four masses are aligned and each test mass oscillates between a pair of attracting masses. Each test mass determines with the adjacent spheres a small meatus (estimated about 4 mm) and a large meatus (about 16 mm). During the experiment the authors found the presence of an abnormal period of the torsion pendulum, which resulted independent of the material wire, test mass, torsion beam and could not be explained with external magnetic or electric fields. Adopting a magnetic damper system, the abnormal mode was suppressed, but the variance of the fundamental period of the pendulum introduced an uncertainty as large as 1400 ppm, testifying the presence of a systematic disturbance in determining G.

We applied to this problem the analysis carried out in this paper. From the air density in the vacuum chamber, we calculate the optical thickness of the small meatus and the related air depression, Eq. (5), which substituted in Eq. (7) gives upon the test mass a disturbing force rising up to $F(p_0) \approx \approx 10^{-14}$ Newton, equivalent to about 10^{-4} times the gravitational force, which alters the pendulum period. This fact agrees with the author conclusions [9] that the torsion balance configuration would have an inherent accuracy of about 10 ppm in determining G, but the uncertainty in the fundamental period reduces this accuracy to 1400 ppm.

The presence of an abnormal disturbance was previously described (1998) by Z. K. Hu, J. Luo, X. H. Fu et al. [10] in dealing with the time-of-swing method. They found the presence of "important non-linear effects in the motion of the pendulum itself, independent of any defect in the detector, caused by the finite amplitude of the swing". Their configuration consisted in a torsion balance with heavy masses external to the vacuum chamber, where the pressure was lowered to $p_0 = 2\times10^{-10}$ bar. The test mass, diameter about 19 mm, was suspended within a stainless vacuum tube placed between two heavy masses distant 60 mm apart. Since the test mass oscillates up to 8 mm from the centre of the vacuum tube, the optical thickness of the small meatus can be deduced. The smaller this thickness, the greater the disturbing force $F(p_0)$. Repeating the analysis carried out for the preceding experiment, we found a force $F(p_0)$ which represents a lower fraction of the gravitational force thanks to the heavy attractor masses. Comparing with many measurements made in last decades with high vacuum technology [11–19] we notice that the vacuum pressures (when reported) were not

comprised between the millibar and the nanobar. The reasons for this avoidance do not appear to have been discussed.

4 Scattering of molecules upon smooth surfaces

The scattering of gas molecules hitting a smooth surface does not generally follow the optical reflection because that which collide about orthogonally may interact with a few atoms of the lattice. As it happens when two free particles come in collision, these molecules may be scattered randomly. Conversely, the molecules hitting the surface from a nearly parallel direction interact softly with the field of the atomic lattice. In fact these molecules, whose momentum $q = mv$ makes an angle $\alpha = \pi/2$ with the vertical axis, receive from the lattice field a small vertical momentum $\Delta q \approx 2\,mv\cos\alpha$ which redirects the molecules along a nearly optical reflection. It is usefull to recall that the momentum hv/c of the UV rays (which observe the reflection law) is comparable to the momentum of air molecules at normal temperature.

To resume: after scattering on a smooth surface a fraction of the nearly orthogonal molecules becomes quasi parallel.

As a consequence an isotropic flux ϕ_0 of molecules hitting a smooth surface, after scattering becomes non-isotropic. This condition may be described by the relationship

$$\psi_0(\alpha) \backsimeq \phi_0\left(1 - \Delta_1\cos\alpha + \Delta_2\sin\alpha\right) \tag{1}$$

where the parameters Δ_1, Δ_2 satisfy the total flux condition $\int_0^{\pi/2}\sin\alpha\,\psi_w(\alpha)\,d\alpha = \phi_0$. Moreover we assume that about χ percent of the nearly orthogonal molecules become quasi-parallel after scattering on the wall. Applying these two conditions one obtains the figures $\Delta_1 \simeq 1.46\,\chi$, $\Delta_2 \simeq 2\Delta_1/\pi \simeq$ $\simeq 0.928\,\chi$, where χ may range between 0.10 down to 0,0001 for smoothed glass walls. This physical condition makes easy to understand the molecular flux depression within the meatus around the test mass. This phenomenon becomes particularly evident at low air pressures. For instance when the vacuum pressure is about a millibar, then 99.99% molecules hitting the test mass, Fig. 1, come from scattering with other molecules within the meatus, whereas 0.01% molecules come directly from the scattering on the chamber wall. To feel a sensible flux depression in the meatus it is necessary that the molecules coming from wall-scattering be about a half of the total. Within an air meatus of thickness "s" this happens when the optical thickness $\Sigma s = s\sigma\delta_0/m \simeq 10^7 s\,\delta_0$ equals 1 mean free path, i.e. when the air density equals $\delta_0 \simeq 10^{-7}/s$. For usual torsion balances the critical vacuum pressure which maximizes the flux depression is $p_0 \approx 1\times10^{-5} \div 3\times10^{-5}$ bar.

The old G measurements adopted a torsion balance at atmospheric pressure, so the meatus effect took place between the test mass and the attracting sphere. This happens also to G measurements in vacuum when the heavy masses are comprised within the chamber. But in general the G measurements in vacuum are made with the heavy masses outside the chamber. In this case we define "meatus" the air comprised between the test mass and the adjacent wall of the vacuum chamber (Fig. 1). At pressures higher than some millibars the molecular flux upon the moving mass is highly uniform, so the sum of every momentum discharged by the molecules on the sphere is null for any practical purpose. However, when the pressure in the chamber is further reduced, the molecular flux begins to show a little depression in the meatus. The flux depression in the circular meatus may be expressed along the radial direction x

$$\phi(x) \backsimeq \phi_m\left(1 + kx^2\right), \tag{2}$$

where ϕ_m is the minimum figure the flux takes on the meatus centre. Since the flux on the boundary, i.e. $x = L$, is the unperturbed flux ϕ_0, then one gets $\phi_m\left(1 + kL^2\right) = \phi_0$ which shows that k is linked to the flux parameters of the meatus

$$k = \left(\phi_0/\phi_m - 1\right)/L^2, \tag{3}$$

where $L \backsimeq R\cos\beta$ is the radius of the area of the test mass experiencing the flux depression. The angle β, defined by $\sin\beta = R/(R+s)$ (where R is the radius of the moving mass, s is the minimum thickness of the meatus), plays a fundamental role since it describes (Fig. 1) the "shadow" of the moving mass on the adjacent chamber wall. Choosing spherical co-ordinates with the same axis of the meatus and origin (Fig. 1) in the point B, the monokinetic transport theory gives us the angular flux of incident molecules $\psi_B(\alpha)$ integrating the scattered molecules along the meatus thickness $s(\alpha)$ and adding the flux $\psi_s(\alpha)$ of uncollided molecules scattered on the surface of the moving mass

$$\psi_B(\alpha) = \int_0^{s(\alpha)} \Sigma\phi(r)\exp(-\Sigma r)dr + \\ + \psi_s(\alpha)\exp\left[-\Sigma s(\alpha)\right], \tag{4}$$

where Σ is the air macroscopic cross section, $\Sigma\phi(r)$ is the density of isotropically scattered molecules, $s(\alpha)$ is the meatus thickness along α. This angular flux holds for $\alpha \leqslant \beta$. The above presentation of the problem has only an instructive character denoting the complexity of the problem, because the fluxes $\phi(r)$ and $\psi_s(\alpha)$ are unknown.

5 Calculation of the molecular flux in the meatus

To solve the problem of calculating the molecular flux within the meatus we adopt the principle of superposition of the effects. Let's consider the test sphere surrounded by the air in the vacuum chamber at pressure p_0. To obtain the disturbing force $F(p_0)$ on the test mass we must calculate the flux in the point A of the sphere and in the point C diametrically opposite (Fig. 1). Let's now remove the sphere and substitute an equal volume of air at pressure p_0, so to fill the chamber with the uniform molecular flux ϕ_0. Let's calculate the flux incident on both sides of the point A considering a spherical coordinates system with origin in this point (Fig. 1). The

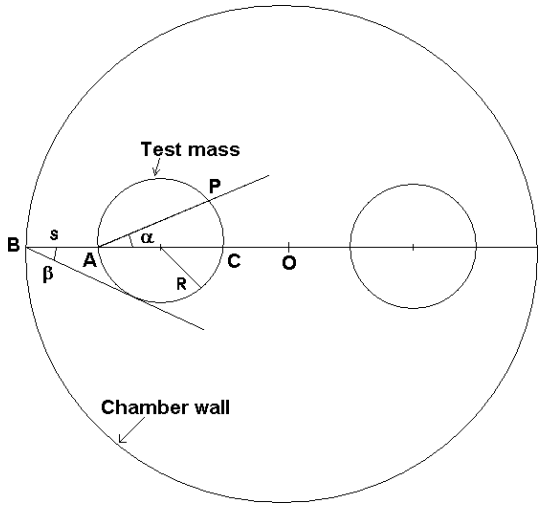

Fig. 1: Schematic drawing of a torsion balance in a vacuum chamber (meatus thickness arbitrarily large).

angular flux on the right-side of the point A is due to the scattering on the molecules within the sphere volume and to the uncollided molecules coming from the surface of the sphere (point P) where there is the uniform flux ϕ_0

$$\psi_A(\alpha) = \int_0^{t(\alpha)} \Sigma\phi_0 \exp(-\Sigma r)dr + \phi_0 \exp\left[-\Sigma t(\alpha)\right] \quad (5)$$

where $t(\alpha) = 2R\cos\alpha$ is the distance between the points A and P (Fig. 1) placed on the (virtual) surface of the removed mass. Let's notice that the first term in Eq. (3) represents the flux due to the scattering source occupying the sphere volume. When we cancel this source term (for instance reintroducing the test mass), Eq. (5) gives the flux

$$\psi_{A+}(\alpha) = \phi_0 \exp(-2\Sigma R\cos\alpha). \quad (6)$$

On the left-side of the point A the flux comes from scattering on the air within the meatus and from the uncollided molecules coming from the chamber wall

$$\psi_{A-}(\alpha) = \phi_0\left[1 - \exp(-\Sigma z(\alpha))\right] + \\ + \psi_w(\alpha)\exp(-\Sigma z(\alpha)), \quad (7)$$

where $z(\alpha)$ is the wall distance and $\phi_w(\alpha)$ is the flux scattered on the chamber wall, as defined by Eq. (1). Since in general the size of the chamber is much larger than R, one may assume the distance $z(\alpha) \simeq s/\cos\alpha$. Subtracting the flux $\psi_{A+}(\alpha)$ from $\psi_{A-}(\alpha)$ gives the actual flux on the point A of the test mass

$$\psi_A(\alpha) \simeq \phi_0\left[1 - \exp(-2\Sigma R\cos\alpha)\right] - \\ - \left[\phi_0 - \psi_w(\alpha)\right]\exp(-\Sigma s/\cos\alpha). \quad (8)$$

Now we calculate with the same procedure the incident flux on the point C

$$\psi_C(\alpha) \cong \phi_0\left[1 - \exp(-2\Sigma R\cos\alpha)\right] - \\ - \left[\phi_0 - \psi_w(\alpha)\right]\exp(-\Sigma(s+2R)/\cos\alpha). \quad (9)$$

The disturbing force on the moving mass is linked to the different pressures on the points A and C due to the momentum discharged by the molecular flux on these points. The molecular flux shows the following difference across the test mass diameter $\phi_C - \phi_A = \phi_0 \int_0^{\pi/2} \sin\alpha\left[\psi_C(\alpha) - \psi_A(\alpha)\right] d\alpha$.

Substituting and putting $w(\alpha) = \psi_w(\alpha)/\phi_0$, one gets the flux difference

$$\Delta\phi_0 = \phi_0 \int_0^{\pi/2} \sin\alpha\left[1 - w(\alpha)\right]\left[\exp(-\Sigma s/\cos\alpha) - \right. \\ \left. - \exp(-\Sigma(s+2R)/\cos\alpha)\right] d\alpha, \quad (10)$$

which confirms that the flux depression depends on the anisotropy of the flux $\psi_w(\alpha)$ scattered on the wall. Through Eq. (1) we also have $w(\alpha) = 1 - \Delta_1\cos\alpha + \Delta_2\sin\alpha$ which, substituting in the above equation gives the air depression

$$\Delta p_0/p_0 = \Delta\phi_0/\phi_0 = \\ = \Delta_1\Gamma(\Sigma s,\ \Sigma R) - \Delta_2\Omega(\Sigma s,\ \Sigma R), \quad (11)$$

where the functions

$$\Gamma(\Sigma s,\ \Sigma R) = \int_0^{\pi/2} \sin\alpha\cos\alpha\left[\exp(-\Sigma s/\cos\alpha) - \right. \\ \left. - \exp(-\Sigma(s+2R)/\cos\alpha)\right] d\alpha \quad (12)$$

and

$$\Omega(\Sigma s,\ \Sigma R) = \int_0^{\pi/2} \sin^2\alpha\left[\exp(-\Sigma s/\cos\alpha) - \right. \\ \left. - \exp(-\Sigma(s+2R)/\cos\alpha)\right] d\alpha \quad (13)$$

depend on the meatus geometry and on the air density δ_0 in the vacuum chamber. These functions do not appear to have been already tabulated. Fitting functions have been used for calculations, whose accuracy is not completely satisfying.

To give a quantitative idea of the phenomenon, the relative depression $\Delta p_0/p_0$ has been calculated assuming the usual size of a torsion balance, as specified in Table 2. Substituting in Eq. (12) the macroscopic cross section $\Sigma = \sigma\delta_0/m$ for any air density δ_0, one obtains the depressions $\Delta p_0/p_0$ reported in Table 2. Notice the high uniformity of the molecular flux within the meatus at 1 millibar vacuum level.

Conversely, the chamber pressure $p_0 = 10^{-5}$ bar corresponds to a sensible depression $\Delta p_0/p_0 \approx 3.4\times10^{-3}$ which may alter the gravitational force between the gravitational masses.

The disturbing force due to the small depression within the meatus $\Delta p(r) = mv\left[\phi_0 - \phi(r)\right]$ is defined by

$$F = \int_0^L 2\pi\, r\, \Delta p(r)\, dr, \quad (14)$$

where $L = R\cos\beta$ is the radius of the meatus periphery where $p(L) = p_0$. Substituting the flux distribution given by Eq. (2) one gets the corresponding depression within the meatus

$$p_0 - p(r) = p_0\left[1 - (\phi_m/\phi_0)\left(1 + kr^2\right)\right]. \quad (15)$$

Vacuum pressure p_0 Pascal	Air density δ_0 kg/m^3	Meatus optical width Σs m.f.p.	Flux depression $\Delta\phi_0/\phi_0$	Disturbing force $F(p_0)$ Newton
100	10^{-3}	40	1.4×10^{-22}	3.6×10^{-25}
50	5×10^{-4}	20	1.2×10^{-11}	1.5×10^{-14}
10	10^{-4}	4	2.8×10^{-6}	7.2×10^{-10}
1	10^{-5}	0.4	3.4×10^{-5}	8.4×10^{-10}
0.1	10^{-6}	4×10^{-2}	6.8×10^{-5}	1.7×10^{-10}
10^{-2}	10^{-7}	4×10^{-3}	1.8×10^{-5}	4.5×10^{-12}
10^{-3}	10^{-8}	4×10^{-4}	4.4×10^{-6}	1.1×10^{-13}
10^{-4}	10^{-9}	4×10^{-5}	1.1×10^{-6}	2.8×10^{-15}
10^{-5}	10^{-10}	4×10^{-6}	2.8×10^{-7}	7×10^{-17}
10^{-6}	10^{-11}	4×10^{-7}	8×10^{-8}	2×10^{-18}

Table 2: Calculation of the disturbing force due to the air molecules within the vacuum chamber of a gravitational torsion balance. The assumed geometrical characteristics are: meatus thickness $s = 4$ mm, moving mass radius $R = 5$ mm.

Substituting the expression of k by Eq. (3) one obtains

$$p_0 - p(r) = p_0 \left[1 - \phi_m/\phi_0\right]\left(1 - r^2/L^2\right) \qquad (16)$$

which, substituted in Eq. (15), gives us the force

$$F(p_0) = (\pi/2)\, p_0 L^2 \left(\Delta p_0/p_0\right) \qquad (17)$$

where the relative depression is given by Eq. (12). Assuming for smoothed chamber walls a value $\xi = 0.001$ we obtain the disturbing force reported in Table 2. One can notice that in the assumed torsion balance apparatus with light test mass ($R = 5$ mm) the disturbing force $F(p_0)$ takes a maximum at a pressure $p_0 \approx 2$ Pascal $= 2\times10^{-5}$ bar which makes the optical thickness of the meatus about equal to 1. This maximum is estimated to be comparable to the measured gravitational force F_{gr}. Even taking into account the questionable accuracy of the fitting functions, the values of the disturbing force explain "ad abundantiam" why the region of the intermediate pressures between millibar and nanobar was avoided by the experimenters. Obviously, what is of interest in the measurements is the systematic error due to $F(p_0)$. For instance in the Gershteyn's light torsion balance (where F_{gr} may be of the order of 10^{-11} Newton) the measurement was made at a pressure $p_0 = 10^{-11}$ bar (10^{-6} Pascal), so the disturbing force $F(p_0)$ gives a negligible systematic error $\epsilon \approx 2\times10^{-7}$.

In the Heyl's heavy balance experiment (where the measured F_{gr} was of the order of 10^{-9} Newton) the disturbing force $F(p_0)$ at a pressure $p_0 = 1$ millibar (100 Pascal) gives $\epsilon \approx 10^{-16}$. However the random error due to the air convection was probably around $\epsilon \approx 10^{-4}$, that is much larger than the systematic error due to the vacuum pressure.

Submitted on February 07, 2009 / Accepted on May 18, 2009

References

1. Speake C.C., Quinn T.J. The gravitational constant: theory and experiment 200 years after Cavendish. *Meas. Sci. Technol.*, 1999, v. 10, 420.
2. Heyl P.R. A determination of the Newtonian constant of gravitation. *Proc. Nat. Acad. Sci.*, 1927, v. 13, 601–605.
3. Gillies G.T. The Newtonian gravitational constant: an index of measurements. *Metrologia*, 1987, v. 24, 1–56.
4. Luo J., Hu Z.K. Status of measurement of the Newtonian gravitational constant. *Class. Quant. Grav.*, 2000, v. 17, 2351–2363.
5. Kritzer R. The gravitational constant. http://www.physics.uni-wuerzburg.de
6. Gundlach J.H., Merkowitz S.M. Mesurement of Newton's constant using a torsion balance with angular acceleration feedback. arXiv: gr-qc/0006043.
7. Gershteyn M.L. et al. Experimental evidence that the gravitational constant varies with orientation. arXiv: physics/0202058.
8. Michelini M. The common physical origin of the gravitational, strong and weak forces. *Apeiron*, 2008, v.15, no. 4, 440.
9. Hu Z.K., Luo J. Progress in determining the gravitational constant with four acttracting masses. *Journal Korean Phys. Soc.*, 2004, v. 45, 128–131.
10. Luo J., Hu Z.K., Fu X.H., Fan S.H., Tang M.X. Determination of the Newtonian constant with a non linear fitting method. *Phys. Rev. D*, 1998, v. 59, 042001.
11. Luther G.G., Towler W.R. Redetermination of the Newtonian G. *Phys. Rev. Lett.*, 1981, v. 48, 121–123.
12. Gundlach J.H., Smith G.L., Adelberger E.G. et al. Short-range test of the Equivalence Principle. *Phys. Rev. Lett.*, 1997, v. 78, 2523.
13. Su Y., Heckel B.R., Adelberger H.G., Gundlach J.H. et al. New tests of the universality of free fall. *Phys. Rev. D*, 1994, v. 50, 3614.
14. Sanders A.J., Deeds W.E. Proposed new determination of G and test of Newtonian gravitation. *Phys. Rev. D*, 1991, v. 46, 489.
15. More G.I., Stacey F.D., Tuck G.J. et al. *Phys. Rev. D*, 1991, v. 38, 1023.
16. Karagioz O.V., Izmailov V.P., Gillies V.P. Gravitational constant measurement using a four-position procedure. *Grav. and Cosmol.*, 1998, v. 4, 239.
17. Ritter R.C., Winkler L.I., Gillies G.T. Precision limits of the modern Cavendish device. *Meas. Sci. Technol.*, 1999, v. 10, 499–507.
18. Fitzgerald M.P., Armstrong T.R. The measurement of G using the MSL torsion balance. *Meas. Sci. Technol.*, 1999, v. 10, 439–444.
19. Gundlach J.H. A rotating torsion balance experiment to measure Newton's constant. *Meas. Sci. Technol.*, 1999, v. 10, 454–459.

LETTERS TO PROGRESS IN PHYSICS

Additional Explanations to "Upper Limit in Mendeleev's Periodic Table — Element No. 155". A Story How the Problem was Resolved

Albert Khazan

E-mail: albkhazan@gmail.com

This paper gives a survey for the methods how a possible upper limit in Mendeleev's Periodic Table can be found. It is show, only the method of hyperbolas leads to exact answering this question.

True number of elements in Mendeleev's Periodic Table is the most important problem to the scientists working on the theory of the Periodic Table. The theory is based in the core on our views about the properties of the electron shells and sub-shells in atoms, which obviously change with increasing nuclear change (the nuclei themselves remains unchanged in chemical reactions). The electron shells change due to redistribution of electrons among the interacting atoms. Therefore, it is important that we know the limits of stability of the electron shells in the heavy elements (high numbers in the Periodic Table); the stability limits are the subjects of calculation in the modern quantum theory which takes into account the wave properties of electron and nucleons. To do it, the scientists employ a bulky mathematical technics, which gives calculations for the 8th and 9th periods of the Table (a hundred new elements are joined there).

Already 40 years ago the physicists proved that no chemical elements with mass higher than 110 can exists. Now, 118th element is known (117th element, previous to it, is still non-discovered). In the last time, the scientists of Joint Institute for Nuclear Research, Dubna, talked that the Periodic Table ends with maybe 150th element, but they did not provided any theoretical reason to this claim. As is probable, the regular method of calculation, based on the quantum theory, gives no exact answer to the question about upper limit of the Table.

It should be noted that 10 new elements were synthesed during the last 25 years: 5 elements were synthesed in GSI*, 4 elements were synthesed in JINR† (2 of these — in common with LLNL‡), and 1 element was synthesed in LBNL§. All the laboratories produced new elements as a result of nuclear reactions in accelerators: new elements were found after analysis of the products of the reactions. This is a very simplified explanation, however the essence of the process is so: problem statement, then components for the nuclear reaction and the necessary physics condition, then — identification of the obtained products after the reaction. This method gives new elements, of course, but it gives no answer to the question about their total number in the Periodic Table.

In contrast to this approach, when I tackled this problem, I used neither calculation for the limits of stability of the electron shells in atoms, nor experiments on synthesis of new elements, but absolutely another theoretical approach which allowed me for formulation of a new law in the Periodic Table and, as a result, the upper limit in it. Here I explain how. (I published all the results, in detail, in a series of papers [1–6], then collected in a book [7]).

First. Contents Y of every single element (say, of a K-th element in the Table) in a chemical compound of a molecular mass X can be given by the equation of an equilateral hyperbola $Y = K/X$, according to which Y (in parts of unit) decreases with increasing X.

Second. After as I created the hyperbolic curves for not only all known elements, but also for the hypothetical elements, expected by the aforementioned experimentalists, I looked how the hyperbolas change with molecular mass. To do it, I determined the tops of the hyperbolas, then paved a line connecting the tops.

Third. The line comes from the origin of the coordinates, then crosses the line $Y = 1$ in a point, where the top of one of the hyperbolas meets atomic mass of element, $K = X$, that is the boundary condition in the calculation. The calculated coordinates of the special point are $X = 411.663243$ and $Y = 1$. Because no elements can be above the point (contents Y of an element in a chemical compound is taken in parts of unit), the element with mass $X = 411.663243$ is the heaviest in the Periodic Table, so the Table ends with this element.

Fourth. In the next stage of this research, I was focused on the functions of atomic mass of element from its number along the Periodic Table. As a result, I have deduced the number of the last (heaviest) element in the Table. It is No. 155.

Thus, the last (heaviest) element in the Periodic Table was proved and its parameters were calculated without calculation of the stability of the electron shells in atoms on the basis of the quantum theory, but proceeding only from the general considerations of theoretical chemistry.

Of course, the methods of theoretical chemistry I applied in this reseach do not cancel the regular methods of the quan-

*Gesellschaft für Schwrionenforshung — Helmholtz Centre for Heavy Ion Research, Darmstadt, Germany.

†JINR — Joint Institute for Nuclear Research, Dubna, Russia.

‡LLNL — Lawrence Livermore National Laboratory, USA.

§LBNL — Lawrence Berkeley National Laboratory, USA.

tum theory; both methods are also not in competition to each other. Meanwhile calculations for the stability of the electronic shells of super-heavy elements can be resultative only in the case where the last element is known. Also, the experimentalists may get a new super-heavy element in practice, but, in the absence of theory, it is unnecessary that the element is the last in the Periodic Table. Only the aforementioned theory, created on the basis of the hyperbolic law in the Periodic Table, provides proper calculation for the upper limit in the Periodic Table, for characteristics of the last (heaviest) element, and hence sets a lighthouse for all futher experimental search for super-heavy elements.

P.S. This short paper was written due to the readers who, after reading my papers and just published book, asked me about the rôle of the calculations for the stability of the electron shells in my theory.

Submitted on April 03, 2009 / Accepted on May 20, 2009

References

1. Khazan A. Upper limit in the Periodic Table of Elements. *Progress in Physics*, 2007, v. 1, 38–41.
2. Khazan A. Effect from hyperbolic law in Periodic Table of Elements. *Progress in Physics*, 2007, v. 2, 83–86.
3. Khazan A. The rôle of the element Rhodium in the hyperbolic law of the Periodic Table of Elements. *Progress in Physics*, 2008, v. 3, 56–58.
4. Khazan A. Upper limit of the Periodic Table and synthesis of superheavy elements. *Progress in Physics*, 2007, v. 2, 104–109.
5. Khazan A. Introducing the Table of the Elements of Anti-Substance, and theoretical grounds to it. *Progress in Physics*, 2009, v. 2, 19–23.
6. Khazan A. On the upper limit (heaviest element) in the Periodic Table of Elements, and the Periodic Table of Anti-Elements. 2009, v. 2, L12–L13.
7. Khazan A. Upper limit in Mendeleev's Periodic Table — element No. 155. Svenska fysikarkivet, Stockholm, 2009.

LETTERS TO PROGRESS IN PHYSICS

Nikolai A. Kozyrev (1908–1983) — Discoverer of Lunar Volcanism

(On the 100th Anniversary of His Birth)

Alexander N. Dadaev*

Central Astronomical Observatory of the Russian Academy of Sciences at Pulkovo, Russia

This paper draws biography of Nikolai A. Kozyrev (1908–1983), the Russian astronomer who was one of the founders of theoretical astrophysics in the 1930's, and also discovered Lunar volcanism in 1958.

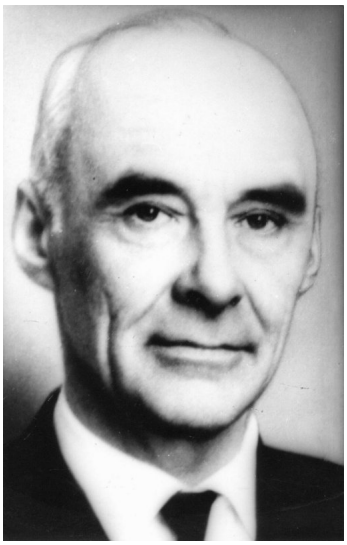

Nikolai A. Kozyrev, the 1970's

Of theories of the internal structure of stars and stellar energy sources scientists nowadays do not show as much interest as in the twenties and thirties of the past century. Interest at that time is explained by the situation then, when thinking about the nature of stellar energy was grounded in the study of the tremendous energy of the atomic nucleus, then new. Already, at the beginning of that century, hypotheses about the structure of the atom had been put forward. That encouraged physicists to study the deep secrets of the atom and its energy. By the end of the 1920's it became a widespread notion amongst astrophysicists that the generation of energy in stars is connected with sub-atomic processes in the chemical elements of which a star is composed. By the end of the 1930's, theoretical physicists had advanced some schemes for nuclear reactions which might explain energy generation in stars, to account for the energy expenditure of a star through radiation into space. Kozyrev's university study and the beginning of his scientific activity was undertaken in the 1920's. Very soon he became known as a serious physicist, and also as an outstanding planetologist. The young scientist had taken a keen interest in the fashionable problem of the origin of stellar energy, but he solved this problem more generally, encompassing not only stars, but also planets and their satellites. He proposed the hypothesis that the genesis of the internal energy of celestial bodies is the result of an interaction of *time with substance*. The discovery of volcanic activity in the Moon, made by Kozyrev when aged fifty, served to confirm his hypothesis. This discovery holds an important place in astronomical history, since a period of some 300 years of telescopic observations until then had not revealed volcanic activity on the Moon; the Moon being regarded as a "dead" heavenly body. Nikolai Kozyrev is rightly considered to be the discoverer of lunar volcanism.

Nikolai Aleksandrovich Kozyrev was born on August, 20 (2nd of September by the New Calendar) 1908, in St. Petersburg, into the family of an engineer, Alexander Adrianovich Kozyrev (1874–1931), a well-known expert in his field, at the Ministry of Agriculture, and who served in the Department of Land Management engaged in the hydrology of Kazakhstan. Originating from peasants of the Samara province, Kozyrev senior, who was born in Samara, was appointed to the rank of Valid State Councillor, in accordance with the 'tables of ranks' in Imperial Russia, which gave to him, and to his family, the rights of a hereditary nobleman. N. A. Kozyrev's mother, Julia Nikolaevna (1882–1961), came from the family of Samara merchants, Shikhobalov. A. A. Kozyrev had three more children: two daughters — Julia (1902–1982); Helena (1907–1985); and a son, Alexei (1916–1989).

Upon finishing high school in 1924, Nikolai Kozyrev went on up to the Pedagogical Institute, and thence, under the insistence of professors at the Institute, was admitted to the Physical and Mathematical Science faculty of Leningrad University, to become an astronomer. He finished university in 1928 and went on to postgraduate study at Pulkovo Observatory.

At the same time two other Leningrad University graduates went on to postgraduate study at Pulkovo — Victor A. Ambartsumian and Dmitri I. Eropkin. Academician Aristarch A. Belopolsky became the supervisor of studies of all three.

The "inseparable trinity" has left its imprint on the Pulkovo Observatory. Each of them was endowed with much talent,

*Submitted through Markian S. Chubey, Pulkovo Observatory. E-mail: mchubey@gao.spb.ru

but they differed in character. Life at Pulkovo proceeded separately from "this world", monotonously and conservatively, as in a monastery: astronomical observations, necessary relaxation, processing of observations, rest before observations, and the constant requirement of silence. The apartments of the astronomers were located in the main building of an observatory, in the east and west wings, between which there were working offices and premises for observations — meridian halls and towers with rotating domes.

The low salary was a principal cause of latent discontent. The protests of the three astrophysicists supported many employees of the Observatory, including the oldest — Aristarch A. Belopolsky.

After postgraduate study, in 1931, Ambartsumian and Kozyrev were appointed to the staff of the observatory as scientific experts category 1. The direction taken by the work of their supervisor is reflected in the character of the publications of the young scientists. But an independent approach was also outlined in these works in the solving of solar physics problems. Their work in the field of theoretical astrophysics was already recognized thanks to the writings of Milne, Eddington, and Zanstr, which they quickly developed on the basis of the successes of quantum mechanics, of the theory of relativity and of atomic and nucleus physics, was quite original. Ambartsumian and Kozyrev closely connected to a group of young theoretical physicists working at universities and physico-technical institutes: George A. Gamov (1904–1968), Lev D. Landau (1908–1968), Dmitri D. Ivanenko (1904–1994), Matwey P. Bronstein (1906–1938). Gamov, Landau and Ivanenko, along with their works on physics, were publishing articles on astrophysics. Ivanenko and Bronstein frequently visited Pulkovo for 'free discussions' of the essential problems of theoretical physics and astrophysics [1]. It was an original "school of talent".

Ambartsumian taught university courses in theoretical physics (for astrophysicists) and theoretical astrophysics. Kozyrev read lectures on the theory of relativity at the Pedagogical Institute. Both participated in working out the problems of a developing new science — theoretical astrophysics.

Courses of study in physics and astrophysics are essentially various. The study of the physics of elementary processes of interaction of matter and radiation is in astrophysics a study of the total result of processes in huge systems that stellar atmospheres as a whole represent. In such difficult systems the process of elementary interaction is transformed into the process of transfer of radiation (energy) from a star's internal layers to external ones, whence radiation leaves for space. The study methods are also various. In physics, a directed action of radiation on matter is possible, and the researcher operates by this action, and the studied process can be modified by the intervention of the researcher. In astrophysics intervention is impossible: the researcher can only observe the radiations emitted into space, and by the properties of observable radiation conjecture as to the internal processes of a star, applying the physical laws established in terrestrial conditions. Meaningful conclusions can be made by means of correctly applied theory. Study within these constraints is of what theoretical astrophysics consists.

The problem cannot be solved uniformly for all objects because astrophysical objects are very diverse. The process of transfer of radiation (energy) in stars of different spectral classes does not occur by a uniform scheme. Still more diversity is represented by stars of different types: stationary, variable, and non-stationary. Besides the stars, astrophysical objects include the planetary nebula, diffuse nebula (light and dark), white dwarfs, pulsars, etc. Theoretical astrophysics is a science with many branches.

From Kozyrev's early publications it is necessary to single out articles about the results of spectro-photometrical studies of the solar faculae and spots on the basis of his own observations. One work dealt with the temperature of sun spots, another the interpretation of the depth of dark spots, and Kozyrev proved that sun spots extend to much deeper layers of the solar atmosphere than was generally believed at that time. Kozyrev's arguments have since found verification.

In 1934 Kozyrev published in *Monthly Notices of the Royal Astronomical Society* a solid theoretical research paper concerning the radiant balance of the extended photospheres of stars [2]. Concerning the problem of transfer of radiant energy, atmospheric layers are usually considered as plane-parallel, for stars with extended atmospheres (photospheres), but such a simplification is inadmissible. Considering the sphericity of the photospheric layers, Kozyrev made the assumption that the density in these layers changes in inverse proportion to the square of the distance from the star's centre and corresponds to the continuous emanation of matter from the star's surface. He used available data on observations of stars of the Wolf-Rayet type and of P Cygni and theoretically explained observable anomalies, namely appearance in their spectral lines of high ionization potentials, which demands the presence of considerably more heat than actually observed on the surface of these stars. In the issue of the above-mentioned Journal, S. Chandrasekar's paper, containing the more common view of the same problem, was published, although received by the Journal half a year after Kozyrev's paper. The theory is called the "theory of Kozyrev-Chandrasekar".

A considerable part of the work during the Pulkovo period was carried out by Kozyrev and Ambartsumian. Together with Eropkin, Kozyrev published two articles containing the results of their expedition research work on polar lights by a spectral method; luminescence of the night sky and zodiac light. Research on the terrestrial atmosphere in those years was rather physical. However, works of a geophysical character stood outside the profile of the astronomical observatory; besides, these works demanded considerable expenditure that led to conflict with observatory management.

In May 1934, Belopolsky died — to the end a defender

Nikolai Kozyrev, 1934

of his pupils. Ambartsumian, in the autumn of 1935, had moved to Leningrad university. The "trinity" has broken up. The Director of Pulkovo Observatory, Boris P. Gerasimovich (1889–1937) decided to remove the two remaining "infractors of calmness". An infringement of financial management during the Tadjik expedition was fashioned into a reason for the dismissal of Dmitri Eropkin and Nikolai Kozyrev. In those years appointment and dismissal of scientific personnel of the observatory were made not by the director, but only with the permission of the scientific secretary of the Academy of Sciences, who upheld the action of the Director. A subsequent investigation for the reinstatement of Eropkin and Kozyrev conducted by the National Court and the commission of the Presidium of the Academy of Sciences occupied more than half a year.

In the meantime, in October, 1936, in Leningrad, arrests of scientists, teachers of high schools, and scientific officers had begun. One of the first to be arrested was the corresponding member of the USSR Academy of Sciences, Boris V. Numerov (1891–1941), the director of the Astronomical Institute, an outstanding scientist in the field of astronomy and geodesy. He was accused of being the organizer of a terrorist anti-Soviet group amongst intellectuals [3].

The wave of arrests reached Pulkovo. Kozyrev was arrested on the solemn evening of the 19th anniversary of October revolution, in the House of Architects (the former Jusupovsky palace). The choice of the date and the place of the repressive operation was obviously made for the purpose of intimidation of the inhabitants. On the night of December 5th (Day of the Stalin Constitution, the "most democratic in the world") Eropkin was arrested in Leningrad. These "red dates" are not forgotten in Pulkovo: all victims of the repression are not forgotten.

The Director of the observatory, Boris P. Gerasimovich was arrested at night, between the 29th and 30th of June 1937, in a train between Moscow and Leningrad. On November 30, 1937, Gerasimovich was sentenced to death and was shot that same day.

The Pulkovo astronomers, arrested between November and the following February, were tried in Leningrad on May 25, 1937. Seven of them, Innokentiy A. Balanovsky, Nikolai I. Dneprovsky, Nikolai V. Komendantov, Peter I. Jashnov, Maximillian M. Musselius, Nikolai A. Kozyrev, Dmitri I. Eropkin; were each sentenced to 10 years imprisonment. The hearings lasted only minutes, without a presentation of charges, without legal representation, with confessions of "guilt" extracted by torture — no hearings, only sentence.

According to the legal codes at the time, the 10 year imprisonment term was the maximum, beyond which was only execution. However, almost all the condemned, on political grounds, were died before the expiry of the sentences. Of the condemned Pulkoveans, only Kozyrev survived.

Boris V. Numerov was sentenced 10 years imprisonment and whilst serving time in the Oryol prison, was shot, on September, 15th, 1941, along with other prisoners, under the threat of occupation of Oryol by the advancing fascist army.

In Pulkovo arrests of the wives of the "enemies of the people", and other members of their families, had begun. It is difficult to list all arrested persons. They were condemned and sentenced to 5 year terms of imprisonment.

Until May 1939, Kozyrev was in the Dmitrovsk prison and in the Oryol prison in the Kursk area, then afterwards he was conveyed through Krasnoyarsk into the Norilsk camps. Until January 1940, he laboured on public works, and then, for health reasons, he was sent to the Dudinsky Permafrost Station, as a geodesist. In the spring of 1940 he made topographical readings of Dudinka and its vicinities, for what Kozyrev was permitted free activity, for to escape there was no possibility: the surrounds were only tundra.

In the autumn of 1940 he worked as an engineer-geodesist, and from December 1940 was appointed to Chief of Permafrost Station. On October 25, 1941, "for engaging in hostile counter-revolutionary propaganda amongst the prisoners" he was again arrested, and on January 10, 1942, he was sentenced to an additional 10 years imprisonment. On the same charges, Dmitri I. Eropkin had been condemned repeatedly, and was shot in Gryazovetsky prison of the Vologda area, on January 20, 1938 [3].

The Supreme Court of the Soviet Russia reconsidered the sentence on Kozyrev as liberal one and replaced it with death execution. But the Chief of the Noril-Lag (a part of the well-known GULAG) tore up the order of execution before the eyes of Kozyrev, referring to the absence in the regional centre, Dudinka, of any "executive teams". Probably, in all reality, this was a theatrical performance. Simply, Kozyrev was

needed, as an expert, for the building of a copper-nickel integrated facility, as another nickel mine near the Finnish border was then located within a zone of military action.

After the court hearing Kozyrev was transported to Norilsk and directed to work on a metallurgical combine as a thermo-control engineer. By spring of 1943, owing to his state of poor health, Kozyrev was transferred to work at the Norilsk Combine Geological Headquarters as an engineer-geophysicist. Until March 1945, he worked as the construction superintendent for the Hantaysky lake expedition and as the Chief of the Northern Magneto-Research Group for the Nizhne-Tungus geology and prospecting expedition.

Some episodes of the prison and camp life of Nikolai A. Kozyrev testify to his intense contemplations during this period. Certainly, some stories, originating from Kozyrev himself, in being re-told, have sometimes acquired a fantastic character.

The episode concerning Pulkovo's *Course of Astrophysics and Stellar Astronomy* [4] whilst being held in Dmitrovsky Central (the primary prison in Dmitrov city), is an example. Being in a cell for two people, Kozyrev thought much of scientific problems. His mind went back to the problem of the source of stellar energy. His cell-mate had been sent to solitary confinement for five days and when he returned he was very ill, and died. Kozyrev was then alone in his cell. He was troubled by the death of this cell-mate and his thoughts ceased to follow a desirable direction. A deadlock was created: there were no scientific data which could drive his thoughts. He knew that the necessary data were contained in the second volume of the *Course of Astrophysics*. Suddenly, in a day of deep meditation, through the observation port of his cell was pushed the book most necessary — from the *Course of Astrophysics*.

By different variants in the re-telling of the tale, the prisoner used the book for between one and three days, thumbing through it and memorising the necessary data. Then the book was noticed by a prison guard, and as it was deemed that the use of such specialist material literature was not allowed, the book was taken from him. Kozyrev thought that this book ,which so casually appeared, was from the prison library. That is almost impossible: someone delivered to the prison the special reference book, published in such a small circulation? Was there really a book in the hands of the prisoner or it was a figment of his tormented and inflamed imagination? Most likely mental exertion drew from his memory the necessary data. Something similar happens, sometimes, to theoreticians, when some most complicated problems steadfastly occupying the brain, are solved in unusual conditions, for example, as in a dream.

Another episode: consumed by his thoughts, Kozyrev began to pace his cell, from corner to corner. This was forbidden: in the afternoon the prisoner should sit on a stool, and at night lie on his bunk. For infringement of the rules Kozyrev was sent to solitary confinement for five days, in February 1938. The temperature in the confinement cell where daylight did not penetrate, was about zero degrees. There the prisoners wore only underwear, barefooted. For a meal they got only a piece of black bread and a mug of hot water per a day. With the mug it was possible to warm one's freezing hands but not the body. Kozyrev began to intensely pray to God from which he derived some internal heat, owing to which he survived.

Upon his release from solitary, Kozyrev reflected, from where could the internal heat have come? Certainly he understood that in a live organism the heat is generated by various vital processes and consumption of food. And it happens that a person remains vigorous and efficient, rather long term, without consumption of food, and "lives by the Holy Spirit"? What is Holy Spirit? If He pours in energy then energy can appear through Him, in a lifeless body. What factor of universal character can generate the energy? So Kozyrev's "time theory", advanced by him twenty years later, thus arose.

Both episodes contain mystical elements, but the mysticism accompanied Kozyrev both in imprisonment and in freedom, both in his life and in his scientific activity.

In June 1945 Kozyrev was moved from Norilsk to Moscow for "choice jugée revision". According to the official enquiry [3], choice judgée revision was made under the petition of academician Grigory A. Shayn, requesting liberation of the exiled Kozyrev, for his participation in restoration of astronomical observatories that were destroyed during the war; in Pulkovo, Simeis, Nikolaev, and Kharkov. However the petition of the academician was too weak an argument. Previously, in 1939, the academicians Sergey I. Vavilov and Grigoriy A. Shayn petitioned for revision of the choice jugées of the Pulkovo astronomers, not knowing that some of them were then already dead. The petition by the outstanding academicians was of no consequence.

The petition which was sent to the Minister of Internal Affairs, in August 1944, and registered with the judicial-investigatory bodies as the "letter of academician Shayn", but had actually been signed by three persons [5], namely, the full members of the Academy of Sciences of the USSR, Sergei I. Vavilov and Gregory A. Shayn, and by the correspondent-member of the Academy, Alexander A. Mihailov, the Chairman of the Astronomical Council of the Academy. This petition concerned only Kozyrev. The fate other condemned astronomers was known only to elements of the People's Commissariat of Internal Affairs. The petition for liberation of Kozyrev was obviously initiated those elements of the People's Commissariat of Internal Affairs. How to explain this?

When the Soviet intelligence agencies had received information about research by the USA on the creation of nuclear weapons, the State Committee of defence of the USSR made, in 1943, a secret decision on the beginning of such works in the USSR. As the head of the programme had been appointed Laurentiy P. Beriya, the National Commissar of Internal Affairs [6, p. 57]. Many physicists were in custody. Many were already dead. Those who still lived in prison camps it was

necessary to rehabilitate. Kozyrev numbered amongst them.

The "choice jugée revision" is an unusual process, almost inconceivable then. It was a question of overturning the decision of Military Board of the Supreme Court of the USSR, the sentences of which then were not reconsidered, but categorically carried out. The decision was made in the special prison of the People's Commissariat of Internal Affairs on Lubyanka (called then the "Felix Dzerzhinsky Square", in the centre of Moscow) where Kozyrev was held for one and a half years. At last, by decision of a Special Meeting of the KGB of the USSR on December 14, 1946, Kozyrev was liberated "conditionally ahead of schedule". This meant that over Kozyrev's head still hung the sentence of the Taymyrsky court, and with the slightest pretext he could appear again behind bars. Only on February 21, 1958, was the sentence of the Taymyrsky court overruled and Kozyrev completely rehabilitated.

After liberation Kozyrev has spent some days in Moscow that were connected mainly with an employment problem. Gregory A. Shayn, appointed in December 1944 as the Director of the Crimean Astrophysical Observatory (CrAO) then under construction, invited him to work in the Crimea. Kozyrev agreed. He devoted himself once again to scientific work.

But first he went to Leningrad for a meeting with kinsfolk and old friends, for restoration of scientific communications and, primarily, to complete work on his doctoral thesis, the defence of which took at Leningrad University on March 10th, 1947, i.e. only two and a half of months after his liberation. Many colleagues were surprised; when did he have time to write the dissertation? But he had more or less composed the dissertation during his ten years in prison. The strange episodes which occurred in Dmitrovsky Central had been connected with its theme. Kozyrev had some free time in Taymyr, when he was free to wander there for the one and a half years he worked as the Chief of the Topographical Group, and as the senior manager of the Permafrost Station. Besides, during his stay in Lubyanka, the possibility of being engaged within a year on the dissertation with use of the specialist literature been presented itself to him. Then he could write down all that at he had collected in his head. After liberation, possibly, it was only necessary to "brush" the draft papers.

Defence of the dissertation by Kozyrev occurred at the Department of Mathematics and Mechanics of Leningrad University: the dissertation theme, *Sources of Stellar Energy and the Theory of the Internal Constitution of Stars*. Attending as official examiners were the corresponding member of the Academy of Sciences of the USSR, Victor A. Ambartsumyan, professor Cyrill F. Ogorodnikov, and Alexander I. Lebedinsky. As a person working, after demobilization, at the Astronomical Observatory of Leningrad University, I was permitted to be present at this defence. Discussion was rather animated, because, beyond the modest name of his dissertation, Kozyrev put forward a new idea as to the source of the stellar energy, subverting the already widespread conviction that thermonuclear reactions are the source of energy in the entrails of stars. The discussion ended with a voting in favour of the Author's dissertation. On this basis the Academic Council of the University conferred upon Kozyrev the award of Doctor of Physical and Mathematical Sciences (the Soviet ScD), subsequently ratified by the Supreme Certifying Commission.

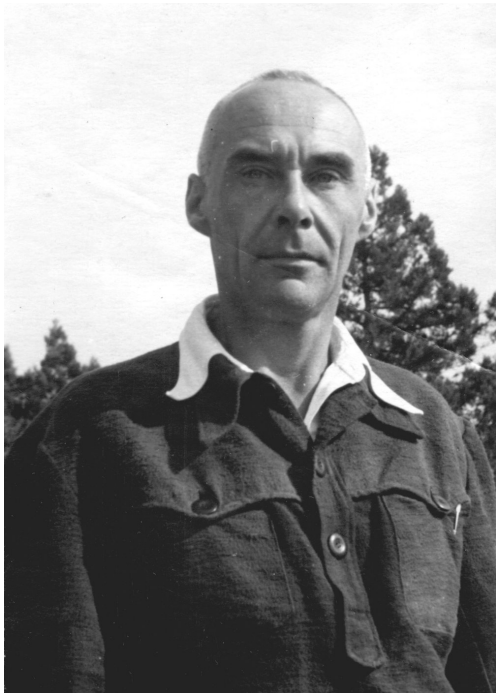

Kozyrev in Crimean Observatory, after the liberation

Kozyrev's dissertation was published in two parts, in the *Proceedings of the CrAO* [8], in 1948 (a part I), and in 1951 (a part II).

With scheme for nuclear reactions in the Sun and stars proposed by the German theoretical physicist Hans Bethe, in 1939, the question of stellar energy sources seemed to have been solved, and so nobody, except Kozyrev, reconsidered the problem.

Arguing by that the age of the Earth means that the Sun has already existed for some billions of years, and intensity of its radiation has not changed for some millions of years, which geological and geophysical research testifies, Kozyrev concluded the Sun is in a rather steady state, both in its mechanical and its thermodynamic aspects. This necessitates a study of the sources of its energy by which it is able to operate continuously for millions, even billions, of years.

Certainly the character of the source depends on the internal structure of the Sun (a star). Theories of the internal structure of stars are constructed on the basis of many assumptions about a star's chemical composition (percentage of hydrogen and other chemical elements), about the ionization conditions, about the quantity of developed energy per unit mass per second, about the nature of absorption of radiation,

etc. The reliability of all these assumptions is determined by comparison of the theoretical conclusions with the data of observations.

The key parameters of a star are its luminosity L, its mass M and its radius R. Kozyrev deduced theoretical dependencies of type M-L and L-R, and compared them with observable statistical dependencies "mass-luminosity" and "luminosity — spectral class" (Herzsprung-Russell diagram). The spectral class is characterized by the star's temperature, and the temperature is connected through luminosity with the star's radius (Stefan-Boltzman's law), i.e. the observable dependence of type L-R obtains. Comparison of the theoretically derived dependencies with observations statistically leads to the conclusion that the temperature at the centres of stars of the same type as the Sun does not exceed 6 million degrees, whereas the temperature necessary for reactions of nuclear synthesis is over 20 million degrees.

Moreover, by comparison of theoretical indicators of energy generation in a star and the emitted energy, these indicators are cancelled out by a star. Hence, in the thermal balance of a star, the defining factor is the energy emitted. But the estimated energy generation of thermonuclear reactions (if they operate in a star) far exceeds the observed emitted energy. Thus, reactions of nuclear synthesis are impossible because of insufficient heat in the stellar core (a conclusion drawn in the first part of Kozyrev's dissertation), and are not necessary (a conclusion of the second part).

Kozyrev drew the following conclusions: 1) a star is not a reactor, not a nuclear furnace; 2) stars are machines that develop energy, the emitted radiation being only a regulator for these machines; 3) the source of stellar energy is not Einstein's mass-energy interconversion, but of some other combination of the physical quantities. He also wrote that the "third part of this research will be devoted to other relations". Kozyrev held that stellar energy must be of a non-nuclear source, and must be able to operate for billions years without spending the mass of a star. The energy generation should not depend on temperature, i.e. the source should work both in stars, and in planets and their satellites, generating the internal energy of these cooler bodies as well. Accordingly, Kozyrev carried out observations, in order to obtain physical substantiation of his fundamental assumptions.

Kozyrev paid special attention to observations of the Moon and planets. About that time the 50-inch reflector, which Kozyrev grew so fond of, had been installed at the Crimean Observatory.

In 1954 Kozyrev published the paper *On Luminescence of the Night Sky of Venus* on the basis of spectral observations made at the Crimean Observatory in 1953. The observations for the purpose of recording the spectrogram of the night sky of a planet possessing a substantial atmosphere, required great skill: it was necessary to establish and keep on a slit of the spectrograph the poorly lighted strip to be completely fenced off from the reflected light of the day side of the planet, the brightness of which is 10,000 times the luminescence of the night sky. Dispersion of light from the horns of the bright crescent extend far into the night part, and can serve as the source of various errors, as the exposure must be long, to embody on a photographic plate the spectrum of the weak luminescence of the atmosphere of the planet. His observations went well; their processing and interpretation led to the detection of nitrogen in the atmosphere of Venus in the form of molecules N_2 and N_2^+.

The English astrophysicist Bryan Warner, in 1960, on the basis of a statistical analysis of Kozyrev's observations, proved identification of nitrogen and, additionally, that part of the spectral lines belong to neutral and ionized oxygen [9]. The presence of nitrogen and oxygen on Venus was definitely verified by direct measurements of its atmosphere by the interplanetary space missions "Venus-5", "Venus-6" (1969) and in the subsequent missions.

The observations of Mars in opposition, 1954 and 1956, inclined Kozyrev to the new conclusions concerning the Martian atmosphere and polar caps. Studying the spectral details of the planet's surface, he has come to the conclusion that observable distinction of the colour of continents and the seas on Mars can be explained by optical properties of the Martian atmosphere. This contention drew sharp objections from Gabriel A. Tihov, the well-known researcher of Mars. The scientific dispute remained unresolved. Kozyrev reasoned, that the polar cap observed in 1956 was an atmospheric formation, similar to "hoarfrost in air". Independently, Nikolai P. Barabashev and Ivan K. Koval (1956), and later also Alexander I. Lebedinsky and Galina I. Salova (1960), came to similar conclusions.

Kozyrev systematically surveyed with spectrograph various sites on the Moon's surface. The purpose of such inspections was to look for evidence of endogenetic (internal) activity which, as Kozyrev believed, should necessarily exist in the Moon. With the help of spectrographs it is possible to locate on the surface the sites of gas ejection, and he was sure that, sooner or later, he would see such phenomena.

In the beginning of the 19th century, William Hershel had reported observation of volcanoes on the Moon. François Arago later showed that visual observations do not permit detection of eruption of a lunar volcano as in the absence of atmosphere the eruption is not accompanied by ignition and luminescence. Kozyrev however approached the question with a belief in the existence of a "cold source" of energy in stars and planets.

His dissertation is devoted to the energy sources of stars. Concerning accumulation and action of the internal energy of planets, Kozyrev had expounded in the years 1950–1951 in the articles *Possible Asymmetry in Llanetary Figures* [10] and *On the Internal Structure of the Major Planets* [11].

The Moon does not differ from the planets in that the non-nuclear energy source should exist in the Moon as well. Its continuous operation should lead to accumulation of energy

which will inevitably erupt onto the surface, together with volcanic products, including gas. The gas can be observed with the help of the spectrograph. Before Kozyrev nobody used such methods of observation of the Moon. Difficulties in the observations are due to the necessity of catching the moment of emission because the ejected gas will quickly dissipate. The gases ejected by terrestrial volcanoes consist of molecules and molecular composites. The temperature of eruptions on the Moon cannot be higher. At successful registration the spectrogram should embody the linear spectrum of the Sun, reflected by the Moon, and molecular bands superimposed upon this spectrum, in accordance with the structure of the emitted gas.

Kozyrev found that luminescent properties are inherent to the white substance of the beam systems on the Moon. Supporters of the theory of a volcanic origin of craters on the Moon consider that the beam systems are recent formations of volcanic origins. One night in 1955 the crater Aristarkh differed in luminescence, exceeding the usual by approximately four times. It was possible to explain the strengthening of the luminescence by the action of a corpuscular stream as the light stream from the Sun depends only on inclination of the solar beams to the Moon's surface. As a stream of the charged corpuscles is deviated by a magnetic field, the luminescence should be observed on a dark part of the lunar disc that was not marked. Hence, "the Moon does not have a magnetic field" [12].

Kozyrev had drawn this conclusion three to four years prior to spacecraft missions to the Moon (1959). The discovery of an absence of a magnetic field for the Moon is considered an important achievement of astronautics. But in those years the prediction made by Kozyrev, went unnoticed, as did the results of his research on the atmosphere of Venus.

Also went unacknowledged was his doctoral dissertation which concluded an absence of thermonuclear synthesis in stars. It would seem that his work should have drawn the attention of physicists and astrophysicists in connection with Raymond Davis' experiments on the detection of the solar neutrino.

In 1946 Bruno Pontekorvo described a technique of neutrino detection through physical and chemical reaction of transformation of chlorine in argon. Any thermonuclear reactions are accompanied by emission of neutrino or antineutrino. R. Davis organized, in the 1950's, a series of experiments on the basis of Pontekorvo's method. The observations revealed little evidence for the expected reaction, in accordance with an absence of thermonuclear reactions in the Sun's entrails as had been predicted by Kozyrev.

Throughout the years 1967–1985, Davis continued experiments to measure neutrino streams from the Sun, with an advanced technique. Results were no better: the quantity of detected neutrinos did not surpass one third of the theoretically calculated stream. In the 1990's the experiments were performed in other research centres by other means, reaffirming Davis' results. The Nobel Prize [13] was awarded to Raymond Davis in 2002.

From August 15th, 1957, Kozyrev began to work at Pulkovo Observatory in the same post of senior scientific researcher. He had received a small apartment in Leningrad, on the Moscow Prospect, on a straight line connecting the city with Pulkovo. Twice a year he went to the Crimea to carry out observations, in the spring and autumn, with the 50-inch reflector.

In August, 1958 Kozyrev published his book *Causal or Asymmetrical Mechanics in the Linear Approximation* [14], where he generalized the results of laboratory experiments and astrophysical observations to a conclusion on the non-nuclear energy source of stars. It was a continuation of his thesis for his doctor's degree. Thus, this third part is in style and character very unlike the first two. Discussion of this book began before the death of Kozyrev, and continues.

The non-nuclear energy source of stars and planets is attributed in Part III to time. Kozyrev however did not explain what time is, but asserted that time proceeds by physical properties, and he tried to reveal them. He believed that in rotating celestial bodies, time makes energy, which he tried to prove experimentally by weighing of gyroscopes at infringement of the usual relationships between cause and effect.

To consolidate his ideas about transformation of time into energy Kozyrev tried to create a corresponding theory. Postulating an infinitesimal spatial interval between cause and effect, and the same time interval between them, he defines the relation of these intervals as the velocity of transition of a reason into a consequence. After a series of postulates, Kozyrev defined the course of time as the speed of transition of a reason in a consequence, and designates it c_2, unlike the velocity of light c_1. He considered that c_2 is a universal constant, as well as c_1; the value of c_2 he finds experimentally and theoretically, as $c_2 = 1/137 c_1$, where 1/137 is dimensionless value equal to Sommerfeld's fine structure constant. Besides that

$$c_2 = a\,\frac{e^2}{h} = a \cdot 350 \text{ km/sec},$$

where e is the elementary charge, h is Planck's constant, a a dimensionless multiplier which is subject to definition.

To describe the character of interaction of the causes and effects by means of mathematical formulae, Kozyrev gave to these phenomena the sense of mechanical forces: reason is active force, and effect is passive force. Thereby Kozyrev *materialized* these concepts just as the definition of force includes mass. Though cause and effect phenomena had already been *materialized* by postulation of the spatial and time intervals between them, Kozyrev used representations about the compactness of bodies and the impossibility of the simultaneous location of two bodies at one point of space. In the same manner Kozyrev also materialized time, or the *course of time*, owing to which there is an intermediate force $\frac{mdv}{dt}$ between the active and passive forces. Values of m and v are not

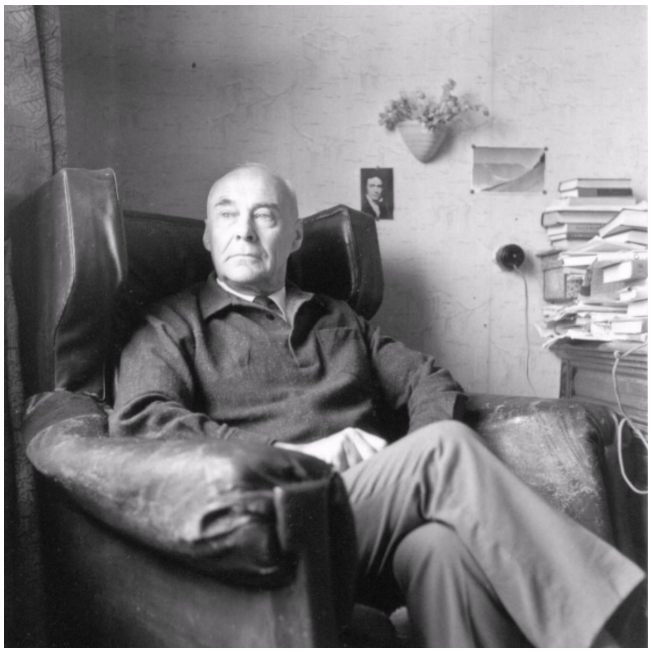

Kozyrev at home, in Leningrad

explained. Nor does Kozyrev explain how the course of time causes the occurrence of the additional force. It was simply a postulate, which he had not formulated. The *materialization* of causes and effects is also just postulated.

The long chain of postulates included in the long theoretical reasoning is reduced to a statement about the subliminal *flow of time* which exists from extreme antiquity. Directly about the flow Kozyrev does not write; but if the *course of time* proceeds by mechanical force, then the force, over some distance, does work. So the river flow actuates a water-mill.

That is why, according to Kozyrev's theory, energy is created at the expense of time only in rotating bodies. To prove this thesis experimentally, Kozyrev engaged in experiments with gyroscopes, to which a separate chapter in his book is devoted. Later, Kozyrev reconstructed the theory on the basis of Einstein's theory.

The physical essence of the *course of time* nobody has been able to elucidate. However there are no bases to deny that time action promotes energy generation in stars and planets, as Kozyrev's theory specifies. Kozyrev's discovery of lunar volcanism, as a result of his persevering research on the basis of his own theory, also specifies that.

On November 3, 1958, at the Crimean observatory, Kozyrev was observing a region on the surface of the Moon for the purpose of its detecting endogenetic activity. This time Kozyrev concentrated his attention on the crater Alphons, in the central part of the lunar disc. According to American astronomer Dinsmor Alter, a haze observed in the crater Alphons prevented clarification of the details of crater [15].

Kozyrev made a pair of spectrograms. On one of them, in the background of the solar spectrum, with its specific dark lines, the light bands of molecular carbon C_2 and carbon dioxide gas CO_2 were visible. On the other spectrogram taken half an hour after the first, the bands were absent. The slit of the spectrograph crossed the crater through the central hill of the crater. Hence, the gas eruption occurred from the central hill of the crater Alphons. So the discovery was made.

Soon Kozyrev published a short letter in *The Astronomical Circular* (No. 197, 1958) and an article containing the detailed description of a technique and circumstances of the observations, with a reproduction of the unique spectrogram, in *Sky and Telescope* (vol. 18, No. 4, 1959). In response to this article the well-known astronomer and planetologist, Gerard Kuiper, sent a letter to the Director of Pulkovo Observatory in which he declared that Kozyrev's spectrogram was a fake.

From December 6 to December 10, 1960, in Leningrad and Pulkovo, there was held an international symposium on lunar research by ground-based and rocket means (the Symposium No. 14 "Moon"), assembled in accordance with the calendar schedule of the International Astronomical Union (IAU). Well-known planetologists took part in the Symposium sessions and scientists from many countries were present: Gerard Kuiper, Garald Jurys, John Grey (USA), Zdenek Copal (Great Britain), Auduin Dolfus (France), Nicola Bonev (Bulgaria), Nikolai A. Kozyrev, Alexander V. Markov, Nadezhda N. Sytinskaja (USSR), etc.

Kozyrev's report *Spectroscopic Proofs for the Existence of Volcanic Processes on the Moon* [16], with presentation of the original spectrogram, was favourably received. Concerning the decoding of the emittance spectrum which had appeared when photographing the lunar crater Alphons, the skilled spectroscopists Alexander A. Kalinjak and Lydia A. Kamionko reported. Their identification of the spectrum proved the authenticity of the spectrogram. G. Kuiper was also convinced of the validity of the spectrogram, and withdrew his claims of forgery.

Kozyrev's detection of endogenetic activity in the "dead" Moon has not received either due consideration or support in relation to his search for a "cold source" of the energy of the Earth and in stars. Kozyrev's book *Causal Mechanics*, putting forward the flow of time as an energy source, has received inconsistent responses in the press. The first was by the Leningrad publicist and physicist Vladimir Lvov, who published in the newspaper *Evening Leningrad*, from December 20, 1958, the article *New Horizons of Science*. The article's title indicates a positive reception of Kozyrev's book. Subsequently, Lvov repeatedly published in newspapers and periodicals, strengthening the arguments in favour of statements that Kozyrev's theory, in essence, amounts to discovery of a third origin of thermodynamics, which counteracts thermal death of the Universe.

In the same spirit, in *The Literary Newspaper*, from November 3rd of 1959, an article by the well-known writer Marietta Shaginyan, entitled 'Time from the big letter', was published. Meanwhile, in Pulkovo Observatory, Kozyrev's lab-

oratory experiments, which he conducted to substantiate the conclusions of *Causal Mechanics* and his "time theory", had been organized. It was found that the experimental data did not exceed the "level of noise" and so did not reveal the effects predicted by the theory. On the basis of these results, the full members of Academy, Lev A. Artsimovich, Peter L. Kapitsa and Igor E. Tamm reported in the newspaper *Pravda*, on November 22, 1959, in the article *On the Turn in Pursuit of Scientific Sensations*, in which they condemned the article by M. Shaginjan as an "impetuously laudatory" account of the "revolution in science" made by professor Kozyrev.

The Branch of General Physics and Astronomy of the Academy of Sciences organized another more careful check of the experiments and Kozyrev's theory. The examination and analysis was made by scientists in Leningrad and Moscow, appointed by the Branch, with involvement of some Leningrad institutes. The results were discussed by the Academic Council of Pulkovo Observatory on July 1, 1961. Kozyrev's theory, detailed in the book *Causal Mechanics*, was deemed insolvent, and recommendations to improve equipment and to raise the accuracy of experimental data were given.

The book *Causal Mechanics* met with a negative reception, although it deserved some measure of positive evaluation. Kozyrev's theory as it is presented in the book is an investigation, which, before Kozyrev, nobody had undertaken. The investigation occurred in darkness, blindly, groping, producing an abundance of postulates and inconsistent reasoning. Before Kozyrev, time was mostly perceived subjectively as sensation of its flow, from birth to death. The great philosopher Immanuel Kant considered time to be the form of our perception of the external world. It is defined still now as the form of existence of matter. The modern theory of relativity has fixed this concept also, having defined time as one of the dimensions of four-dimensional space-time, by which it amplifies the idea that space and time are the *essence of the form* of the physical world. Kozyrev searched not for formal time, but for time that is actively operating.

Despite criticism of his efforts, Kozyrev continued his investigations in the same direction, following his intuition. He did not change his belief that time generates energy, only his methods of inquiry. After July 1961, Kozyrev almost entirely disengaged from experiments of mechanical character.

Kozyrev was carried along by a great interest in the laboratory study of irreversible processes which might visually reveal time action. For this purpose he designed a torsion balance, with an indicating arm rotating in a horizontal plane and reacting to external processes. Having isolated the device from thermal influences, Kozyrev interpreted any deviations of an arm from its "zero" position as the effect of time. Generally speaking, all processes in Nature are irreversible, by which the orientation of time manifests. This orientation should cause a deviation of the balance arm in one and the same direction, though deviations are possible to different angles, depending on the intensity of the process. In Kozyrev's experiments the deviation of the arm occurred in both directions (to the right and to the left), for which he devised explanations.

Intensive irreversible processes are especially evident. Cases Kozyrev used included the cooling of a heated wire or a piece of metal; the evaporation of spirit or aether; the dissolution of sugar in water; the withering of vegetation. Processes carried out near the device caused deviations the arm which could occur from electromagnetic influence, or waves in the range of ultrasonic or other. Such influences Kozyrev did not study, but any deviations of the arm he considered to be produced by time. He introduced the concept of "time density" in the space surrounding the device. He explained the balance arm deviations in both directions as the passing of a radiant time process ("time density" arises) or the absorption of time ("density" in the surrounding space goes down). What is "time density" Kozyrev did not explain. In some experiments the same irreversible process yielded different results on different days (deviations in opposite directions). Kozyrev explained this by the action of a remote powerful process deforming the laboratory experiment.

In studying irreversible processes by the methods described above, Kozyrev investigated the possibility of time shielding. Kozyrev conjectured that if time signals come from space, these signals can be captured by means of aluminium coated telescopic mirrors. This offered a method for "astronomical observations by means of the physical properties of time". In February, 1963, Victor Vasilevich Nassonov (1931–1986), a skilled engineer and expert in electronics with work experience at a radio engineering factory, visited Kozyrev's laboratory. Nassonov expressed his desire to work as a voluntary assistant to Kozyrev. As such he worked in laboratory until Kozyrev died. Nassonov immediately began improvement of equipment and introduced automatic data recordings which raised their accuracy. Nassonov usually went to laboratory in the evenings, after his work at the radio factory. Kozyrev too worked mainly in the evenings. When Kozyrev was away on observations in the Crimea, Nassonov took holiday leave from the radio factory and, at his own expense, accompanied Kozyrev. Nassonov became Kozyrev's irreplaceable assistant and close colleague.

Kozyrev worked not only in the laboratory or at home behind a desk. He did not alter his periodic trips to the Crimean Observatory where he used the 50-inch reflector. Planets and the Moon were primary objects of his observations. At any opportunity he undertook spectrographic surveys of the lunar surface for the purpose of detection of any changes characterizing endogenic activity. He noted some minor indications but did not again obtain such an expressive spectrogram as on November 3, 1958 — that was a unique find by good luck.

For observations of planets he used the configurations (opposition, elongation), most convenient for the tasks he had in mind. He took every opportunity; adverse weather the only

Nassonov and Kozyrev in front of Pulkovo Observatory

hindrance. In April 1963, Kozyrev conducted observations of Mercury when the planet was at elongation — the most remote position from the Sun, visible from the Earth. He aimed to determine whether or not hydrogen is present in the Mercurian atmosphere. Such an atmosphere could be formed by Mercury's capture of particles which constitute the solar wind; basically protons and electrons. The captured particles, by recombination, form atomic and molecular hydrogen. The task was a very difficult one. First, observations of Mercury are possible only after sunset or before sunrise, when the luminescence of the terrestrial atmosphere is weak. However Mercury is then close to horizon, and noise from the terrestrial atmosphere considerably amplified. Second, Mercury shines by reflected sunlight, in the spectrum of which the hydrogen lines are embedded. It is possible to observe the hydrogen lines formed in the atmosphere of a planet by taking into account the shift of lines resulting from the planet's motion (toward the red when receding from the observer, toward the violet on approach). This shift can be seen as distortion of a contour of the solar line from the corresponding side. In April 1963, Mercury was to the west of the Sun and was visible after sunset. Kozyrev detected the presence of an atmosphere on Mercury. In autumn of the same year, Mercury was east of the Sun, and it was observed before sunrise; its atmosphere was not detected (details are given in [17]).

By means of observations of the passage of Mercury across the Sun's disc on November 10th of 1973, Kozyrev again detected signs of an atmosphere on Mercury [18]. However his conclusion contradicted the results of direct measurements by the spacecraft "Mariner-10", in 1974–1975. This spacecraft, first sent to Venus, and then to Mercury, during a flight around the Sun, took three sets of measurements as it approached Mercury. Concerning the atmosphere of the planet, the gathered data had demonstrated that it contains helium and oxygen in minute quantities, and almost no hydrogen.

Kozyrev's disagreement with the Mariner-10 data can be explained by the instability of hydrogen in the atmosphere because of the great temperature of Mercury's Sun-facing surface (above 500°C) and by Mercury's small force of gravitational attraction (escape velocity 4.2 km/s). Observations of Kozyrev fell to the periods of capture of a corpuscular solar stream; soon the grasped volume of a stream dissipated. Anyway, Kozyrev's observations and conclusions to write-off there are no bases.

Observing Saturn in 1966, Kozyrev detected the presence of water vapour in its rings [19]. Emergence of the water bands in the spectrum of the planet, which is so removed from the Sun, Kozyrev explained as the "photosublimation" process (the term coined by Kozyrev), i.e. by the direct transformation of crystals of ice into water vapour under the influence of solar radiation. G. Kuiper an opponent, argued that the Saturnean rings consist not of the usual ice, but of ammoniac, upon which Kuiper's objections were been based, but subsequently retracted by him.

Only in 1969 did Kozyrev's discovery of lunar volcanism receive official recognition, owing to findings made by the American Apollo-11 mission on the Moon in July, 1969. Astronauts Neil Armstrong, Buzz Aldrin and Michael Collins brought back to Earth a considerable quantity of lunar soils, which consisted mainly of volcanic rocks; proving intensive lunar volcanic activity in the past, possibly occurring even

now. Kozyrev's discovery has thus obtained an official recognition.

The International Academy of Astronautics (IAA, Paris, France) at its annual meeting in late September, 1969, in Cloudcroft (New Mexico, USA), made the resolution to award Kozyrev a nominal gold medal with interspersed seven diamonds in the form of constellation of the Ursa Major: "For remarkable telescopic and spectral observations of luminescent phenomena on the Moon, showing that the Moon remains a still active body, and stimulating development of the methods of luminescent researches world wide". Kozyrev was invited to Moscow for the award ceremony, where, in solemnity, the academician Leonid I. Sedov, vice-president of the International Astronautic Federation (a part of which is the IAA) gave Kozyrev the medal.

In December 1969, the State Committee for Affairs of Discovery and Inventions at the Ministerial Council of the USSR, awarded Kozyrev the diploma for discovery for "tectonic activity of the Moon".

Despite the conferring of medal and diploma, the question of a non-nuclear stellar energy source was not acknowledged. To Kozyrev the recognition of his discovery was also recognition of his work on the source of stellar energy. His theoretical research was amplified by his publication of a series of articles detailing his results, along with the formulation of his new considerations about the physical properties of time.

He no longer spoke about time generating energy in celestial bodies. In experiments with irreversible processes the properties of bodies to "emit" or to "absorb" time, forming around bodies a raised or lowered "time density" seemed to have been established, though Kozyrev did not explain how this is to be understand; but he nonetheless used the idea. It is especially strange that in works after 1958 he avoided the interpretation of time as material essence. In the seventies he gradually passed to the representation of immaterial time.

Upon the idea of time "emitting" and "absorption" is based Kozyrev's work *Features of the Physical Structure of the Double Stars Components* [20]. Therein Kozyrev did not investigate the interaction of double star components by light and other kinds of electromagnetic and corpuscular radiation; he postulated the presence of "time radiations" — the main star (primary star) radiates time in the direction of the companion-star (secondary star) owing to which the time density in the vicinity of both stars becomes identical, which finally leads to the alignment of the temperatures of both stars and their spectral classes in accordance with statistical studies of double stars.

By a similar method, Kozyrev investigated the mutual influence of tectonic processes on the Earth and on the Moon [21]. In consideration of tectonic processes Kozyrev could not neglect their gravitational interaction and put forward two kinds of interaction: 1) a trigger mechanism of tidal influences; 2) a direct causal relationship which is effected "through the material properties of time".

For comparison of lunar processes with terrestrial ones Kozyrev used the catalogue of recorded phenomena on the Moon, published by Barbara Middlherst et al. [22]. It is conditionally possible to suppose that all considerable phenomena on the Moon, observed from the Earth, are caused by tectonic processes. Records of the same phenomena on the Earth for the corresponding period (1964–1977) are easy to find. From comparison of the records Kozyrev drew the conclusion that there are both types of communication of the phenomena on the Earth and on the Moon, "independently of each other", though they are inseparable. To reinforcement his conclusions about the existence of relationships "through the material properties of time", Kozyrev referred to such relationships established for double stars, although alternative and quite obvious relations for double stars systems were not considered.

Some words are due about appearance and habits of Kozyrev. Since the age of fifty, when Kozyrev worked in Pulkovo, his appearance did not change much. He was of tall stature, well-built, gentlemanly, with a high forehead, short haircut and clean shaven, and proudly held his head high. He resembled a military man although he never served in the army, and went about his business in an army style, quickly, and at meetings with acquaintances kindly bowed whilst on the move or, if not so hastened, stopped for a handshake. He was always polite, with everybody. When operating a telescope and other laboratory devices Kozyrev displayed soft and dexterous movements. He smoked much, especially when not observing. In the laboratory he constantly held the hot tea pot and cookies: a stomach ulcer, acquired in prison (which ultimately caused his death), compelled him to take often of any food.

When at the Crimean Observatory, he almost daily took pedestrian walks in the mountains and woods surrounding the settlement of Nauchny (Scientific). He walked mostly alone, during which he reflected. Every summer, whilst on holiday, he took long journeys. He was fond of kayaking the central rivers of Russia for days on end. On weekends he travelled by motorbike or bicycle along the roads of the Leningrad region. On one occasion he travelled by steam-ship, along a tourist route, from Moscow, throughout the Moscow Sea, then downwards across the Volga to Astrakhan. He loved trips to Kiev and in to places of Russian antiquity. In the summer of 1965 Kozyrev took a cruise by steam-ship, around Europe, visiting several capitals and large cities. Separately he visited Bulgaria, Czechoslovakia, and Belgium.

In scientific work, which consumed his life, Kozyrev, even in the days of his imprisonment and exile, he, first of all, *trusted in himself*, in his own intuition, and considered, in general, that intuition is theomancy emanating from God. According to Kozyrev, postulates should represent the facts which are not the subject to discussion. Truth certainly sometime, will appear in such a form that it becomes clear to all who aspire to it.

Nikolai Aleksandrovich Kozyrev died on February 27, 1983. He is buried in the Pulkovo astronomer's memorial cemetery. Victor Vasilevich Nassonov continued some laboratory experiments with irreversible processes relating to biology. Nassonov, through overwork that could not be sustained, died on March 15th 1986, at the age of fifty-five.

Submitted on March 27, 2009 / Accepted on May 20, 2009

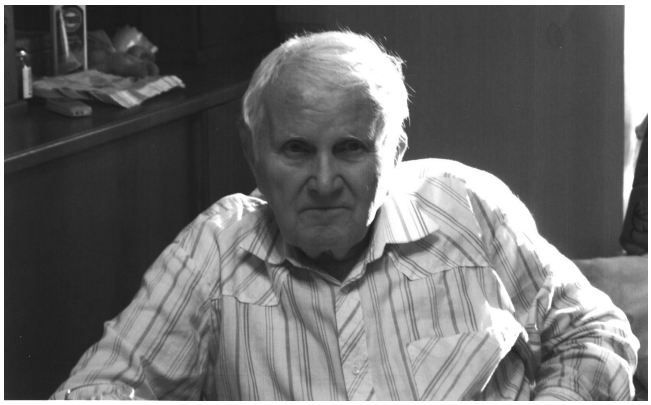

About the Author: Alexander Nikolaevich Dadaev was born on October 5, 1918 in Petrograd (now — St. Petersburg), Russia. In 1941 he completed his education, as astronomer-astrophysicists, at Leningrad University. He participated in the World War II, in 1941–1945, and was wounded in action. During 1948–1951 he continued PhD studies at Pulkovo Observatory, where he defended his PhD thesis *Nature of Hot Super-Giants* in 1951. He was the Scientific Council of Pulkovo Observatory in 1953–1965, and Chief of the Laboratory of Astrophysics in 1965–1975. Alexander N. Dadaev is a member of the International Astronomical Union (IAU) commencing in 1952. The Author would like to express his gratitude to Dr. Markian S. Chubey, the astronomer of Pulkovo Observatory who friendly assisted in the preparation of this paper.

References

1. Martynov D. Ja. The Pulkovo observatory 1926–1928. *Historical Astronomical Research*, issue 17, Nauka, Moscow, 1984 (*in Russian*).
2. Kozyrev N. A. Radiative equilibrium of the extended photosphere. *Monthly Notices of the Royal Astron. Society*, 1934, v. 94, 430–443.
3. Official data about the destiny of the Pulkovo astronomers. *Historical Astronomical Research*, issue 22, Nauka, Moscow, 1990, 482–490 (*in Russian*).
4. Course of astrophysics and stellar astronomy. Ed. by B. P. Gerasimovich. Part I. Methods of astrophysical and astrophotographic researches. ONTI, Leningrad, 1934; Part II. Physics of the Solar system and stellar astronomy. ONTI, Leningrad, 1936 (*in Russian*).
5. In protection of the condemned astronomers. *Historical Astronomical Research*, issue 22, Nauka, Moscow, 1990, 467–472 (*in Russian*).
6. Zalessky K. A. Stalin's empire. Biographic encyclopedia. "Veche" Publ., Moscow, 2000, 120 (*in Russian*).
7. Kozyrev N. A. Sources of stellar energy and he theory of the internal constitution of stars. *Proceedings of the Crimean Astron. Observatory*, 1948, v. 2, 3–13 (*in Russian*).
8. Kozyrev N. A. The theory of the internal structure of stars and sources of stellar energy. *Proceedings of the Crimean Astron. Observatory*, 1951, v. 6, 54–83 (*in Russian*).
9. Warner B. The emission spectrum of the night side of Venus. *Monthly Notices of the Royal Astron. Society*, 1960, v. 121, 279–289.
10. Kozyrev N. A. Possible asymmetry in figures of planets. *Priroda*, 1950, no. 8, 51–52 (*in Russian*).
11. Kozyrev N. A. On the internal structure of major planets. *Doklady Akademii Nauk USSR*, 1951, v. 79, no. 2, 217–220 (*in Russian*).
12. Kozyrev N. A. Luminescence of the lunar surface and intensity of corpuscular radiation of the Sun. *Proceedings of the Crimean Astron. Observatory*, 1956, v. 16, 148–158 (*in Russian*).
13. Davis R., Jr. Solar neutrinos, and the Solar neutrino problem. http://www.osti.gov/accomplishments/davis.html
14. Kozyrev N. A. Causal or asymmetrical mechanics in the linear approximation. Pulkovo Observatory, Pulkovo, 1958 (*in Russian*).
15. Alter D. A suspected partial obscuration of the floor of Alphonsus. *Publications of the Astronomical Society of the Pacific*, v. 69, no. 407, 158–161.
16. Kozyrev N. A. Spectroscopic proofs for the existence of volcanic processes in the Moon. *The Moon*, Proceedings from IAU Symposium No. 14 held in Leningrad, Pulkovo, December 1960, 263–271.
17. Kozyrev N. A. The atmosphere of Mercury. *Sky and Telescope*, 1964, v. 27, no. 6, 339–341.
18. Kozyrev N. A. The atmosphere of Mercury in observations of its passage cross the Sun's disc on November 10, 1973. *Astron. Circular*, 1974, no. 808, 5–6 (*in Russian*).
19. Kozyrev N. A. Water vapour in a ring of Saturn and its hothouse effect on a planet's surface. *Izvestiya Glavnoy Astronomicheskoy Observatorii*, 1968, no. 184, 99–107 (*in Russian*).
20. Kozyrev N. A. Relation masse-luminosité et diagramme H-R dans le cas des binaires: Physical peculiarities of the components of double stars. *On the Evolution of Double Stars*, Proceedings of a Colloquium organiced under the Auspices of the International Astronomical Union, in honor of Professor G. Van Biesbroeck. Edited by J. Dommanget. *Communications Obs. Royal de Belgique*, ser. B, no. 17, 197–202.
21. Kozyrev N. A. On the interaction between tectonic processes of the Earth and the Moon. *The Moon*, Proceedings from IAU Symposium No. 47 held at the University of Newcastle-Upon-Tyne England, 22–26 March, 1971. Edited by S. K. Runcorn and Harold Clayton Urey, Dordrecht, Reidel, 1971, 220–225.
22. Middlehurst B. M., Burley J. M., Moore P., Welther B. L. Chronological catalogue of reported lunar events. *NASA Techn. Rep.*, 1968, R-277, 55+IV pages.

Progress in Physics **is an American scientific journal on advanced studies in physics, registered with the Library of Congress (DC, USA): ISSN 1555-5534 (print version) and ISSN 1555-5615 (online version). The journal is peer reviewed and listed in the abstracting and indexing coverage of: Mathematical Reviews of the AMS (USA), DOAJ of Lund University (Sweden), Zentralblatt MATH (Germany), Scientific Commons of the University of St. Gallen (Switzerland), Open-J-Gate (India), Referential Journal of VINITI (Russia), etc.** ***Progress in Physics*** **is an open-access journal published and distributed in accordance with the Budapest Open Initiative: this means that the electronic copies of both full-size version of the journal and the individual papers published therein will always be acessed for reading, download, and copying for any user free of charge. The journal is issued quarterly (four volumes per year).**

Electronic version of this journal:
http://www.ptep-online.com

Postal address for correspondence:

Department of Mathematics and Science
University of New Mexico
200 College Road, Gallup, NM 87301, USA

Printed in the United States of America